# Energy Prediction and Optimization of the Hybrid Community District Heating System (H-CDHS)

Behrang Talebi

A Thesis

In the Department

Of

Building, Civil and Environmental Engineering

Presented in Partial Fulfillment of the Requirements

For the Degree of

Doctor of Philosophy (Building Engineering) at

Concordia University

Montreal, Quebec, Canada

June 2018

CONCORDIA UNIVERSITY

SCHOOL OF GRADUATE STUDIES

This is to certify that thesis prepared

By: Behrang Talebi

Entitled: Energy Prediction and Optimization of the Hybrid Community District Heating System (H-CDHS)

and submitted in partial fulfillment of the requirements for the degree of

DOCTOR OF PHILOSOPHY (Building Engineering)

complies with the regulations of the University and meets the accepted standards with respect to originality and quality.

Signed by the final examining committee:

_____ Chair
Dr. V. S. Hoa

_____ External Examiner
Dr. G. Fraisse

_____ External to Program
Dr. A. Dolatabadi

_____ Examiner
Dr. R. Zmeureanu

_____ Examiner
Dr. L. Wang

_____ Thesis Supervisor
Dr. F. Haghighat

_____ Co-Supervisor
Dr. P. Mirzaei Ahranjani

Approved by

_____
Dr. F. Haghighat, Graduate Program Director

Aug, 20, 2018

_____
Dr. A. Asif, Dean
Faculty of Engineering and Computer Science

# Abstract


## Energy Prediction and Optimization of the Hybrid Community District Heating System (H-CDHS)

**Behrang Talebi, Ph.D.**

**Concordia University, 2018**

The ever-increasing demand for energy in different sectors, such as building sector as one of the main consumers of the energy, is a result of a considerable surge in the world population, starting since the beginning of the industrial revolution in the late 18th century until the present. One of the direct consequence of this rapid growth was the overuse of fossil fuels as the world's main energy source resulting in a rapid depletion of them and thereby increasing the level of $CO_2$ equivalent emissions at an atmospheric level known as greenhouse gasses. Increasing the concentration of these gasses at atmospheric level, exceeding the 400 PPM level for the first time in history, puts the earth at the point of no return. In order to sustain the economic growth while reducing the greenhouse gas concentration at an atmospheric level at the current stage, providing a clean sustainable solution which allows for a steady flow of energy is one of the most vital challenges facing the politician and energy planners. One of the solutions proposed by the energy planners which touches the higher level of energy management is to promote the usage of District Heating Systems (DHS).

While designing an efficient DHS is highly dependant on accurate modeling of the thermal performance of the buildings, district users; yet, limited simulation tools capable of modeling the district energy systems, at a larger scale with a numerous user's types and with an appropriated

level of precision which can potentially be a very laborious and time-consuming process, have been developed. Besides many associated limitations, providing a realistic demand profile of the district energy systems is not a straightforward task due to a high number of parameters involved in predicting a detailed demand profile. To this end, this dissertation focuses on the development of the procedure for energy modeling and optimization of the Hybrid Community District Heating System (H-CDHS) with integrated centralized thermal storage, the 4$^{th}$ generation of district heating systems.

To do so, this study describes the procedure used to develop two types of simplified models to predict the thermal load of a variety of buildings (residential, office, attached, detached, etc.). The predictions were also compared with those made by the detailed simulation models. The simplified model was then utilized to predict the energy demand of a variety of district types (residential, commercial or mix), and its prediction accuracy was compared with those made by detailed model: A good agreement was observed between the results. In next step, the proposed procedure was utilized to predict the heating demand profile of an existing community, WWH community in Glasgow. High prediction accuracy and low computational time of the proposed method illustrates the potential of the proposed method in predicting the heating demand profile of larger scale communities.

In the last step, the proposed load prediction method was coupled with energy simulation tool (TRNSYS) and optimization tool (MATLAB/Simulink) in order to develop a simplified methodology for dynamic optimization of a hybrid community-district heating system (H-CDHS) integrated with a thermal energy storage system. Two existing and newly built community have been defined and the results of the optimization on the equipment size of both communities have been studied. The results for the newly build community is then compared with the one obtained

from the conventional equipment sizing methods as well as static optimization methods to obtain potential reduction in equipment size using the proposed method.

# Acknowledgment

First and foremost, I would like to express my deepest gratitude to my supervisor, Dr. Fariborz Haghighat, for his continuous motivation, inspiration and support throughout my study. I am grateful for the invaluable advice, both professional and personal, which he gave me over these years. I also want to thank my co-supervisor, Dr. Parham Mirzaei, for his advice and support throughout my study. His guidance was invaluable and greatly contributed to my success in my research.

Also, I would like to gratefully acknowledge other members of my dissertation committee: Dr. Radu Zmeureanu, Dr. Ali Dolatabadi, Dr. Leon Wang and Dr. Gilles Fraisse for their knowledgeable advice.

I would like to thank all my friends and collogues in our research group, Energy and Environment, and Annex 31. I appreciate their help, stimulating exchange of idea, and most importantly, their friendship.

Last but not least, I wish to express my warmest appreciation and love to my wonderful parents, Behrooz and Zakieh, my trustworthy brothers and friends, Babak and Roozbeh, for their continuous inspiration and support. I am indebted to their unconditional love and encouragement.

*This thesis dedicated to my lovely family.*

# Contributions of Author:

## Journal Papers

| A Review of District Heating Systems: Modeling and Optimization | |
|---|---|
| Authors | Behrang Talebi, Parham A. Mirzaei; Arash Bastani; Fariborz Haghighat |
| Date | 04 October 2016 |
| Abstract | The ever-increasing demand for heating in different sectors, along with more preventative regulations on greenhouse emissions, has forced different countries to seek new alter-natives to heat buildings such as district heating system (DHS). Although rudiments of DHSs can be observed over the centuries, it was not widely implemented until last two decades when the DHS became a strategy to design more energy-efficient way of heating the buildings. This paper suggests a new approach in categorizing DHSs based on their geographical location, scale, heat density, and end-user demand. Furthermore, this paper reviews system and component modeling approaches with a focus on DHS load prediction. Main limitations of the existing methods are also addressed and discussed with a comprehensive review of the recent studies. Finally, the state of the art in optimization of the different DHSs has been reviewed and categorized based on their objective functions and the techniques used for solving optimization problems (deterministic and heuristic). |
| Chapters | Chapter 2 |
| Journal | Frontiers in Built Environment; https://doi.org/10.3389/fbuil.2016.00022 |

| Simplified Model to Predict the Thermal Demand Profile of Districts | |
|---|---|
| Authors | Behrang Talebi, Parham A. Mirzaei; Fariborz Haghighat |
| Date | 07 April 2017 |
| Abstract | Extensive research works have been carried out over the past few decades in the development of simulation tools to predict the thermal performance of buildings. These validated tools have been used in the design of the building and its components. However, limited simulation tools have been developed for modeling of district energy systems, which can potentially be a very laborious and time-consuming process. Besides many associated limitations, providing a realistic demand profile of the district energy systems is not a straightforward task due to high number of parameters involved in predicting a detail demand profile. This |

| | |
|---|---|
| | paper reports the development of a simplified model for predicting the thermal demand profile of a district heating system. The paper describes the method used to develop two types of simplified models to predict the thermal load of a variety of buildings (residential, office, attached, detached, etc.).The predictions were also compared with those made by the detailed simulation models. The simplified model was then utilized to predict the energy demand of a variety of districts types (residential, commercial or mix), and its prediction accuracy was compared with those made by detailed model: good agreement was observed between the results. |
| Chapters | Chapter 2,3,4 |
| Journal | Energy and Buildings; https://doi.org/10.1016/j.enbuild.2017.03.062 |

## Validation of a Community District Energy System Model Using Field Measured Data

| | |
|---|---|
| Authors | Behrang Talebi; Fariborz Haghighat; Paul Touhy; Parham A. Mirzaei |
| Date | 13 December 2017 |
| Abstract | Load prediction is the first step in designing an efficient community district heating system (CDHS). Even though several methods have been developed to predict the heating demand profile of buildings, there is a lack of method that can predict this profile for a large-scale community with a numerous user types in a timely manner and with an appropriate level of precision. This paper, first briefly describes the 4-step procedure developed earlier, utilizing a Multiple Non-Linear Regression (MNLR) method, for predicting the heating demand profile of district, followed by description of the community structure, and its district system. It also reports the field measurement procedure for collecting the data required and the preliminary analysis data. Results obtained from a continuous monitoring of the CDHS over a two-year period is employed to validate the accuracy of the developed model in the predicting the CDHS's heating load profile. Finally, using the 4-step procedure, the district's energy demand profile is predicted, and compared with both the measured data and the initial prediction. The outcome shows a less than 11.2% in the mean square root error (MSRE) of the predicted and measured load profiles. |
| Chapters | Chapter 3,4 |
| Journal | Energy; https://doi.org/10.1016/j.energy.2017.12.054 |

## Optimization of a Hybrid Community District Heating System integrated with Thermal Energy Storage system

| | |
|---|---|
| Authors | Behrang Talebi; Fariborz Haghighat; Paul Touhy; Parham A. Mirzaei |

| | |
|---|---|
| Date | Submitted (Under Review) |
| Abstract | Evidence from a variety of research suggests that buildings hold a critical role in climate change by significantly contributing to the global energy consumption and the production of greenhouse gases emissions. Considering the trend of higher energy consumption in building sector, it is important to influence this sector toward decreasing its energy demand. District generation and cogeneration systems integrated with the energy storage system have been suggested as a potential solution to achieve such planned goals.<br><br>Unlike older generation of the DHS, where the main focus of the design was on minimizing the system heat loss, in 4th generation DHS the higher system efficiency is achievable through picking the optimal equipment size as well as adopting the right control strategy. Different design methods have been adopted by designers for selecting the equipment size but finding the optimal size is a challenge most designer facing.<br><br>This paper reports the development of a simplified methodology for dynamic optimizing a hybrid community-district heating system (H-CDHS) integrated with a thermal energy storage system by coupling the simulation and optimization tools together. Two existing and newly built community have been defined and the results of the optimization on the equipment size of both community have been studied. The results for newly build community later on compared with the one obtained from the conventional equipment size methods whereas static optimization methods and potential size reduction with conventional method has been obtained. |
| Chapters | Chapter 2,5 |
| Journal | Submitted (Under Review) |

# Conference Papers:

## A Procedure to Predict the Energy Demand Profile of District System

| | |
|---|---|
| Authors | Behrang Talebi; Fariborz Haghighat |
| Date | May 2016 / Aalborg Denmark |
| Abstract | The ever-increasing demands for heating in different sectors, along with more preventative regulations on greenhouse emissions, have compelled designers to seek new alternatives to design energy-efficient buildings. One of these alternative approaches is the Community-District System (CDS). Different methods have been proposed for improving the energy efficiency of CDSs. One of these methods focusses on decreasing peak demand load and regulating energy consumption via energy management. In order to implement this approach it is essential to predict the detailed energy consumption profile of the CDS. Several methods have been developed to model the demand profiles of CDSs. In a small-scale systems, due to the small number of users, the energy demand profile will be predicted by the detailed-modeling of the users using different energy simulation software whereas in large district scale system, due to large volume of users, a comprehensive modeling of the users is time consuming and can be unfeasible. To overcome this problem, a variety of simplified models have been developed and utilized by designers. One of the main drawbacks of the existing simplified models is that they mostly determine the total energy consumption of the users as opposed to the detailed annual profile of the energy consumption. This paper describes the development of procedure to predict the energy consumption profiles of the large-scale CDS. This model have been validated by comparing the model prediction with the results obtained from simulation of the community scale CDS using comprehensive model |
| Chapters | Chapter 2,3 |
| Publisher | CLIMA 2016 - proceedings of the 12th REHVA World Congress |

## Developing a Simplified Model to Predict the Heating Energy Demand Profile of a District

| | |
|---|---|
| Authors | Behrang Talebi; Fariborz Haghighat |
| Date | October 2016 / Republic of Korea |
| Abstract | The ever-increasing demands for heating in different sectors, along with more preventative regulations on greenhouse emissions, have compelled designers to seek new alternatives to design energy-efficient buildings. One of these alternative approaches is the Community-District System (CDS). Different methods have been |

| | |
|---|---|
| | proposed for improving the energy efficiency of CDSs. One of these methods focusses on decreasing peak demand load and regulating energy consumption via energy management. In order to implement this approach it is essential to predict the detailed energy consumption profile of the CDS.<br><br>Several methods have been developed to model the demand profiles of CDSs. In a small-scale systems, due to the small number of users, the energy demand profile will be predicted by the detailed-modeling of the users using different energy simulation software whereas in large district scale system, due to large volume of users, a comprehensive modeling of the users is time consuming and can be unfeasible. To overcome this problem, a variety of simplified models have been developed and utilized by designers. One of the main drawbacks of the existing simplified models is that they mostly determine the total energy consumption of the users as opposed to the detailed annual profile of the energy consumption. This paper describes the development of procedure to predict the energy consumption profiles of the large-scale CDS. This model have been validated by comparing the model prediction with the results obtained from simulation of the community scale CDS using comprehensive model. |
| Chapters | Chapter 2,3 |
| Publisher | IAQVEC 2016, 9th International Conference on Indoor Air Quality Ventilation & Energy Conservation In Buildings |

## Optimization of the Thermal Energy Storage of a Hybrid District Heating System

| | |
|---|---|
| Authors | Behrang Talebi; Fariborz Haghighat; Parham A. Mirzaei |
| Date | April 2018 / Adana Turkey |
| Abstract | Having the demand profile of the H-CDHS, using a simplified procedure, a TRNSYS model has been utilized to develop a work frame for dynamic optimization of the thermal storage of a CDHS. Different scenarios for energy behavior of the community have been assumed and the corresponding demand profile predicted based on the simplified model coupled with the TRNSYS file. The TRNSYS framework, developed based on two different configurations of the thermal storage within the community. The model has been optimized to determine the optimal size of the thermal storage considering both CO2 emission and operational cost of the building. |
| Chapters | Chapter 2,5 |
| Publisher | EnerSTOCK2018; 14TH INTERNATIONAL CONFERENCE ON ENERGY STORAGE |

# Table of Contents

## List of Figures:

## List of Tables:

# Chapter 1: Introduction

## 1.1.Background

Since the beginning of the industrial revolution in the late 18th century until the present, the world population increased from roughly 700 million to more than 7 billion people. Based on world energy outlook developed by the International Energy Agency [1], with the same growth pattern, the world's population will be projected to exceed 9.7 billion by the end of 2050. Along with this considerable surge in the world population, the number of households is expected to elevate to 3.2 billion in 2050, which represent a 70% increase of worldwide households since 2010 [2].

Providing a secure and clean source of energy to respond the households' demand is one of the upmost fundamental challenges faced by the energy planners. In effect, households represent a significant share of the total energy demand while they are responsible for 40% and 26% of the total energy consumptions as well as 38% and 36% of the total $CO_2$ emission in North America and Europe, respectively [1]. In the last few decades, the overuse of the fossil fuels as the world's main energy source has resulted in their rapid depletion and thereby increasing the level of $CO_2$ equivalent emissions. Based on the atmospheric measurements done by NASA [3], over the last few decades, for the first time, there was an unprecedented level of the atmospheric $CO_2$ equivalent level at atmosphere passed the 300 ppm, in 1950. Since that time this level increased rapidly, which exceed 400 ppm in latest measurements. Such evidences indicate that the Global warming is at the point of no return. In other words, for the first time in past 650,000 years, the earth will not be able

to recover from a glacial cycle. This fact becomes more important, knowing the fact that earth went through 7 glacial cycles, but it always recovered [3].

Unequivocally, the above-mentioned statistics, emphasize the necessity of a global objective to reduce the $CO_2$ emission and to increase efforts and market uptake from the building sector as a major energy consumer. Given the expected rise in household energy consumption, the building sector is now required to adapt itself to the new ambitious demand of developing Net-Zero Energy Buildings/communities (NZEB) by 2050, which is described as an Energy Technology Perspective 2017 Roadmap (IEA) goal, aiming to reduce $CO_2$ emissions by 50% by 2050. In order to reach this goal[1], different rigorous preventative codes and regulations at regional and continental levels have been adopted by many countries, forcing their building sectors to seek new alternatives to the conventional systems mainly focused at enhancing the energy conservation with a higher level of energy management.

For instance, the European Union is obliged to commit a 9% reduction in energy use by 2016 based on the 2006/32/EC directives [4]. Also in 20-20-20 as the climate change package legislation [5], the mandate of all European countries is to decrease the greenhouse gas emissions as well as primary energy consumption by 20%. European countries must also increase the share of renewable energy sources to 20% by 2020. Based on the energy supply and demand projection of Canada, the non-hydro renewable energy share should be doubled by 2035 [6]. Paris climate change accord, COP21 [7], as the most recent regulation on $CO_2$ emission production, also mandates involved countries to limit the total $CO_2$ emission to 40 billion tonnes emitted per year in order to limit the global warming to 1.5°C.

[1] Energy Technology Perspective 2012 Roadmap (IEA)

As a result, different energy conservation strategies have been applied at various levels, including energy production, conversion, and user-demand, but the most promising solutions touch a higher level known as energy management.

One of the suggested strategies focusing on the energy management at a higher level is using District Heating System (DHS). Hybrid Community-District Heating System (H-CDHS), **Figure *1-1***, as sustainable forms of heating systems designed to distribute safe, clean, and sustainable energy within the network of users at a higher efficiency and a lower $CO_2$ production level. Although limited evidence of using DHS could be addressed over the span of several centuries, it was not until last two decades that it has become an established method to design green and energy efficient heating for buildings. Within different types and generations of DHS, H-CDHS, or the fourth generation DHS, is a unique alternative for energy management purposes as it also integrates thermal storage systems and renewable sources.

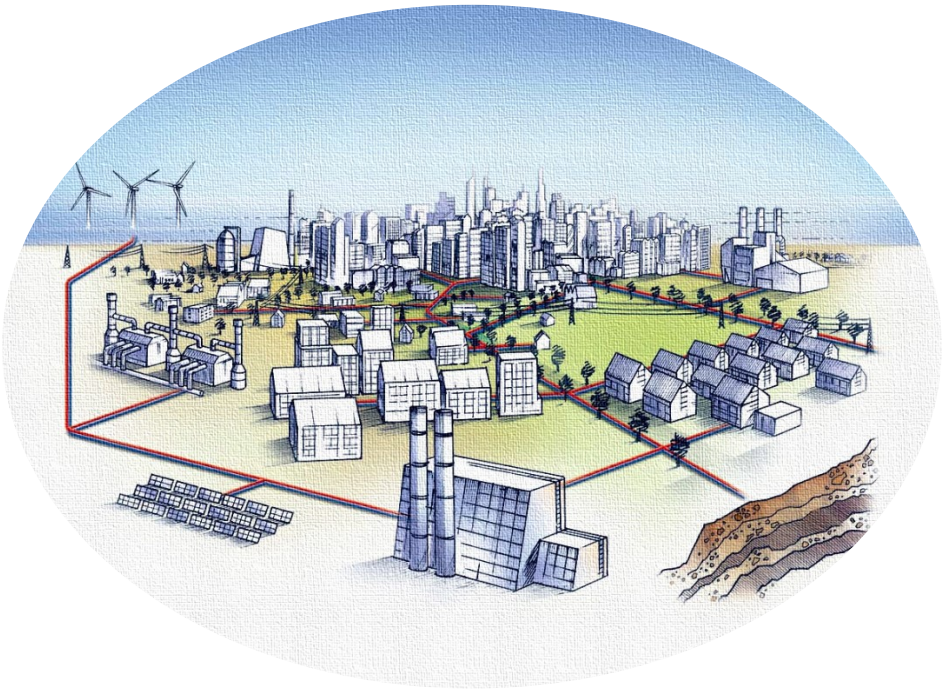

**Figure 1-1: Schematic View of H-CDHS; [*https://www.ecopolis.danfoss.com*]**

Since the energy generated by renewable sources such as solar and wind are inherently intermittent in order to solve the problem of the mismatching between supply and demand sides, a thermal storage system has been proposed to be integrated into H-CDHSs. To implement such idea effectively, it is essential to predict the energy demand of H-CDHSs at smaller intervals such as hourly bases.

This led to the development of several methods to model buildings' energy demand profile. Given its restricted number of users, a small-scale H-CDHS energy demand profile can be predicted using a detailed model of users' consumption created with energy simulation models.

Conversely, in large district scale systems, due to the large volume of users, a comprehensive modeling is time-consuming, computationally expensive and sometimes impractical. To overcome this problem, a variety of simplified models were developed to predict the energy demand profile or the total energy demand of large communities. Though these simplified models could reduce the computational time to a fraction of that of comprehensive models, their simplicity would compromise the prediction accuracy as a consequence of using the simplified models. In general, three major drawbacks can be addressed for most of these simplified modes. First, the low prediction accuracy emerging from assumptions made in modeling of individual buildings/units, i.e. presentation of the occupants' behavior and, the interaction of each building with its surrounding buildings in an urban setting. Second, scaling effects impair accuracy by oversimplifying scaling methods that extrapolate results from building level to the district level. And third, flexible methods that predict community load profile containing diverse building types. A closer analysis of existing models reveals that the current research requires further validation of models that predict heating demands using measured data.

Having the detail of users' heating energy demand profile, dynamic optimization of a district, to obtain the optimal size equipment and control strategy, is a challenge that designers facing. Most existing districts have been sized based on the conventional sizing methods such as design date method. These methods pick the equipment size by matching the maximum generation, supply, with pick demand load one to one multiplied by the safety factor without considering the interaction between different equipment. Using the safety factors along neglecting the interaction between equipment results in oversizing of the energy generation equipment while this further results in operation of the equipment at their partial load, which is not favorable due to a lower operation efficiency.

## 1.2. Objectives

To this end, three main objectives have been defined for this thesis:

1. Development and validation of a simplified procedure to accurately predict the detail heating energy demand profile of the mid to large size community in a timely manner
    a. Development of a simplified procedure for accurately predicting the heating energy demand profile of the mid to large size community in a timely manner
    b. Validation of the developed procedure using a set of measured data obtained from a midsize community
2. Developing a dynamic optimization framework by coupling the developed prediction tool, one of the exisitng simulation software (TRNSYS) and an optimization tool (MATLAB/Simulink) to determine the optimal equipment size and operational schedule with a target in minimizing the cost and $CO_2$ emission of the whole system

# Chapter 2: Literature Review

A District Heating System, hereinafter referred to as "DHS", is a heat generation/distribution system consists of a network of users, hereinafter referred to as "Users", connected together through a set of insulated pipes hereinafter referred to as "Network" in order to provide the heating energy demand required by users, hereinafter referred to as "Heating Energy Demand Profile" or "HEDP". The heat generation in a DHS could be in form of a centralized heat generation station form or a set of smaller substations. The distributed energy could be used for a variety of applications such as Space Heating, "SH", or Domestic Hot Water, "DHW".

Different classifications of DHSs have been suggested, which the one has been introduced by Lund et al. [8] is the most well-known and well-recognized classification. Lund et al. classified existing DHSs into four categories based on the heat transfer media type, its operating temperature and the type of technologies have been used in them.

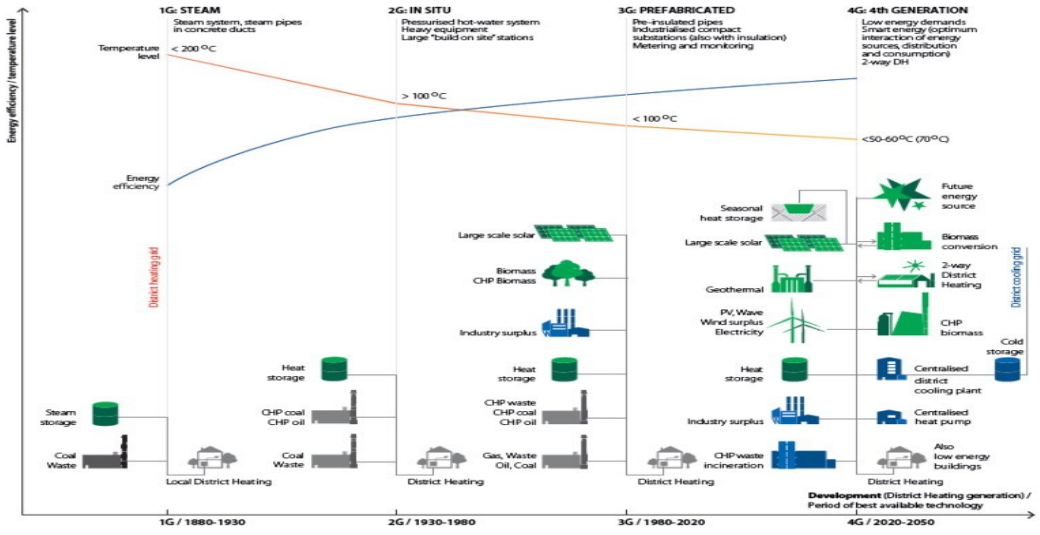


**Figure 2-1: District Heating System Generations [8]**

However, an essential step toward designing an efficient DHS, regardless of its generation type, is detailed predictions of the demand user profile of the users of that district.

## 2.1. DHS Energy Prediction

Modeling the HEDP of a series of buildings at a district level is a complex task and requires a high level of expertise. The demand profile of each individual building is varying as a function of a time, this variation has a stochastic behavior in comparison with a deterministic behavior model, which is resulting in increase of the complexity level of the model. In case of large-scale district systems, with more varying occupants' behavior, this complexity level further increase as the building heterogeneity in district system is elevated, particularly in the urban setting where each building has its own properties and corresponding HEDP.

Generally, the energy required by a DHS at each time-step is equal to the summation of the energy required by individual users of that DHS in addition to the heat loss from the network. Since most DHS operates within a specific temperature range, the heat loss from the network could be considered as a function of the network size and not a function of time. As a result, the total energy consumption of a DHS could be presented as:

$$Q_{Total} = Q_{loss} + \sum_{n=1} \int_1^t Q_i\,(t).\,dt \qquad \textbf{Equ. 2-1}$$

where $Q_{Total}$ is the total energy consumption of the DHS, $Q_i(t)$ is the energy consumption of the individual users at the time ***t*** and $Q_{loss}$ is the heat loss from the distribution network. To predict the total energy required by a DHS, both heat loss of the network as well as HEDP of the individual users of the DHS should be separately predicted.

### 2.1.1. Energy Prediction for Distribution Network

A DHS distribution network is mainly designed in accordance with the system scale, geographical considerations, type of the users and utilized heat generations sources. Beside the role of the distribution network in linking the energy generation source with the users' demand and defining the inter-communication between different components of the system, it also effects on the whole energy consumption of the system. Since most distribution networks operate within a specific temperature range, the heat loss from the system could be again considered as a function of the size of that network and not a function of time. The total energy requirement of the system is equal to the summation of different users' profiles in addition to the heat loss per network length. Since a DHS is a type of hydronic system, the modeling technique to design the distribution system can be either based on hydraulic or thermal equilibrium.

#### 2.1.1.1. Hydraulic Equilibrium

The distribution system in the DHS operates based on the heat transfer through a heated fluid; therefore, it should be designed based on the requirements of the hydraulic system regardless of the flow rate and energy level of the fluid.

***Mass flow balance:***

The mass flow balance could be written for each point of the system as [9], [10]:

$$\sum_{in} Q_{in} - \sum_{out} Q_{out} - \sum_{user} Q_{user} = 0 \qquad \text{Equ. 2-2}$$

where $Q_{in}$ is the mass flow rate entering the point, $Q_{out}$ is the mass flow rate exiting the point, and $Q_{user}$ is the mass flow rate required by the utility. Depending on the type of the system (e.g. open or closed loop), $Q_{user}$ could be considered as zero. It is important to note that the system and network are assumed to be leak free without any loss of the fluid mass.

***Energy balance***

In the energy balance techniques, the energy balance could be written between any two points in the system as [11]:

$$\Delta H_{i,j} - (H_i - H_j) = 0 \qquad \text{Equ. 2-3}$$

where $\Delta H_{ij}$ represents the energy loss between points $i$ and $j$; $H_i$ and $H_j$ are the energy content of the fluid at points $i$ and $j$, respectively. Considering the DHS as a closed system and without any loss in the liquid mass, the energy loss in the system could be written as a correlation of the pressure loss in the system represented in two different ways:

$$\Delta H = f.{}^{L}/_{D}.\rho.{}^{V^2}/_{2} \qquad \text{Equ. 2-4}$$

$$\Delta H = \beta.\rho.{}^{V^2}/_{2} \qquad \text{Equ. 2-5}$$

where f is the pipe friction coefficient, $\beta$ is the resistance coefficient, L is the length of the pipe, D is the pipe diameter, $\rho$ is the density of the fluid and V is the flow velocity. In the distribution pressure drop, the friction loss due to the viscous effect, generated by the pipe surface, is the key parameter. The hydraulic diameter of the pipe, the mass flow rate of the system, and roughness of the pipe surface are the parameters affecting the distribution pressure loss of the system [10]. Additionally, in a concentrated pressure loss, the head loss due to fittings and changes in the pipe diameter is taken into the account [11].

### 2.1.1.2. Thermal Equilibrium

Thermal equilibrium can be represented as either a steady-state or dynamic equation. A DHS with an operational temperature lower than 70 °C or with a low heat propagation (well

insulated) can be represented as a steady state system. Inversely, a DHS operating with temperatures higher than 110 °C or with a high heat propagation can be considered as a dynamic system [12], [13]. The thermal model could be then written based on two major sources of the temperature drop in the system, including temperature drop across the users and due to the heat loss in the system. The temperature drop across the users can be modeled based on a simple convection heat transfer equation [14],[15]:

$$Q = U.\Delta T \quad \text{Equ. 2-6}$$

where $Q$ is the amount of the energy required by the system, $U$ is the heat transfer coefficient and $\Delta T$ is the temperature drop across the users.

On the other side, the temperature drop due to heat loss in the system occurs in both longitudinal and radial directions. The longitudinal heat loss is along the system between different locations, whereas the radial heat loss occurs in the surrounding environment. Both types of the heat transfer in the system could simply be modeled by an enthalpy balance developed between any two points [16], [17]:

$$\frac{\partial(mh)}{\partial(t)} = \sum_{in} h_{in} - \sum_{out} h_{out} - \sum_{loss} h_{loss} \quad \text{Equ. 2-7}$$

$$\frac{\partial(mh)}{\partial(t)} = \dot{Q}_c(x) - \dot{Q}_c(x+dx) - d\dot{Q}_1 \quad \text{Equ. 2-8}$$

where $\dot{Q}_c(x)$ is the convective heat flow and $d\dot{Q}_1$ is the radial heat flow expressed as:

$$d\dot{Q}_1 = k.dx.(T - T_{earth}) \quad \text{Equ. 2-9}$$

$$\dot{Q}_c(x) = q_{mx}.T_x.C_p \quad \text{Equ. 2-10}$$

where $k$ is the radial heat transmission coefficient and $q_{mx}$ is the flow rate. By replacing the $d\dot{Q}_1$ and $\dot{Q}_c(x)$ in the ***Equ. 2-8***, the temperature at any point can be calculated as (see ***Figure 2-2***):

$$T_i^{n+1} = T_i^n + {}^{\Delta T}/_{m_i.C_p}\left(q_{m_{i-1}}.C_p.T_{i-1}^n - q_{m_i}.C_p.T_i^n - d\dot{Q}_1\right) \qquad \text{Equ. 2-11}$$

where $C_p$ is the fluid heat capacity, $T^n$ is the temperature, $\Delta t$ is the time step, and $m_i$ is the water mass.

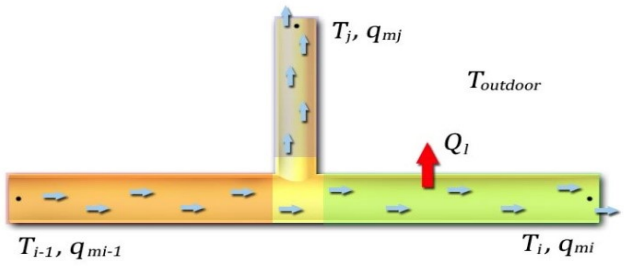


**Figure 2-2: Heat flow in the piping system**

Based on the definition of $d\dot{Q}_1$, one of the main factors, influencing the amount of heat loss, is the soil temperature. In systems with high operating temperature, the higher differences in temperature could result in higher amounts of heat loss in the system. Similarly, the increased heat losses in a system could result in an increase in surrounding temperatures over a period of time, which itself can consequently decrease the associated heat loss.

#### 2.1.1.3. Holistic Modeling

Deterministic and black box models are the approaches conducted in the holistic modeling of the DHS [18]. The network has been considered as a whole package in the black box models where the individual design of the components is disregarded. The entire system is then modeled by techniques such as the transfer function or Artificial Neural Network (ANN) [19]. On the other

hand, in deterministic models, each component of the DHS has been designed separately with a set of equations describing the flow and pressure losses of each element. For instance, [20] categorized DHS with the link flow ($Q$), the loop corrective flow ($\Delta Q$), the nodal heads ($H$) and finally the mixed node-loop.

Due to the high number of the elements, obtaining a solution from such a system can be computationally expensive. Therefore, numerical approaches have been widely used as categorized as below [20]:

- **Numerical minimization method:** finding the minimum value of a nonlinear function subjected to linear constraints.
- **Hardy-Cross method:** solving a system of nonlinear equations [21].
- **Newton-Raphson method:** solving a system of nonlinear equations [22].
- **Linear theory method:** solving a system of nonlinear equations [23].

Based on the simplicity of the input data, the number of equations and size of the matrix of the equations [17], [24] as well as the accuracy of the results, the most frequently used method is a combination of Newton-Raphson and nodal head methods [17], [20]. Furthermore, due to the weak convergence of the nodal equation algorithm for networks with a low flow rate, the loop equation method has been suggested, which is a combination of the loop corrective and Newton-Raphson methods [20].

Further to the above-mentioned studies, several commercial software has been developed based on the loop equation method using the graph theory such as TERMIS and SpHeat. ***Table 2-1*** summarizes different modeling level in respect with district scale.

**Table 2-1: Summary of the Network Modeling for DHS**

| Modeling Different Components of the DHS | | | | | | | | | | |
|---|---|---|---|---|---|---|---|---|---|---|
| No. | Description | Country Climate | Modeling level | | | Scale | Energy source | Utilized tool | Validation | Ref. |
| | | | Source | Building | System | | | | | |
| 1 | 34 Users | Italy | | GD | P | M | CHP | ODS | TERMIS | [11] |
| 2 | Combined sources | | SM | | | M | Combined | UC | | [25] |
| 3 | Multi-unit apartment building | | | GD | P | S | CHP | UC | | [14] |
| 4 | 8 units, different supply temperature | Geneva | SM | GD | | M | CHP | UC | | [26] |
| 5 | 7 users with $L_p$ > 13.5 km | Germany | | GD | P/T | L | Biomass | ODS | | [27] |
| 6 | Compares HT and LT supply | Ottawa | | LF | P/T | L | CHP | Logster | TERMIS | [28] |
| 7 | Effect of human behavior | Denmark | | LF | P | M | HP | IDA-ICE | TERMIS | [29] |
| 8 | Thermal storage | Stuttgart | | GD | P/T | L | CHP/Biomass | | spHeat | [9] |
| 9 | Solar district heating | | SM | GD | | M | Solar/CHP | UC | | [30] |
| 10 | Solar thermal heating network | Sonnenberg | SM | Software | P/T | M | Geothermal/Solar | | spHeat | [31] |
| 11 | CHP with thermal storage for 100 units | Flanders | SM | Measurement | P | M | CHP | UC | | [32] |
| 12 | Biomass-fired CHP with storage | Leini/Turin | SM | Measurement | | L | CHP/Biomass | UC | | [33] |
| 13 | For 50% heating load calculation | Zaragoza | SM | TRNSYS | | L | Solar | UC | | [34] |
| 14 | Source optimization | Estonia | SM | | | L | CHP | UC | | [35] |
| 15 | Different flow control strategy | | | GD | P/T | M | CHP/HP | UC | | [16] |
| 16 | Different control strategy | Wales | | HDD | TPL | M | CGP | PSS SINCAL | | [36] |
| 17 | City level | Yazd | SM | GD | | L | Combined | EMD | | [37] |
| 18 | Neighborhood | Turin | | HDD | | | | | | [38] |

**Keys:** SM: source modeling, GD: given data, LF: load factor, HDD: heating degree day, P: pressure model, T: thermal model, ODS: own developed software, UC: user code, L: large, M: medium.

### 2.1.2. HEDP Prediction of the Users

Accurate prediction of the HEDP of the users in a smaller time interval such as the hourly basis can affect the efficiency of a DHS and its optimization procedure [39]. In order to define the size of the heating equipment, predicting the heating demand profiles of users is essential.

#### 2.1.2.1. HEDP Prediction at a Building Level

Regardless of the method used, the energy consumption of each individual building is a function of physical and environmental characteristics of a building (i.e. R-value, infiltration rate, ambient air temperature, solar radiation, and humidity), human-related factors or social behavior of the occupants, and random factors that account for uncertainties.

$$Q_{total}(t) = \sum(\dot{q}_{buiding\ assemblies}(t) + \dot{q}_{Solar\ gain}(t) + \dot{q}_{internal\ gain}(t) + \dot{q}_{inf.,vent}(t)) \quad \text{Equ. 2-12}$$

Different techniques have been suggested in the literature to predict the users demand profile considering one or all of the above factors, including:

- Historical methods.
- Deterministic or simulation-based methods.
- Time series predictive methods.

Historical methods use historical data obtained from both demand and supply sides to model the demand profile. Energy Use Intensity (EUI) and Load Factor (LF) are historical methods utilized to estimate the users demand profile whereby the historical consumption data is provided. EUI is the rate of energy use per unit area [40] and LF is the ratio of energy consumption over the maximum possible energy generation from the supply side [29] and [28]:

$$LF = {Consumption\ [kWh]}/{Peak\ Demand\ [kW] \times Time\ [hr]} \quad \text{Equ. 2-13}$$

Knowing the EUI and LF of different users[2,3] results in the calculation of the total energy and peak heating demand required for each user. The supply energy demand calculates the annual average LF per area for different users. Mainly, the values are accessible based on region or reference archetype [*Footnote 2&3*]. Barnaby et al. [41] used this method for load prediction of different users. One of the main problems with this method is associated with the nonexistence of separated factors allocated to ambient conditions. For instance, even though the social behavior[4] of the users, does not fluctuate dramatically over time, the method does not allow for long-term generalizations.

Another common approach in predicting the demand profile of the buildings is to use deterministic methods. Deterministic methods, also referred to as simulation-based modeling, use the mathematical representation of the thermal behavior of the buildings. Based on the amount of information used in these methods, deterministic methods could be categorized under two major subdivisions: 1) comprehensive or software-based simulation modeling, which uses different simulation software, taking into account all the different parameters affecting the demand profile of a building and 2) simplified modeling, which approximate the energy consumption by taking into account only few parameters.

Different commercial energy simulation software, such as TRNSYS [42], eQUEST, Energy-Plus [43] and etc., are developed for modeling any arbitrary type of buildings. Although they yield highly accurate demand profiles, the main disadvantages of these models are their

---

[2] Commercial and institutional consumption of energy survey summary. Available at: http://oee.rncan.gc.ca/publications/statistics/scieu09/scieu_e.pdf

[3] Energy Use Data Handbook. (1990-2011). Available at: http://publications.gc.ca/collections/collection_2014/rncan-nrcan/M141-11-2011-eng.pdf

[4] Social behavior is the effects of the social status of the occupants on their energy behavior. For instance lower income family due to their lower budget tends to be more conservative in consuming energy.

requirements in terms of data quantity and time for modeling of each building [34], [44], [45]. Thus, simplified deterministic methods have emerged as another effective solution. Simplified methods are used when the adaption of the comprehensive method is relatively extensive due to lack of detail data or high computational time. These methods simplify physical characteristics of the buildings to predict their demand profile. For example, Kim et al. [46] considered the parameters including shape, orientation, and occupancy type in the modeling of the end-users' profile. They used the average energy required per square meter of a dwelling area of a building based on its monthly/yearly outdoor design temperature. In order to take into account the shape and orientation of the building, new sets of coefficients were introduced: (1) the ratio of the outdoor surface to volume of the building (the shape factor) and (2) the orientation relative to the south (orientation factor) [45]. Wang et al. [47] used a simplified deterministic method to predict the demand profile within which they also included the effect of thermal mass on load prediction by means of a genetic algorithm. Results obtained from their simulations illustrate a good correlation with actual data for a residential building, which has a lower internal heat gain density. Inversely, this method is unsuitable for larger buildings with higher internal heat gain density.

Another simplified method used for modeling the demand profile of buildings is the degree-day method widely used for modeling of small buildings in which the main source of energy is lost through their envelope. Al-Homoud [48] compares this method with another simplified method known as the bin method. Unlike the degree day method, the bin method is mainly used for larger scale buildings in which the internal load generation has a higher effect, which would render the degree day method unfeasible. In both cases, the main concern in modeling is the outdoor air condition of the buildings and the average building envelope thermal resistance. The fact that factors such as the occupants behavior and the thermal mass of the buildings have

not been taken into account result in predominantly poor findings [39]. Furthermore, the low frequency of available data adds to obtaining inaccurate results. In the degree-day method, the indoor and outdoor temperature differences on the daily, weekly and yearly bases were measured and, as a result, the profile does not reflect the distribution of heat requirement for smaller intervals such an hourly demand profile. In order to consider the effect of the occupants on the demand profile in residential buildings, Yao et al. [49] developed a model to predict the load profile of domestic buildings in the UK. In their model, they consider both "Behavioral Deterministic Factors", which are not/little related to climate and "Physical Determinist Factors", which are highly related to climate conditions and the building design. In their method, Yao et al. divided the demand profile of each building into five different segments and added them up together in order to define the entire profile of the building. According to their method, the heating profile of the building could be estimated as:

$$C\frac{dT}{dt} = \varphi_{aux} + \varphi_{solar} + \varphi_{vent} + \varphi_{cond} + \varphi_{sp} \qquad \text{Equ. 2-14}$$

where C is the thermal capacity of the building, $\varphi_{aux}$ is the auxiliary heating cooling load of the building, $\varphi_{solar}$ is the solar gain of the building, $\varphi_{vent}$ is the ventilation load and finally the $\varphi_{sp}$ is the internal load due to occupants activity. The main contribution of Yao et al. [49] was in adding the component representing the internal load generation related to the occupants in residential buildings. In order to do so, they did an extensive statistical analysis on the data gathered from residential households in the UK for a period of 15 years. They presented the results in eight different possible load profile scenarios in which they considered the number of occupants, usage schedule and equipment load. In spite of all advantages of their model, the main limitation was associated to the simplicity of the model in consideration of a same daily profile for the internal gain throughout the

year. Furthermore, they only focused on the number of occupants and not on the effect(s) of the buildings' characteristics.

Time series predictive methods is another approach adopted for predicting the demand profile of buildings. Numerical predictive time series methods rely on the mathematical curve fitting relation(s) between the influential parameter selected as input file and the demand profile at previous time-steps. The predictive models themselves are categorized further to classical approaches (i.e. time series ARMA models, regressions [50], [51], [34], Kalman filter) and artificial intelligence (AI) methods (i.e. artificial neural network algorithms (ANN) [52] and fuzzy neural network (FNN) [53] and Support Vector Machine (SVM)).

In ARMA time-series, the prediction will be done by implementation of a linear combination between the previously predicted values along with previous and current values weather and the noise [53]. For the demand profile prediction, Gross et al. used the ARMA time-series method in a form of:

$$z(t) = Y_p(t) + Y(t) \qquad \text{Equ. 2-15}$$

where $Y_p(t)$ represents the day and the normal weather condition for the design day and Y(t) indicates the effect of deviation from the normal weather pattern. With slight difference from the general form, different kinds of ARMA-type models can be developed, e.g., Box-Jenkins [54], time-series [55], and ARIMA [56].

Another predictive method has been used for the energy prediction was Kalman Filter. Similar to other predictive methods, this technique estimates the value of the variables for future time-steps ($t+\Delta t$) based on the values of the variables at its current time step (t). In order to make the best estimation, Kalman filter determines the best variable set, which minimizes the source

function using the residual sequence method. In each step, the Kalman filter checks the difference between the measurements and the model output, and choose the variable set to minimize the difference. Since the deviation from the measurement can be positive or negative, two different sets of residual sequences could be assumed for the system such as residual for the hot side and residual for the cold side of the profile [57].

Regression-based methods are another type of predictive methods used for demand prediction, usually divided into two subcategories: multiple linear autoregressive models (MLR), and multiple non-linear autoregressive models (MNLR). While the main objective of the MLR is to find a linear relationship between the number of independent variables and one dependent variable (**Equ. 2-16**), the non-linear regression methods assumes a nonlinear behavior between the dependent variable and independent variables (**Equ. 2-17**).

$$Y = \alpha_0 + \alpha_1 X_1 + \alpha_2 X_2 + \cdots + \alpha_n X_n \qquad \textbf{Equ. 2-18}$$

$$Y = \alpha_0 + \alpha_1 X_i + \alpha_2 X_j + \alpha_3 X_k + \alpha_4 X_i^2 + \alpha_5 X_j^2 + \alpha_6 X_k^2 + \cdots + \alpha_p X_j X_j X^k \qquad \textbf{Equ. 2-19}$$

In some cases, the results of the dependent variable at the time t is highly influenced by the value of the independent variables at the time t as well as some previous time-steps. In these cases, such as a building with a higher thermal mass, the dependent variable was predicted based on the previously observed set of independent variables. Due to its usefulness for predicting the dependent variable, this method became a popular tool to forecast future results [58].

Using artificial intelligence predictive methods is another approach to predict the demand profile of the building. The most common artificial intelligence methods used in the field of load prediction are Artificial Neural Network [ANN], Fuzzy Neural Network [FNN], and Support Vector Machine [SVM]. The ANN has been widely used in research for predicting the load

particularly in forecasting the electricity consumption of buildings [59]. In most of the cases, ANN shows higher prediction performance compared to other simulation-based methods. This higher accuracy with the ANN method is usually due to its higher adaptability as it considers the social parameters in the load prediction due to the integration of a real case data into the system training [52], [59]. Despite the high accuracy of the predictive methods, their main drawbacks are the over-fitting problem as well as the data requirements for the training proposes. Providing accurate and comprehensive archives of data for ANN is one of the main drawbacks of this method. In cases where the data archive used for training of the system is small, using the SVM method(s) [60] shows a better performance. However, only a limited number of studies were conducted using SVM; hence, the information regarding the utilization of this model is limited.

#### 2.1.2.2. HEDP Prediction at a District Level

As mentioned earlier, building heterogeneity in each district system is different, particularly in the urban setting, and each building has its own properties and demand profile. Therefore, developing a model which could predict the demand profile of the entire district with acceptable accuracy is essential. Most of the existing models used for the demand prediction of DHSs have been developed based on the assumption of a standalone building, barely representing the complexity of an urban/district setting. Indeed, the first assumption in the modeling of a standalone building is that the entire building shell receives solar radiation and exchanges heat with the surrounding environment. Moreover, since the demand profile of a building varies as a function of time, this variation has a stochastic behavior (and not a deterministic behavior). As a result, the level of model complexity is increased [26], [61], [62], especially for large district systems with more varying occupant behaviors. In general, the methods suggested to model and predict the demand profile of DHSs (similar to ***Section 2.1.2.1*** for buildings), can be categorized

as (1) deterministic methods, (2) historical methods [39], [44], and (3) time-series predictive methods [63]. Nevertheless, regardless of the prediction methods used by designers to predict the heating demand profile of the districts, these methods could be divided into two general categories:

- Comprehensive modeling using more detailed information and specifications of the buildings such as commercial simulation software for modeling every individual user within a district.
- Simplified numerical methods adopting times-series predictive or historical methods to predict the district demand profile using some limited properties of individual users within the network.

***Comprehensive Methods:***

A common way to predict HEDP at a district level is to use the deterministic methods. Similar to building models, the deterministic methods are divided into two categories of (1) comprehensive modeles using commercial simulation software and (2) simplified deterministic methods. Over the past few decades, many simulation tools have been developed for predicting the energy demand profile of buildings such as Energy Plus, TRNSYS, eQUEST, etc. These simulation tools are broadly used for modeling various type of buildings. At the district level, although they yield highly accurate demand profiles, their main disadvantages are the dependency on data quantity and high computational cost for modeling of each individual building [34], [44].

For small-scale District Systems (DS) consisting of a limited number of buildings, using the comprehensive method can increase the accuracy of the system. However, for a large-scale DS, providing the required data for modeling of each building and the time required to model them is not realistically feasible. Despite this fact, Zhang [64] used the comprehensive method for

modeling the demand profile of 95,817 buildings in Westminster, UK. Another disadvantage of the comprehensive method is modeling the effect of the occupant's behavior on the final demand profile of buildings. Nevertheless, providing the data and time required for modeling several buildings at a city-wide scale district is very expensive. Since the application of the comprehensive method is relatively unfeasible for a large-scale community such as a city given the individualized and time-consuming modeling involved, simplified methods emerged as a popular option for the prediction of demand profile of district networks.

***Simplified Simulation Models:***

Deterministic methods have been widely used at the building level, while historical/times series methods are more favorable at the district level with more stochastic behaviors. This is due to their high level of dependency to data for training purposes, especially for large DSs with diverse building types [65]. These methods have mainly been adopted to predict buildings' total energy consumption and maximum demand rather than predicting the actual demand of the system in a smaller interval such as an hourly basis [66].

At the district level, to simplify the prediction process and increase the prediction accuracy, the community building stock is segmented into "building archetypes", i.e. a building which can represent a group of similar buildings. In this method, buildings with similar occupancy type are divided into subcategories while a reference building is defined for each building category. The demand profile of other buildings located within each category is later defined based on the reference building with some adjustment. The number of building categories used in this method as well as the number of adjustments required for modeling the entire demand profiles are the key parameters in the simplified method. The most commonly utilized technique is the regression method.

Usually, segmentation of the building stock is carried out based on the type of parameter picked. Although different sets of parameters can be used to generate building archetypes, generally, these parameters are divided into three major categories:

1. Physical characteristics of the building
2. Usage and occupational behavior of the building
3. Climatological properties of the region

To conduct the segmentation, the first step is to investigate the existing building stock, to define different types of occupancy behavior and to categorize the buildings with similar occupancy type. After categorizing the buildings based on their occupancy behavior, they will be grouped based on their physical characteristics and/or type of mechanical systems. Due to the existence of different climates at different regions, these archetypes could be further grouped based on climatological conditions of the region in the case of defining the archetypes at the national level. **Table *2-2***, summarized the influential parameters in defining the number of archetypes required for each building group.

**Table 2-2: Parameters Conceded to in Defining the Number of Archetypes for Each Building Stock**

| Building archetype | | | | | | | | | | |
|---|---|---|---|---|---|---|---|---|---|---|
| Level | Ref. | Statistics | | | Parameters | | | | | |
| | | Country | No. of buildings | No. of archetype | Shape | Area | Age | Usage | System | Climate |
| Urban level | [67] | Japan | 1,128 | 20 | ✓ | ✓ | | | | |
| | [68] | USA | | 30 | ✓ | | ✓ | ✓ | ✓ | |
| | [69] | England | 267,000 | 144 | ✓ | | ✓ | | | |
| | [70] | Italy | 1,320 | 7 | | | ✓ | | | |
| | [71] | Italy | | 56 | ✓ | | ✓ | ✓ | | |
| | [72] | Netherlands | 300,000 | 26 | ✓ | | ✓ | | | |
| | | USA | 200 | 12 | ✓ | | ✓ | ✓ | ✓ | |
| | [73] | Switzerland | 20,802 | 20 | ✓ | | ✓ | ✓ | | |
| National level | [74] | England | 115,751 | 47 | ✓ | | ✓ | | | |
| | [75] | Italy | 11 M | 96 | ✓ | | ✓ | | | ✓ |
| | [76] | Greece | 2.5 M | 24 | ✓ | | ✓ | | | ✓ |
| | [76] | Greece | 2.5 M | 5 | ✓ | | ✓ | ✓ | ✓ | |
| | | Italy | 877,144 | 3,168 | ✓ | | ✓ | | ✓ | ✓ |
| | [77] | Ireland* | 40,000 | 13 | | | | | | |
| | [78] | France | 14.9 M | 92 | ✓ | | ✓ | | ✓ | ✓ |
| | [78] | Spain | 9.8 M | 120 | ✓ | | ✓ | | ✓ | ✓ |
| | [78] | Germany | 18 M | 122 | ✓ | | ✓ | | ✓ | ✓ |
| | [78] | UK | 20.5 M | 252 | ✓ | | ✓ | | ✓ | ✓ |
| | [79] | Finland | 36,000 | 12 | | | ✓ | ✓ | | |

* Ireland: construction, thermal

Although the building shape has been widely used in defining the building archetype, different studies considered different parameters to define the shape. For instance, in a study, the correlation of the building with surrounding buildings was used as the main parameters to define the building shape and shading effect, categorizing them as detached, semi-detached, townhouse [72]. However, in another study, the height of the buildings was added to the previous parameters [78]. Having the number of building archetypes, as well as the number of buildings within each archetype, the demand profile of the users is predicted using different scaling methods. The most common scaling methods are; (1) area weighted in which the demand profile of a reference building is multiplied by the total district area over the reference building area ratio, and (2) number based in which the demand profile of a reference building is multiplied by the number of buildings within an archetype, **Table *2-3***.

**Table 2-3: Summary of the Methods used for HEDP in DHS Using Different Scaling Methods**

| DH Modeling | | | | | | |
|---|---|---|---|---|---|---|
| **Country** | **Year** | **Method** | **Scaling Method** | **Type** | **Output** | **Ref.** |
| Japan | 2004 | Archetype/ survey | Number per archetype | Residential | Total EUI | [67] |
| USA | 2008 | eQuest/ comprehensive modeling/ archetype | Area-weighted | Mixed | Hourly/ total consumption | [68] |
| Italy | 2012 | Regression analysis of measured data | Area-weighted | Residential | Total consumption | [70] |
| Finland | 2014 | Archetype/ linear development using REMA | Number per archetype | Mixed | Total consumption | [79] |
| Italy | 2013 | Archetype/ comprehensive modeling | Area-weighted | Mixed | Total consumption | [71] |
| Italy | 2014 | Simplified equivalent resistance | Area-weighted | Residential | Total consumption | [80] |
| Greece | 2011 | Archetype/ comprehensive modeling | Area-weighted | Residential | Hourly/ total consumption | [76] |
| Germany | 2014 | Simplified/ equivalent resistance / HDD | Building by building | Mixed | Total consumption | |
| | 2015 | Archetype/ simplified model/ adjusted HDD | Area-weighted | Residential | Total consumption | [81] |

In such approaches, the level of simplification in the representation of the building stock modeling is observed to be very high. For example, the orientation and other geometrical diversity of the buildings are mainly neglected compared to the reference building within a defined archetype. The above-addressed shortcomings in demand profile prediction are more magnified in the case of having larger DSs with more uniform building archetypes. For instance, in the case of Japanese district [67], German district [82] or Swiss district [81], with more homogeneous building types, the simulation accuracy is presumably much lower compared with Italian district [71], which has more heterogeneous building archetypes.

### 2.1.3. Limitations

The main limitations of the methods to predict the DHS demand profile include:

**Feasibility of expanding one model to the entire district level:** The first limitation of the presented methods is related to the limitation of these models in prediction of the total energy

consumption of the entire district. Especially, in the case of a larger district system where the heterogeneity of buildings is elevated, this problem becomes more amplified. For instance, HDD should be only used for prediction of small residential buildings while the BIN method is more suitable for larger buildings with much higher internal heat generation density [48]. As a result, an archetype method with a combination of these methods should be used to predict the total energy load of the entire network.

**Type of prediction:** Another limitation of the presented methods is related to the prediction method. Most of the presented methods have been adapted to predict the total energy consumption. Even though DSs are initially designed based on the total energy consumption as well as the maximum peak demand of the system, detailed profile of the network is further required to improve the system efficiency and enhance the energy distribution management. **Table *2-4*** summarizes different prediction methods that have been used to predict the consumption load of DSs. According to the table, most of the studies focused only on the total energy consumption of the networks and not the detailed profile.

**Accuracy:** Prediction accuracy is the next limitation of the previous models. Three primary sources of discrepancies identified for the existing models are occupant behavior, neighborhood interference, and scaling effect.

a) Since most of the models do not directly take into consideration the occupant behavior influence, the accuracy of the prediction, particularly at the building level, is observed to show a much lower value in many cases. In contrast, the accuracy is significantly higher at the district level with more diverse building types due to the fact that several building influencing parameters at a district level overlap on each other and therefore compensate the accumulated error at some points, **Table *2-5***; as a consequence of this misleading

schedule prediction, most of the previous works are only focused on one type of building in order to improve their simulation accuracy.

b) The unmeasured effects of the district/community on buildings such as shared walls between them and also the solar blockage by the adjacent shadow casted from surrounding buildings significantly impact on the prediction of the heating demand schedules. Most of the existing models are designed as a standalone building, barely representing the complexity of an urban/district setting. Indeed, the first assumption in the modeling of a standalone building is that the entire building shell receives solar radiation and exchanges heat with the surrounding environment.

c) Finally, many of the recent studies are utilizing scaling methods to represent the entire housing stocks (see **Table *2-3***), which is another source of discrepancy in the demand schedule prediction of DHSs. Commonly used methods are (1) area-weighted scaling method in which the demand profile of the reference building has been multiply by the total district area divided by the reference building area ratio in order to predict the demand profile of the entire district and (2) number based in which the demand profile of the reference building has been multiplied by the number of buildings within an archetype. In such approaches, the level of simplification in the representation of the building stock modeling is observed to be very high. For example, the orientation and other geometrical diversity of the buildings are mainly neglected compared to the reference building within a defined archetype

**Computational time:** The computational time of the stock modeling is one of the major limitations of the current DHS models.

**Table 2-4: Summary of the methods used for load prediction in DHS**

| Load Prediction Methods in DHS | | | | |
|---|---|---|---|---|
| **Ref.** | **Year** | **Prediction** | **Prediction type/resolution** | **Method** |
| [81] | 2015 | Annual | Total energy demand | Simplified modeling/adjusted HDD |
| [83] | 2014 | Daily | One day forecasting | NARX*, ANN |
| [79] | 2014 | Annual | Total energy demand | Linear development using REMA |
| [80] | 2014 | Annual | Total energy demand | Simplified equivalent RC |
| [84] | 2014 | Annual | Total energy demand | Simplified equivalent RC |
| [85] | 2013 | Daily | Average daily and hourly variation | Time series |
| [71] | 2013 | Annual | Total energy demand | Comprehensive modeling |
| [82] | 2013 | Annual | Total energy demand | Quasi-state monthly energy balance |
| [70] | 2012 | Annual | Total energy consumption | Linear regression analysis |
| [86] | 2011 | Annual | Peak load and total demand | Multivariant regression |
| [87] | 2011 | Annual | Total energy demand | Gray box model |
| [76] | 2011 | Annual | Annual peak demand | Comprehensive modeling |
| [88] | 2010 | Monthly | Peak load forecasting | Linear regression and clustering |
| [69], [89] | 2009 | Annual | Annual heating degree day | Linear regression |
| [90] | 2008 | Annual | Linearized peak day profile | Linear regression |
| | 2008 | Annual | Total energy demand | Gray box |
| [68] | 2008 | Annual | Hourly/total energy demand | Software modeling using eQUEST |
| [63] | 2006 | Annual | Profile | Gray box |
| [91] | 2008 | Annual | Peak demand | Stochastic method |
| | 2005 | Annual | Total energy demand | Gray box |
| | 2004 | Annual | Total energy demand | Multi-variant regression |
| [67] | 2004 | Annual | Total EUI/total energy demand | Software modeling using SCHEDULE |
| | 2004 | Annual | Total energy demand | Simplified equivalent RC |
| [39] | 2002 | Annual | Profile | Linear regression |

*Nonlinear autoregressive network with exogenous inputs

**Table 2-5: Summary of the accuracy level of the previous studies**

| Prediction Accuracy of Different Models | | | | | | | |
|---|---|---|---|---|---|---|---|
| **District Level** | | | | **Building Level** | | | |
| **Year** | **Country** | **Error** | **Ref.** | **Year** | **Country** | **Error** | **Ref.** |
| 2004 | Japan | 18% | [67] | 2014 | USA | 11-23% | [92] |
| 2008 | USA | 10-13% | [68] | 2011 | Greece | 12-55% | [76] |
| 2012 | Italy | 10% | [70] | 2013 | Germany | 5-50% | [82] |
| 2013 | Italy | 4% | [71] | 2013 | Germany | 18-31% | [82] |
| 2014 | Italy | 8% | [80] | 2014 | Germany | 1-60% | [84] |
| 2013 | Germany | 21% | [82] | 2014 | Switzerland | 6-88% | [93] |
| 2013 | Germany | 7% | [82] | 2015 | Switzerland | 8-99% | [81] |
| 2014 | Switzerland | 8% | [93] | | | | |
| 2015 | Switzerland | 9-66% | [81] | | | | |

To this end, this study aims to propose a new procedure for predicting the heating demand schedule of the DHSs using simplified models.

## 2.2.DHS Optimisation

As a major energy consumer, the building sector accounts for about 40% of the total energy consumption in North America and Europe, respectively [94]. Various countries prioritize the implementation of energy enhancement strategies in this sector to respect the Paris Climate Accord, COP21 [7]. Such strategies have been applied at various levels, including energy production, conversion, and user-demand, but the most effective solution touches the higher level known as energy management [95].

As mentioned earlier, a DHS is a unique type of energy system used at a higher level of energy management. This system by storing the energy generated by different sources, such as centralized boiler houses, renewable sources and the excessive heat of the industry, and by distributing it among the network users throughout the distribution network, allows the operators to control and manage the energy. In order to have a more efficient system with a higher level of performance, different optimization methods have been developed to improve the performance and efficiency of DHSs by minimizing the energy consumption of the system as well as the cost associated with operation and construction of the DHSs. ***Table 2-6*** summarizes the previous optimization work at the district level.

While the objective function of most optimization works remains almost the same (See ***Table 2-6*** , cost and emission, the optimization goals and methods are varied. This variation in methods and goals are mainly due to the differences between different types of existing DHSs. While the main structures of DHSs remain almost untouched over the time, the methods in energy generation and distribution have been drastically changed [13]. For an instant, the operating temperature of the system has been dropped from +100°C steam in the earliest generation of the

district heating system to 50-60°C water in the 4th generation DHSs. Even though decreasing the operational temperature of the system alongside with other alterations such as enhancing the energy efficiency of the system results in improving the performance of the DHS, but designing the system, which could operate with a minimal cost and energy level, was always remained as a challenging subject for designers.

**Table 2-6: Summary of the recent DHS optimization studies based on the optimization goals and objective function**

| DHS Optimization | | | |
|---|---|---|---|
| **Ref.** | **Goal** | **Objective Function** | **Method** |
| [14] | Minimizing the initial HE and pump operational cost | 1. Mass flow (construction cost is fixed)<br>2. Thermal conductance (pump power is fixed) | Newton method |
| [25] | Using mitigation strategy to control thermal comfort | Minimizing the departure of the space temperature from thermal comfort temperature | Sequential linear programing |
| [96] | Reduction of the heat demand at the user level by applying the energy efficiency method | Decreasing the operational cost | MODEST optimization model |
| [97] | Finding the energy flow from a different source in order to minimize the operational cost | Minimizing the operational cost | MODEST optimization model |
| [98] | Optimizing the payoff characteristic between the energy cost and occupant thermal comfort | Minimize the pay off the HVAC system operational cost and thermal comfort | Multi-Objective GA |
| [99] | Determining the energy and exergy efficiencies and exergy destruction for thermal optimization | Optimizing the mass flow rate | ANN |
| | Minimizing the investment cost of the system | Minimizing the capitalized cost | Non Linear Optimization Method |
| [100] | Presenting a model for structural and operational optimization of the district system | Minimizing the total cost | MILP programing |
| [101] | Minimizing the global warming potential during the life cycle and maximizing the exergy performance | 1. Maximizing the exergy efficiency<br>2. Minimize the life cycle global warming potential | Multi-Objective GA |
| [25] | Economical optimization of the system | Minimizing the hourly cost of the system | MINLP programing & GA |
| [102], [103] | Minimizing the total energy cost | Minimizing the total annualized cost | Nonlinear programing |
| [38] | Defining a globally optimal system from the energy viewpoint | average unit cost of heat supplied to all users | GA |
| [37] | Improving the design of community scale integrated energy system | Maximizing the exergy efficiency | GRG non-linear |
| [19] | Economical optimization of the system | Minimizing the total annual cost | ANN |
| [104] | Economical optimization of the system | Minimizing the investment and operation cost | MILP programing |
| | Cost and economical optimization of the system | 1. Maximizing the utility company profit | MILP programing |
| | | 2. Minimizing the greenhouse gas emission | MILP programing |

**MILP, mixed-integer linear programing; MINLP, mixed-integer non-linear programing; GRG, generalized reduced gradient.**

The major design issue of the older district heating system (DHS) generations (1st to 3rd generation) was mainly high heat loss in the distribution network due to the high-temperature media (100°C and more) [14], [105] In this regard, the optimization focus was on enhancing the system efficiency by controlling the heat loss from the system and subsequently, improving the system efficiency. As a result, most optimization studies have focused on minimizing the system heat loss. However, the new generation DHS (4th generation) operates at a lower temperature (50-60°C), and hence achieving higher system efficiency is possible by adopting appropriate control strategies and also through optimization of the equipment size [103], [106]. Note that, designing the 4th generation DHS based on the conventional design method, sizing the equipment based on the peak demand load, could lead to oversizing of the equipment and low system efficiency. Therefore, the adoption of an optimal approach (for cost and energy) to enhance the efficiency of the DHS while designing the 4th generation DHS became a standard practice among designers

Aside from the optimization goals, different optimization methods have been developed to improve H-CDHS efficiency and to reduce the system's emission footprint and the overall cost [65], [107]. Among the existing methods, mathematical methods based on continuous or discrete variables [95], [108]–[110], generic algorithms [95], [111]–[113] and neural networks systems are the most implemented techniques for optimizing the hybrid system's efficiency. Based on the defined type of the objective function, the DHS optimization is mainly formed on the basis of a single objective function or multi-objective functions. While most single variable function is solved using the deterministic numerical methods, the multi-objective functions use either weighted factors or pareto-front approaches. In the weighted factor approach, importance factor is fitted to different objectives of the optimization problem, based on a trial-and-error approach to convert the multi-objective function to a single objective problem, which provides a numerical

solution for the problem. **Figure *2-3*** presents different deterministic methods for the numerical optimization approaches:

$$Optimization: \begin{cases} Discrete \begin{cases} Integer\ Programing \begin{cases} Mixed-Integer\ Linear\ Programming\ (MILP) \\ Mixed-Integer\ Mon-Linear\ Programming\ (MINLP) \end{cases} \\ Stochastic\ Programing \end{cases} \\ Continuous \begin{cases} Constrained \begin{cases} Stochastic\ Programing \\ Nonlinearly\ Constrianed \\ Bound\ Constrained \\ Network\ Programing \\ Linear\ Programing \end{cases} \\ Unconstrained \begin{cases} Nonlinear\ Equations \\ Nonlinear\ Least\ Square \\ Global\ Optimization \\ Nondifferentiable\ Optimization \end{cases} \end{cases} \end{cases}$$

**Figure 2-3: Categorization of different numerical optimization approaches**

where the optimization problem can be defined as [71]

$$min\ Z = f(x,y) \quad s.t. \begin{cases} h(x,y) = 0 \\ g(x,y) \leq 0 \\ x \in X\ ; y \in \{0,1\}^m \end{cases} \qquad \textbf{Equ. 2-20}$$

where the objective function $f(x, y)$ is subjected to a set of constraints. $h(x,y) = 0$ defines the performance of the system, and $g(x,y) \leq 0$ stands for a feasible plan of the system. Moreover, two different types of variables could be defined for MIP (MILP/MINLP) problems; the continuous variable ($x$), representing the state variable and the discrete variable ($y$) with the value of 0 and 1, representing the equipment assigned to with a sequential task to the system.

Optimization algorithms consist of both continuous and discrete variables where they furthermore characterized as mixed integer linear programing (MILP) if all the equations are linear or mixed-integer non-linear programing (MINLP) if one of the equations is non-linear. In the cases of having no discrete variable, the optimization algorithm can be addressed with linear programing

and non-linear programing [114]. The schematic of the optimization process, presented in ***Equ. 2-18*** , serves as a basis of several optimization tools, which have been developed for optimization of the DHSs, e.g., general optimization toolboxes such as MATLAB or GenOpt [115], customized DHS optimization tools such as FreeOpt [116], cost-associated optimization tools with the thermal electrical load of the system such as STEFaN [117], network pipe size and routing optimization tool such as MODEST(Model for Optimization of Dynamic Energy System with Time-Dependent and Boundary Condition), the system investment, and operational cost optimization at both supply and demand level [97], [118].

Besides the mathematical approaches (as shown in **Figure *2-3***) adopted to formulate the optimization process, the optimization methods could be categorized either as static or dynamic optimization based on the dependency of the decision-making process with respect to time. In static optimization, the optimization time period remains the same for each iteration and the optimal solution is selected for a particular point of time within the given time period. In other words, in each iteration, regardless of any change in the optimization variables, the optimal solution is always at the same time. For example, static optimization obtains the optimal size of the equipment based only on the annual peak demand load. While in dynamic optimization, the optimization time horizon is split into a set of smaller time periods and the solution for each period affects the future solutions and possibilities. As a result, the optimizing agent takes into account this effect in the decision-making process.

Even though there is a scientific consensus on the mathematical definition of the static and dynamic optimization processes, there are many ongoing debates as to which type of optimization method should be used when it comes to use of the commercial energy simulation and optimization tools. Since similar simulation output could be obtained from all these commercial methods (e.g.

energy demand profile), the interaction between the simulation and optimization tools can be used to identify the optimization type (static or dynamic optimization). For instance, in static optimization, the district component and the interaction between them are modeled either by using the user-defined code or commercial simulation software [119] [120] in order to find the optimal size of the DHSs' equipment [108], [121]–[123]. Subsequently, the energy simulation is performed exclusively from the optimization process and a set of unique solution is obtained per simulation. In other words, the optimization population will be generated by simulating the model over the simulation time period under different scenarios (optimizations variables) and the unique solution is obtained based on the objective function (i.e. cost and emission) under each scenario. Later on, the unique solutions are used by the optimization tools as an optimization population to find the optimized value of the objective function. It is worth mentioning that all unique solutions obtained from static optimization are for the same exact point of time (e.g. the peak demand time). By using the non-interactive model, i.e., separate simulation and optimization model (static model), there exists a higher probability of decreasing the effectiveness of the optimization tool towards predicting the optimal size of the equipment [121].

On the other hand, in dynamic optimization, instead of generating the optimization population by simulating the model for different scenarios, the optimization and simulation are carried out simultaneously. By simultaneously performing the optimization and simulation, not only a more comprehensive spectrum of the solution is generated as an optimization population, but also the generated off-spring population reflect the effects of previous hours. Due to the complexity of coupling the simulation and optimization tool in dynamic optimization, several

research works focused on the dynamic optimization using user-defined codes for system modeling[5] [110], [124], [125].

Since the dynamic optimization of the system using the detailed user-defined codes is computationally expensive, and in many cases not feasible, different simplification approaches have been adopted to decrease the computational time. These approaches resulted in a simplification of the district energy model[6], using the reduced input file and the representative weather or demand file for the design period instead of using the whole year profile, or the combination of two. Considering the above-said research gap, the main objective of this study is to develop a dynamic optimization platform that could explore the optimal equipment size using the detailed demand profile in a timely manner. The developed model predicts the detailed demand profile of the DHS and uses them along with detailed energy model of the DHS and the equipment, and interaction between them to dynamically optimize the entire system. Subsequently, the optimal size of the equipment is obtained. The size of the equipment obtained from the model is later compared with the one obtained from the conventional method (design day method), as well as using a static optimization tool, (Biomass optimization tool). In this regard, data from an existing H-CDHS with an integrated thermal energy storage system is used to optimize its boiler house to minimize its overall cost and $CO_2$ emission.

[5] Modeling the district components and the interaction between them.
[6] Represent the components and the interaction between them with a simplified equation

**Table 2-7: Summary of the DHS optimization studies based on the type of the objective function and objective function**

| DHS Optimization | | | |
|---|---|---|---|
| **Ref.** | **Type of Objective Function** | **Objective Function** | **Solving Method** |
| [126] | Multi-objectives optimization | Cost and $CO_2$ emission | Evolutionary algorithm/Perato front |
| [127] | Multi-objectives optimization | Cost and $CO_2$ emission | Weighted factor/MILP |
| [128] | Single Objective | Pressure drop | Deterministic/MINLP |
| [129] | Multi-objectives optimization | Global cost, operation, and investment | Weighted factor/MINLP |
| [105] | Multi-objectives optimization | Accumulated error | GA/non-linear objectives |
| [130] | Multi-objectives optimization | Exergy efficiency and life cycle global warming | GA/multi-objectives |
| [25] | Single Objective | Hourly cost | GA/MINLP |
| [131] | Multi-objectives optimization | Global cost and CO2 emission | Weighted factor/MILP |
| [14] | Single Objective | Mass flow rate/thermal conductance | Newtown method |
| [19] | Multi-objectives optimization | Total cost | ANN |
| [99] | Single Objective | Mass flow rate | ANN |
| [38] | Multi-objectives optimization | Average unit cost of heat supplied to all users | GA |
| [37] | Single Objective | Exergy efficiency | Non-linear GRC |
| [96] | Single Objective | Operational cost | MODEST optimization model |
| [132] | Single Objective | Capitalized cost | NLP |
| [104] | Multi-objectives optimization | Total cost | Weighted factor/MILP |
| [97] | Single Objective | Operational cost | MODEST optimization model |
| [98] | Multi-objectives optimization | Operational cost and thermal comfort | GA/multi-objectives |

**MILP, mixed-integer linear programing; MINLP, mixed-integer non-linear programing; GRG, generalized reduced gradient.**

# Chapter 3: Methodology

Predicting building energy demand is a complex procedure consisting of different stages. Even though a number of studies have been conducted to forecast the energy consumption of buildings, a general model that can accurately predict the HEDP of different types of DHSs with a wide range of the users in a timely manner is not proposed yet. Therefore, this study aims to propose a new procedure for predicting the heating energy demand profile (HEDP) of the DHSs using simplified models. For this purpose, a 4-step procedure has been developed to accurately predict the hourly heating demand profile of the different type of district systems with a high resolution, in a timely manner. The procedure benefits from multiple linear regression (MLR) and multiple nonlinear regression (MNLR) methods. In this 4-step procedure, the heating energy demand profile of the entire district is predicted by modeling each individual unit in the community using their physical and geometrical characteristics, the regions' meteorological information, and the occupants' behavior.

The proposed 4-steps procedure has been validated both at a building level and at a district level using inter-modal comparison and measured data.

For the purpose of validation, Root Mean Square Error (RMSE) has been used as an indicator to evaluate the correlation between the predicted value using the proposed method and the results obtained from the comprehensive modeling. The RMSE indicator is defined as:

$$RMSE = [\frac{1}{m}\sum_{i=1}^{m}(\hat{Y}_i - Y_i)^2]^{0.5} \qquad \textbf{Equ. 3-1}$$

where $\hat{Y}_i$ is the predicted value obtained from the proposed method, $Y_i$ is the result of the comprehensive simulation or measured data and $m$ is the number of observations.

## 3.1. Development of the 4-Steps Procedure

The proposed procedure consists of four major steps:

***Step 1:*** In the first step, a sample building stock model (BSM) is segmented into different archetypes, and a reference building is defined for each archetype. The initial segmentation is completed by considering the building's construction method, physical and geometrical properties, and construction period. Once the initial archetypes are determined, each archetype is further divided into sub-archetypes based on the occupancy schedule (e.g. residential users with high, medium and low usage) of the building within that archetype. Different methods are used for segmenting the BSM based on the occupancy schedule. While some researchers only segment the BSM based on major occupancy types (e.g. residential, commercial, or office types), others segment it following the user's energy profile. This study presents a more detailed approach for defining the number of archetypes as well as the reference building for each archetype. A hierarchical clustering method was adopted to this end. In this method, the data set is split into a prefixed number of clusters. The building closest to the centroid of that cluster is defined as a reference building for that cluster. To define the number of clusters required for a given data set, prefixed number of clusters, the optimal number of cluster is defined using the elbow method [133].

***Step 2:*** The second step includes the generation of the model's input files. These files are constructed based on the physical properties of individual units, regional meteorological data, and occupants' behavior. In order to determine the input file of the model, extensive sensitivity analysis

is done to identify the most influential parameter on the heating demand profile of the buildings. Based on the results obtained from sensitivity analysis, four different input files are constructed for this study.

***Step 3:*** In the third step, a reference building's heating demand profile is initially defined using the measured data. An ANN model is then trained and tested using the reference building's input file as well as the heating profile to obtain the regression coefficients.

***Step 4:*** Finally, in the fourth step, once the MLR/MNLR model is trained separately for each archetype using the reference building, each individual unit's heating demand profile is then predicted by adopting the input file of them. This procedure is capable of predicting the heating demand profile of both individual buildings and the entire district network.

*Figure 3-1* presents the algorithm for a simplified 4-steps procedure for predicting the HEDP of the DHS.

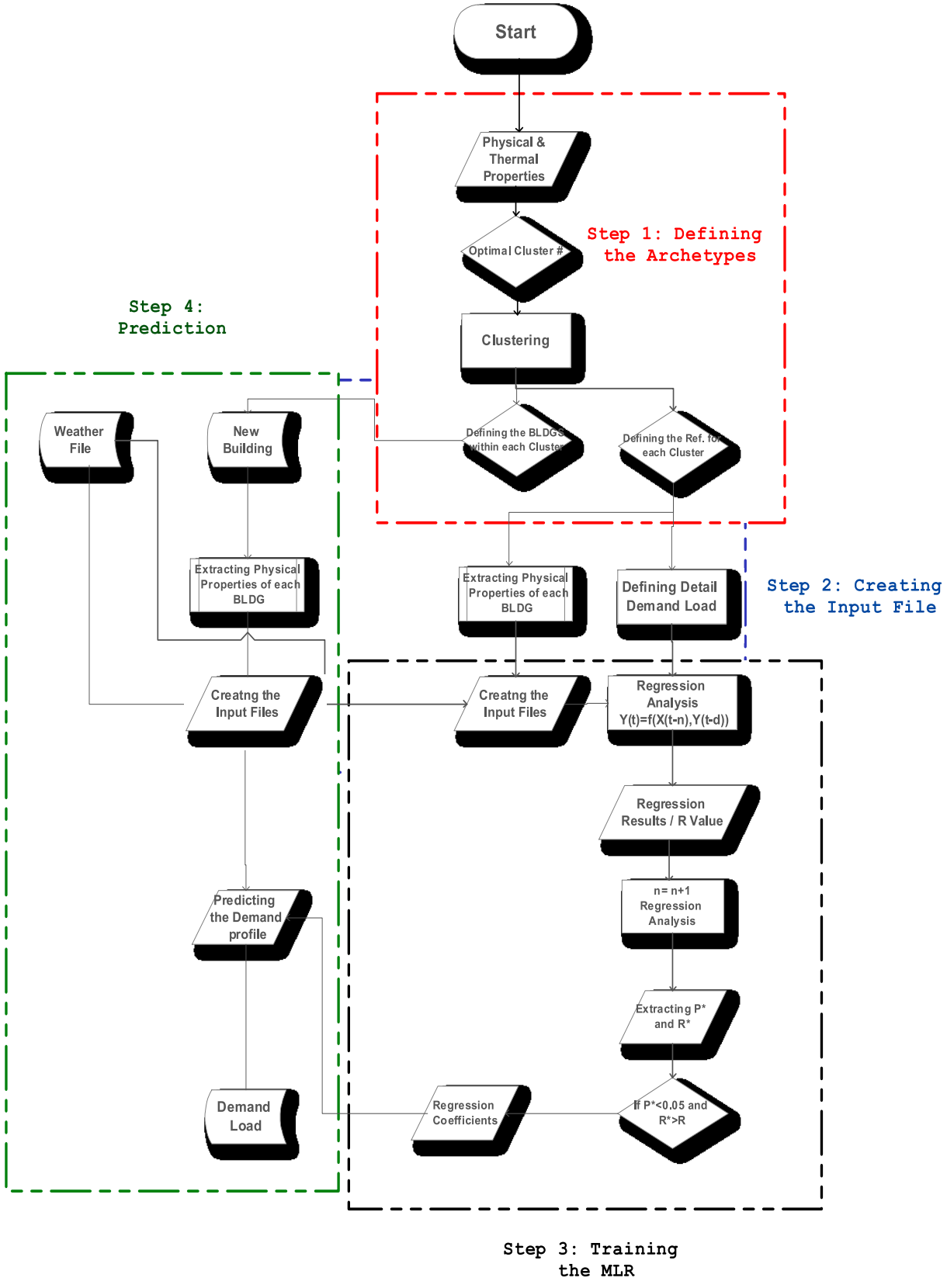


**Figure 3-1: Algorithm for Predicting the HEDP of DHS Using the 4-Steps Procedure**

### 3.1.1. Step 1: Defining the Archetypes

The first step in defining a proposed simplified procedure is to find the number of the archetypes. Therefore, the entire building stock is initially identified and will be segmented into a predefined number of building archetypes, each presenting buildings with similar properties in term of the occupancy behavior and energy demand. Generally, building segmentation in a building stock requires a thorough identification of the attributed parameters in energy demand. **Table *2-2*** presents the addressed parameters used in previous building stock segmentation studies. According to this table, the parameters used for the forming of a building stock model can be divided into the four categories:

1. Building physical characteristics and properties.
2. Building usage and occupant behavior.
3. Regional climate.
4. Building mechanical system.

While the main focus of the building stock segmentation is on the mechanical space conditioning at the national level, in a smaller scale, such as urban/district level, this focus has been shifted toward the usage as well as the building age (see ***Table 2-2***). Regardless of the scale of the segregation procedure, in the first step, the existing building stock is segmented based on the occupancy. The buildings are further grouped based on their physical properties and their type of the mechanical systems. Eventually, the segmented archetypes could be further clustered based on the regional climate in the case of defining the archetypes at the national level. To improve the generation of the building archetypes for predicting the HEDP of the DHS, in this study, the thermal mass of the building has been considered in the clustering process. This element is

recognized to have a significant impact in developing a dynamic model at the district level. Therefore, the modified clustering process is characterized as below:

1. Building mass: high, medium, low density, etc.
2. Building shape: low-rise, high-rise, medium-rise, etc.
3. Construction age: in the case of renovation, time of the renovation was considered to be a construction time for a specific building. Thus, it is reasonable to assume that a constructed building is following the minimum thermal resistance requirements code for that time period.
4. Building occupancy schedule: residential, commercial, etc.
5. Building occupancy behavior: high, medium, low energy usage, etc.

Here, it should be noted that different parameters are suggested to define a building shape. Mastrucci et al. [72] used the shading interaction of a building with its surrounding buildings and categorized them as detached, semi-detached, and townhouse. In another study, Mata et al. [78] have added the building height to the latter parameters. In this study, since exposure area is one of input data, buildings' height and interaction with surrounding building, detached, semi-attached and or stand-alone building, is considered as the shape factor.

After investigating the BSM, and sorting the buildings within the BSM based on the main categorization presented above, the next step is to define the number of sub-cluster required for each main categories. Different methods have been suggested by researchers in order to define the optimal number of cluster required within each main categories such as Information Criterion Method, Information Theoretic Method, Average Silhouette Method and Elbow Method. In this study, the elbow method is used [133].

Elbow method, define the optimal number of the cluster by comparing a difference between the within-cluster sums of the square (WSS)[7] of two consecutive cluster number. In other words, whenever increasing the number of the cluster does not significantly decrease the WSS, the optimal number of the cluster has been reached.

### 3.1.2. Step 2: Creating the Input File

With segmentation of the BSM into a predefined number of archetypes, the next step is to define the model input variables. As mentioned earlier in ***Section 2.1.2***, ***Equ. 2.12***, the HEDP of the building depends on four factors:

1. Building assemblies heat loss
2. Solar heat gain
3. Internal heat gain
4. Heat loss due to infiltration

However, detail calculation of all major heat gains/losses requires an extensive information regarding the physical and geometrical properties of all buildings. Unlike the metrological data, the geometrical properties of buildings can completely change from one building to another; as a result, obtaining all required information for all individual users of the district, especially in a mid to large size DHS is not practical. Thus, for the proposed simplified model, first, a sensitivity analysis has been performed and based on the obtained results, the most influential parameters for each major cause have been identified, and then the input files of the model has been defined.

---

[7] The WSS is the sum of the squared deviations from each observation and the cluster centroid and calculated as $\sum_{k=1}^{K}\sum_{i\in S_k}\sum_{j=1}^{P}(x_{ij}-\bar{x}_{kj})^2$ where $S_k$ is the set of observations in the $k^{th}$ cluster and $\bar{x}_{kj}$ is the $j^{th}$ variable of the cluster center of the $k^{th}$ cluster

### 3.1.2.1. Sensitivity Analysis

Sensitivity analysis is a technique to determine the impact of uncertainty of a particular input variable on the model output. In many literatures, sensitivity analysis considered to be the prerequisite for modeling [134]. Different techniques of sensitivity analysis have been suggested in the literature [135]. In this study, the local sensitivity method using the central differences approach is used. Firth used this method [136] to determine the effects of each parameter on the model output of his community domestic energy model. Even though results obtained from Firth and Salteli [137] show that the local sensitivity analysis cannot provide a thorough uncertainty analysis of the model, but in case of community-level with a wider range of buildings, results could be used with a good level of accuracy [138][137].

In this method, for a model consisting of multiple output variables (M) and multiple input variables (N), the sensitivity coefficient can be determined as:

$$SC_{N,M} = \frac{dY_M}{d\mu_N} \approx \frac{Y_M(\mu_N+\Delta\mu_N)-Y_M(\mu_N-\Delta\mu_N)}{2\Delta\mu_N} \quad \text{Equ. 3-2}$$

where $\mu_N$ is the nominal value of the input variables and $\Delta\mu$ is the small change applied to that variables while other variables kept constant. Chang [138] suggested that the $\mu_N$ could be calculated as the weighted average of the $N^{th}$ input parameter over all sample dwellings. While Turanyi [139], suggested that perturbation size can affect the accuracy of the analysis as a large step-size could result in damaging the local linearity assumption whereas too small step-size could ended up in a high round of error. After calculating the sensitivity coefficient, the normalized sensitivity coefficient is determined as:

$$\delta_{N,M} = \frac{dY_M}{d\mu_N}\frac{\mu_N}{Y_M} \quad \text{Equ. 3-3}$$

Since in real case scenarios, more than one parameter changes from a building to another one, the linearity, and additivity test were also performed [138] to study the effects of change of multiple parameters on the model prediction:

$$Linearity\ Test: Y(\beta.\Delta u) = \beta.Y(\Delta u) \quad \text{Equ. 3-4}$$

$$Additivity\ Test: Y(\Delta u_1 + \Delta u_2) = Y(\Delta u_1) + Y(\Delta u_2) \quad \text{Equ. 3-5}$$

Sensitivity analysis was initially performed by carrying out over 100 simulations using a validated eQUEST model. The simulations were conducted over a range of buildings by multiplying the selected input parameter(s) by a random number within the predefined range. As mentioned earlier, the linearity and additivity test, the simulations were done by changing a single parameter in 15% of the cases. While in the remaining 85%, two parameters in 25% of the cases, and three parameters in 60% of the cases were changed. Then, the heating demand profiles obtained from detailed simulation (eQUEST) were used for the sensitivity analysis as well as performing the linearity and additivity tests. A further simulation was also conducted to study the combined effects of different parameters on the performance of the model archetypes. The input parameters are:

- Occupancy density * Ran(1 ± 0.20);
- Win/Wall * Ran(1–3);
- Area * Ran(1 ± 0.40);
- Aspect Ratio * Ran(1 ± 0.5);
- Infiltration * Ran(1 ± 0.50);
- Area * Ran(1 ± 0.25);
- No. Stories [4,5 and 6 stories];

The results obtained from the sensitivity analysis are presented in **Table *3-1*** and **Figure *3-2*.** In general, it can be concluded that the results of the sensitivity analysis are in a good agreement with those reported in literature [**138**].

**Table 3-1: Results from linearity test and local sensitivity analysis**

| Sensitivity Analysis Results | | | |
|---|---|---|---|
| **Input Parameter μ** | **f(Δμ)** | **$R^2$** | **Norm. Sens. Coeff. δ** |
| **Area** | (L): $\Delta Y=0.7053\Delta\mu+0.2929$ | 0.9998 | 0.71 |
| **Infiltration** | (L): $\Delta Y=0.0133\Delta\mu+0.9867$ | 1 | 0.018 |
| **Story Height** | (NL): $\Delta Y= +0.002\Delta\mu+1.0001$ | 0.9999 | 0.01 |
| **Window Ratio** | (NL): $\Delta Y= 0.0027\Delta\mu^2-0.025\Delta\mu+1.0223$ | 1 | -0.025 |
| **Aspect Ratio** | (NL): $\Delta Y= 0.2454\Delta\mu^2 -0.4555\Delta\mu+1.1643$ | 0.996 | 0.46 |
| **Aspect Ratio** | (NL): $\Delta Y= 0.0486\Delta\mu^2 -0.0895\Delta\mu+0.9943$ | 0.9999 | 0.091 |
| **No Stories** | (NL): $\Delta Y= -0.0101\Delta\mu^2+0.1615\Delta\mu+0.7175$ | 1 | 0.16 |

Knowing the main causes of the heat loss/gain in a building, along with the most influential physical and geometrical properties of the building, four input files have been defined for the proposed simplified model:

1. Solar dependent variable: an equivalent of the solar gain of the building based on its shape, orientation, exposed wall and window to wall ratio;
2. Thermal dependent variable: an equivalent of the heat gains or loss of the building based on the heating/cooling temperature difference and the equivalent thermal resistance;
3. Internal generation: an equivalent of the heat generation based on occupant behavior;
4. The thermal mass of the building: represented in the form of the autoregressive model.

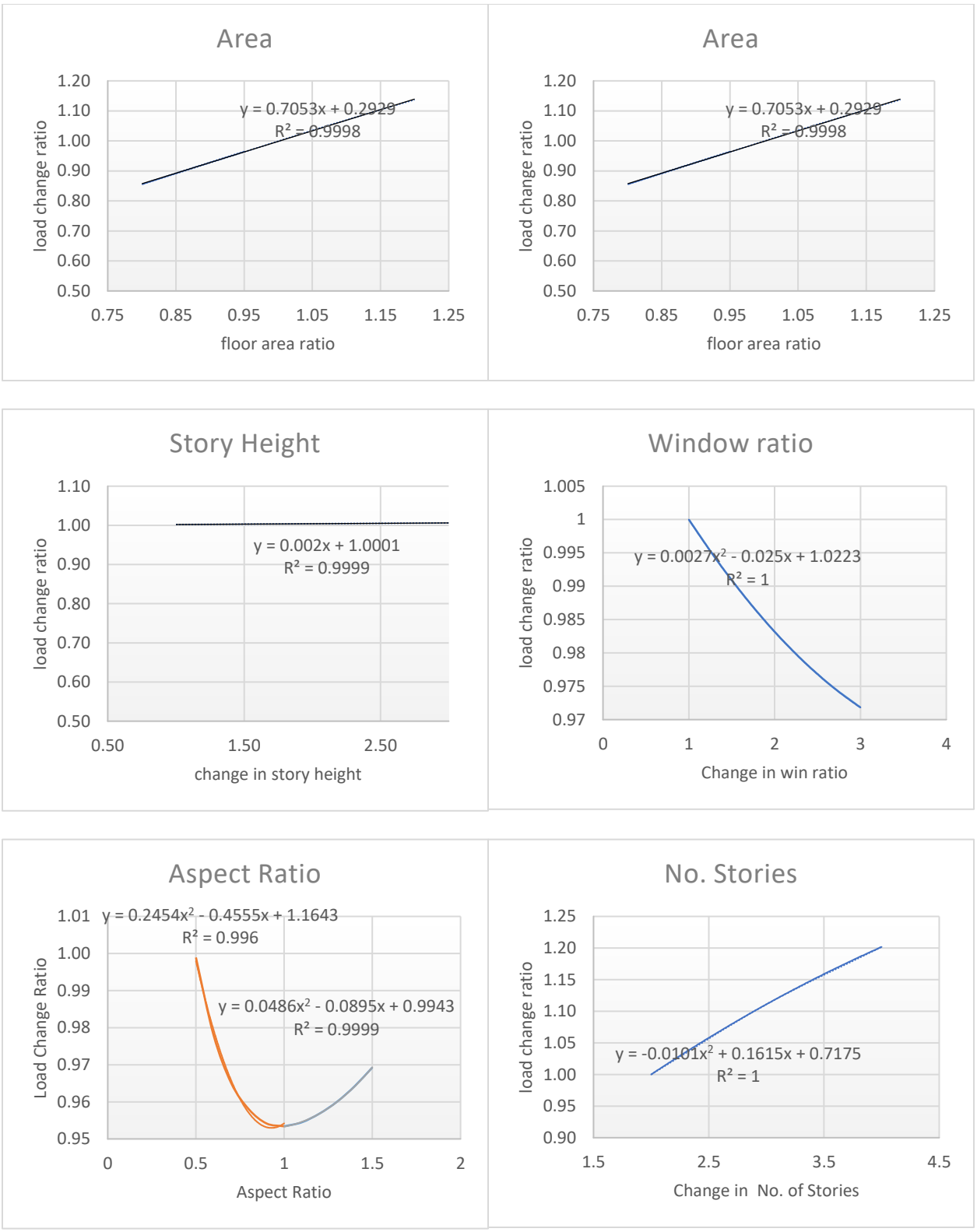


**Figure 3-2: Results of linearity test**

### 3.1.2.2. Solar Dependent Variable

The solar dependent variable was defined based on a measured dataset in the form of a TMY3 file and an isotropic solar model. The TMY3 [140] weather data defined the solar radiation based on the global horizontal radiation (I), direct normal radiation ($I_{bn}$), and diffuse horizontal radiation ($I_d$). The global horizontal radiation is defined as the total amount of direct and diffuse solar radiation on a horizontal surface while the direct normal is the solar radiation received on a surface normal to the sun. By having the incident angle, tilt angle, solar altitude, building orientation as well as the exposed facade of the building, hourly total heat gain profile of a building are calculated as follows:

$$I_{bt} = I_{bn} . \cos\theta \quad \text{Equ. 3-6}$$

$$I_{dt} = I_d(\frac{1+cos\beta}{2}) \quad \text{Equ. 3-7}$$

$$I_{rt} = I . \rho_g . (\frac{1-cos\beta}{2}) \quad \text{Equ. 3-8}$$

$$I_{total} = I_{bt} + I_{dt} + I_{rt} \quad \text{Equ. 3-9}$$

where $I_{bt}$ represents the beam radiation, $I_{dt}$ is the diffuse sky radiation, $I_{rt}$ is the reflected ground radiation, $\rho_g$ is the ground reflectance, $\theta$ is the incident angle and $\beta$ is the tilt angle.

Having $I_{total}$, the solar dependent variable can be written as:

$$SD(t) = \sum_{FO=1}^{N_{FO}}[I_{total,FO}(t). A_{wall,FO} . (1 - \alpha_{wall}) + I_{total,FO}(t). A_{win,FO} . \tau_{win}] + I_{total}(t) . A_{roof} . (1 - \alpha_{roof}) \quad \text{Equ. 3-10}$$

where $\alpha_{wall}$ is the wall albedo, $\alpha_{roof}$ is the roof albedo and $\tau_{win}$ is the window transmittance. This approach allows the model to take into account the effects of the shared wall by only measuring the solar gain on the exposed exterior facade of a building.

#### 3.1.2.3. Thermal Dependent Variable

The exterior façade of a building is the main source of heat exchange between its indoor and outdoor environment. Depending on the type of a building assembly, there are different codes and regulations for the optimal value of the thermal resistance of that assembly. Besides the assembly type, the design method (i.e. passive or active) as well as the building application (i.e. residential and commercial) could affect the thermal resistance of buildings. The thermal dependent variable has been defined in order to represent the equivalent heat loss from the building façade and presented as:

$$TD(t) = {}^{1}/_{R_{eq.}} (\Delta T_{Heating\ Difference}) \qquad \text{Equ. 3-11}$$

where $R_{eq.}$ is the equivalent thermal resistance of the building and defined as:

$$R_{eq.} = \sum_{i=1}^{n} \frac{A_{total}}{\left(\frac{A_i}{R_i}\right)}, \ [\frac{m^2.^{\circ}C}{W}] \qquad \text{Equ. 3-12}$$

where $A_{total}$ is the total building exterior facade area, and $A_i$ and $R_i$ are the area and thermal resistance of each wall, respectively. Also, $\Delta T_{Heating\ Difference}$ or the heating temperature difference can be then determined using the outdoor dry-bulb temperature from the TMY3 file and indoor air temperature set point. For residential buildings with low internal heat generation, it can be concluded that cooling and heating not happen simultaneously, thus, it is logical to separate these load profiles from each other. As a result, a temperature set point was determined as a

cooling/heating threshold, and the difference between the set-point and the dry-bulb outdoor-temperature was used as an input file for the model as shown in **Figure *3-3***.

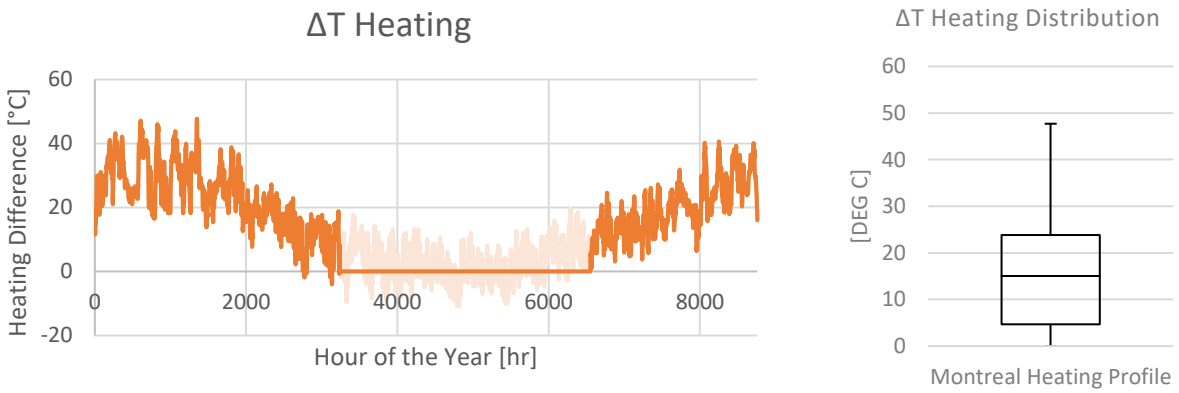


**Figure 3-3: (Left) Heating Temperature Difference; (Right) Temperature Difference Distribution [°C]**

The heating/cooling temperature threshold for different regions/countries could be found using the design code of that regions/countries. For instance, this temperature set-point, heating threshold, for a city of Montreal, Canada could be assumed as 21°C [141]. Since the main focus of the proposed model is to determine the HEDP of the users, the month with an average outdoor temp above 21°C could be assumed as zero, **Figure *3-3***.

### 3.1.2.4. Internal Heat Generation:

Internal heat generation effect on the HEDP of a building, varying from day to day and from a building to building. The variation is due to a different level of occupant density and a minimum internal load associated with their occupancy type. For example, in residential buildings with a low occupant density and a 24-h operational schedule, the effect of internal heat generation on the energy consumption schedule is more or less uniform whereas it becomes more significant for commercial buildings with higher internal heat generation. This implies that the study of the internal heat generation effect requires a comprehensive statistical analysis, which is beyond the

scope of this work. In this study, the typical design schedule suggested by MNECB [142] was used for each building archetype. These schedules can be further expended to all buildings within an archetype. For instance, **Figure *3-4*** & **Figure *3-5*** represent the typical schedules for electricity usage, cooking, lighting and occupancy for a low-density residential building.

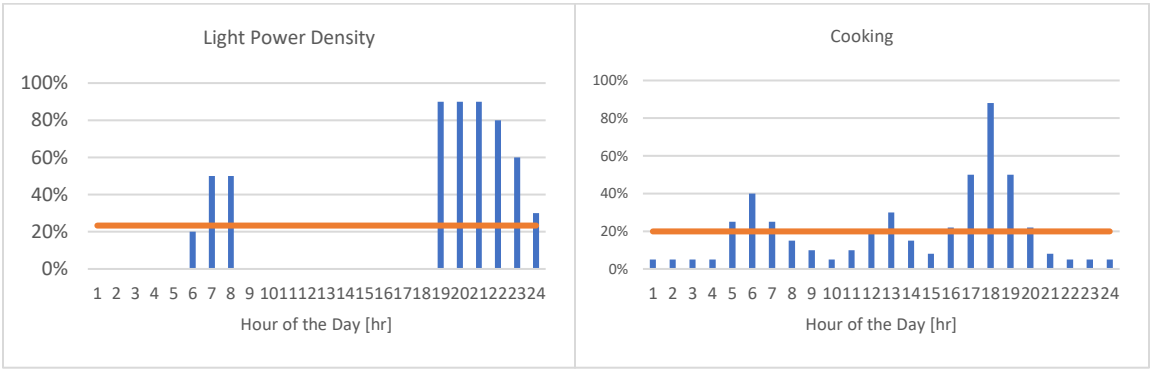


**Figure 3-4: (Left) Typical Lighting Schedule (Right) Typical Cooking Schedule**

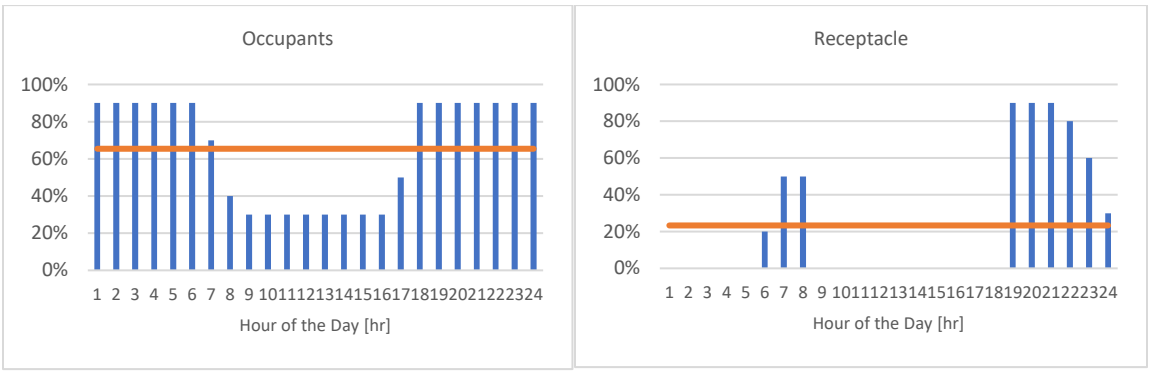


**Figure 3-5: (Left) Typical Occupancy Schedule (Right) Typical Receptacle Schedule**

### 3.1.2.5. Thermal Mass

Thermal mass, as the simplest means of thermal storage in buildings regulates the temperature and heat demand profile. As a result, heat demand of a building at present time can be assumed as a function of the building loads at the previous hours. Pfafferott et al. [143] showed that buildings with a higher thermal mass can regulate the temperature fluctuation for a longer

period of time. In this study, buildings were assumed to have low, medium and high thermal masses [144].

### 3.1.3. Step 3: Model Training

As mentioned earlier two different methods have been used in training the simplified model for predicting the HEDP of the DHS. These two models are the multiple linear autoregressive models (MLR) and multiple non-linear autoregressive models (MNLR).

#### 3.1.3.1. Multiple Linear Autoregressive Model

The main objective of the MLR is to find the relationship between the number of independent variables and one dependent variable. The main assumption of this method is that relationships between independent variables, predictors, and the dependent variable, criterion variable, is linear. ASHRAE fundamental represents the MLR equation as follow:

$$Y = \propto_0 + \propto_1 X_1 + \propto_2 X_2 + \cdots + \propto_k X_k \qquad \text{Equ. 3-13}$$

where Y is the dependent variable, $\propto_k$ are the coefficients, $X_k$ are the independent variables and k is the number of independent variables. Different methods were used to estimate the regression coefficients of which the least square method is the most popular one [145]. In this method, the regression coefficients usually estimated in a way to minimize the sum of the square errors between the predicted and actual dependent variable. Once the regression coefficients were extrapolated based on the verified set of data, the results were used to predict the new Y based on the new set of independent variables.

In some cases, the results of the dependent variable at the time t is highly influenced by the value of the independent variables at the time t as well as some previous time steps. In these cases,

such as a building with higher thermal mass, the dependent variable was predicted based on the previously observed set of independent variables, see ***Section 3.1.2.5***. Due to its usefulness for predicting the dependent variable, this method became a popular tool to forecast future results [146]. There are different types of the time series method among which the simple exponential smoothing is the most famous one. The Autoregressive (AR) method is a linear prediction time series method that works based on the simple exponential smoothing method. Two different autoregressive-based methods were used in this study to develop the simplified model.

The main difference between these two linear methods is the type of input variables that has been used for them. In the first method, the thermal dependent variable, solar dependent variable as well as internal heat generation of the building are used while in the second method the predicted load at previous hours also consider as an extra input for the model. The following equation shows the general format of the MLR used in this study.

$$Y(t) = \propto_1 TD(t) + \propto_2 TD(t-1) + \propto_3 TD(t-2) + \cdots + \propto_n TD(t-n-1)$$

$$+ \beta_1 SD(t) + \beta_2 SD(t-1) + \beta_3 SD(t-2) + \cdots + \beta_n SD(t-n-1)$$

$$+ \gamma_1 IG(t) + \gamma_2 IG(t-1) + \gamma_3 IG(t-2) + \cdots + \gamma_n IG(t-n-1)$$

$$+ \boldsymbol{\varphi_1 Y(t-1) + \varphi_2 Y(t-2) + \varphi_3 Y(t-3) + \cdots + \varphi_n Y(t-n)}$$

$$+ C \qquad \text{Equ. 3-14}$$

where α, β, γ and φ are the coefficients obtained from auto-regression; TD is the thermal dependent variable; SD is the solar dependent variable; IG is the interior heat generation dependent variable; and Y is the energy demand of the building. By running the auto-regression between the input data and the results obtained from DOE/eQUEST, the value of the coefficients α, β, γ and φ are

determined. Once the coefficients and the input data are established, the energy demand of any building can be predicted by the presented formula. In order to verify the results, the energy demand of another building modeled by DOE was predicted by using the presented formula, and the results were compared with those from the detailed simulation.

#### 3.1.3.2. Multiple Non-Linear Autoregressive Model

For the second method, non-linear regression method has been used. The main assumption of the MLR was the linearity between the dependent variable and independent variables. For cases in which this assumption is inaccurate, the multiple nonlinear regression analysis could be used. In this method, the relationship between the dependent variable and independent variables were assumed to be nonlinear. Adamowski [147] represents the MNLR equation as follow:

$$Y = \alpha_0 + \beta_1 X_i + \beta_2 X_j + \beta_3 X_k + \beta_4 X_i^2 + \beta_5 X_j^2 + \beta_6 X_k^2 + \cdots + \beta_p X_i X_j X_k \quad \text{Equ. 3-15}$$

where $\alpha_0$ is the intercept, $\beta$ is the regression coefficient, and p is the number of observations. As in the MLR method, the least squares method was used to estimate the regression coefficients. As for the first model, two different non-linear models have been used to predict the load:

- A nonlinear input-output model, which predicts Y(t) given d as past values of series X(t):

  $$Y(t) = f(X(t-1), \cdots, X(t-d)) \quad \text{Equ. 3-16}$$

- NARX: a Nonlinear autoregressive model with external Input, which predicts the series Y(t) given d as past values of Y(t) and another series X(t):

  $$Y(t) = f(X(t-1), \cdots, X(t-d), Y(t-1), \cdots, Y(t-d)) \quad \text{Equ. 3-17}$$

The main advantage of this method over the MLR is in the associated accuracy of the results due to taking into consideration of a wider range of the buildings in the energy demand prediction.

Inversely, its main disadvantage is related to the need for a large dataset for its training and validation.

#### 3.1.3.3. Model Training

Two different tools were utilized to develop the linear and nonlinear regression models. The first tool adapted for the linear model (MLR) was R-Studio, which has a powerful and user-friendly interface. While the ANN toolbox of MATLAB has been used for the nonlinear model (MNLR). The closed loop forward ANN model was trained and validated using the existing set of data from a detailed simulated schedule of more than 100 buildings. The ANN model was used to predict the heating demand profile of the buildings within a district by finding the correlation between hourly demand profile of a target and other input files defined in ***Step 2***, ***Section 3.1.2***. This nonlinear autoregressive model with an external input (NARX) was therefore used to predict the hourly heating demand profile of the model by taking into consideration of the past target data, demand profile, and other series of input parameters defined earlier. Thus, to predict the demand profile of the future hours previously predicted values and input files were used at the same time. It should be noted that the utilized dataset was initially divided into three parts, including 75 buildings for the training stage (75%), 23 buildings for the validation stage (23%), and finally, two buildings for the testing stage. The number of the hidden layers decided to be 9 based on Lu and Viljanen's suggestion [148]. He suggested the best number of hidden units for the system is equal to two times the number of input layer plus one. To determine the accuracy of the model, the mean square error of the predicted results against the validated data was calculated.

### 3.1.4. Step 4: Load Prediction

After grouping the building stock model (BSM) into different archetypes, obtaining the reference building for each archetype and training the prediction model for each archetypes using the reference model for that specific archetypes, the last step is to obtain the overall load of the entire community. To do so, the earliest extracted physical data for each unit[8] grouped using the archetypes properties and the input files have been fed into the appropriated trained model[9]. The trained model, using the regression coefficients obtained from the training of the model using the reference building of that archetype[10], and the input file generated based on the physical data of induvial units within that archetypes and the outdoor weather data, the HEDP for each individual unit has been obtained. The total HEDP of the entire district is the summation of all the HEDP of individual units of all different archetypes in addition to the heat loss from the distribution network. The heat loss prediction of the distribution network explained in more details later on in ***Section 4.2.4.3***.

[8] Data such as: Window to wall ratio, area, aspect ratio, orientation, etc.
[9] Using the reference building of each archetype, one model for that archetype has been trained.
[10] Based on the method of training, instead of having the regression coefficients, MLR method, we could have an ANN model, the MNLR method.

# Chapter 4: Model Validation Results

After developing the simplified procedure to predict the heating energy demand profile of the DHS, the proposed model was validated both at a building level and community level. For validating the model at building level, only Inter-model comparison was used while for the community level, both intermodal comparison and measured data were used.

## 4.1. Inter-model Comparison

In the first step, the proposed method was validated using the inter-model comparison both at building level and the community level. In both case, first a set of arbitrary buildings were selected and modeled in an energy simulation software, eQUEST/TRNSYS. Using the simulation software, the heating energy demand profile of the simulated buildings were obtained. In next step, the HEDP of the same buildings was predicted using the proposed procedure. Finally, the predicted profile was compared with the one obtained from the detailed simulation.

### 4.1.1. Inter-model Comparison at the Building Level

First, the proposed procedure was used to predict the heating load of the individual building using both MLR and MNLR approaches while the results were compared with the one obtained from the comprehensive modelling.

#### 4.1.1.1. MLR Model

Two new buildings were developed using the verified, DOE based model to validate the proposed simplified procedure (MLR), called buildings "***R1***" and "***R2***". The new buildings were first modeled in DOE-eQUEST, by changing some of the parameters of the verified model in the

reference building. The description of the reference building and tested buildings "***R1***" and "***R2***" could be found in **Table *4-1***.

**Table 4-1: Description of the Verified Building vs. Tested Buildings**

| Building Description | | | | | |
|---|---|---|---|---|---|
| **Building** | **Area[m$^2$]** | **Stories** | **Win/Wall** | **Set Point** | **Note** |
| **Reference** | 1858 | 4 | 30% | Constant 25 | Detached No Shading |
| **R1** | 2044 | 4 | 35% | Constant 24 | Common Wall on East |
| **R2** | 1998 | 4 | 35% | Schedule 1 | 20 ° Rotate to East |

| Schedule 1 | | | | | | |
|---|---|---|---|---|---|---|
| **Month** | **November** | **December** | **January** | **February** | **March** | **April** |
| **Avg. Temp, [°C]** | 2.61 | -6.82 | -9.83 | -9.43 | -2.72 | 6.49 |
| **Set-point, [°C]** | 22 | 23 | 24 | 24 | 22 | 21 |

Having the energy demand profile of the reference building, the MLR model has been trained and the regression coefficients have been obtained, **Appendix A (MLR Method)**. These coefficients later on have been used to predict the heating energy demand profile of the buildings "***R1***" and "***R2***".

Since one of the identified sources of the discrepancy in predicted results was the common wall, one of the newly developed buildings "***R1***" assumed to have a common wall on the east side. Next, the heating demand profiles of the new buildings were obtained using MLR approach and were compared with those obtained from the DOE simulation. Also, to check the accuracy of the model under different circumstance, two different scenarios were defined (**Table *4-1***, ***Schedule 1***) with different air temperature set-points, and the accuracy of the results was compared with those obtained from the comprehensive modeling. In the first scenario, a constant set-point air temperature assigned to the building "***R1***" for the entire year while in the second scenario, a set point schedule was assigned to the building "***R2***" based on the average outdoor temperature. Also, it was assumed that there is no heating load during the cooling season, even if the indoor air

temperature drops below the thermostat set-point. For this study, the heating season was assumed to be from 1st of November until the end of April. As mentioned earlier, to take into account the effect of thermal mass on the heating demand profile of the buildings, set of regression analysis with different "t" past values were performed and the best fit for each archetype was selected. For instance, for a low-rise multifamily residential building, this value determined to be four. To determine the best fit, two criteria were checked; having the highest R-value while maintaining the P value within 95% of the confident interval, less than 0.05. ***Table 4-2***, shows the best fit results of the regression analysis obtained for "t = 4" for a low-rise multifamily residential building, reference building.

**Table 4-2: Regression Analysis of the Reference Building**

| Reference Building | |
|---|---|
| **Best Fit Regression Statistics** | |
| **Multiple R** | 0.9983 |
| **Adjusted R Square** | 0.9966 |

Results obtained from the regression analysis, **Table *4-2***, shows a high correlation between the input file, and target value, heating demand profile. Having the coefficients of the regression analysis of the reference building, further simulations were performed using MLR method to predict the heating demand profile of the "***R1***" and "***R2***" buildings. As shown in **Table *4-1***, building "***R1***" has a common wall with another building on the east side and a constant set-point set of 24°C.

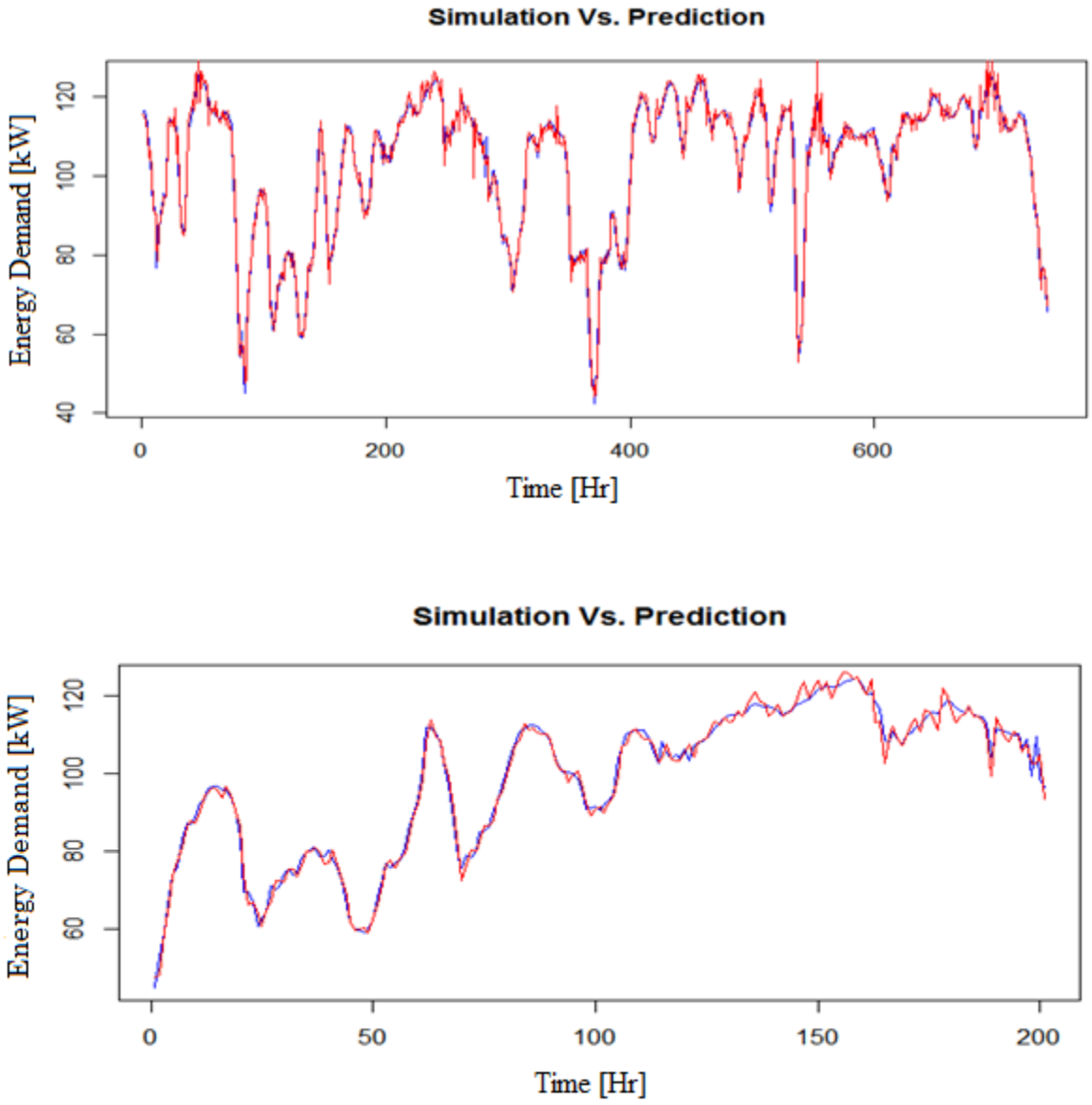


**Figure 4-1: Building "R1" heating demand profile [kW]: (Top) one-month period, December; (Bottom) 8 days' period in mid-December [hr]; Blue Line: simulation, Red Line: prediction.**

Figure *4-1* presents the prediction made by the simplified procedure against one made by comprehensive simulation for the month of December. Results show a good agreement between the predicted and simulated profiles. The R-value and standard error of the prediction are given in Table *4-3*.

Table 4-3: **Prediction vs. simulation for building "R1"**

| Building R1 | | |
|---|---|---|
| **Building** | **MSE** | **R** |
| **R1** | 6.996 | 0.9971 |

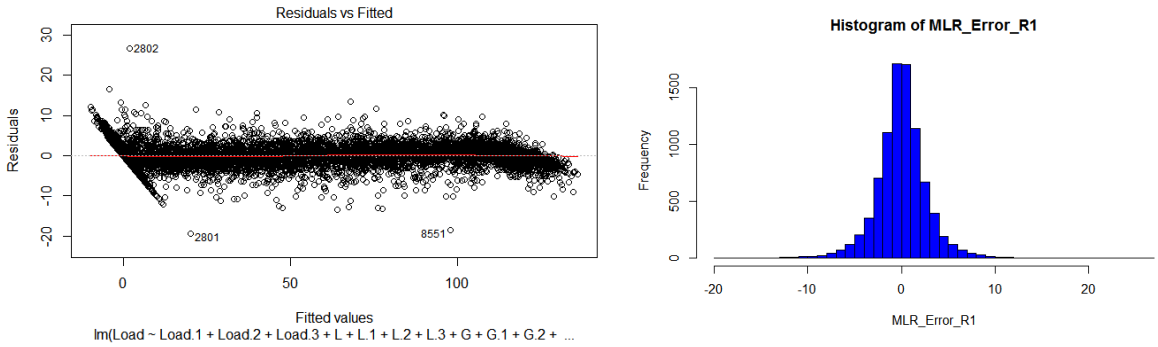


Figure 4-2: **(Left) Residual against fitted value; (Right) error histogram [kW] of the building "R1".**

Since the main assumption in using the MLR method is that there is a linear relation between load at time t and inputs, the linearity assumption was checked. As shown in Figure *4-2 (left)*, redline shows almost a linear relationship between predicted and simulated values. Also, the magnitude of the errors between predicted and simulated profiles is shown in the histogram as depicted in Figure *4-2 (Right)*. In the second scenario, the demand profile of building "***R2***" was predicted only for the heating season (1st of November till 30th of April). Unlike the previous scenario, based on the average outdoor temperature, the set-point was varied between 21°C and 24°C.

Figure *4-3* shows the predicted demand profile against the simulated profile of building "***R2***". Similarly, a good agreement between the predicted and simulated demand profile can be seen. Results obtained from the heating demand prediction for the second building tabulated in Table *4-4*: **Prediction vs. simulation for building "R2"**Table *4-4*.

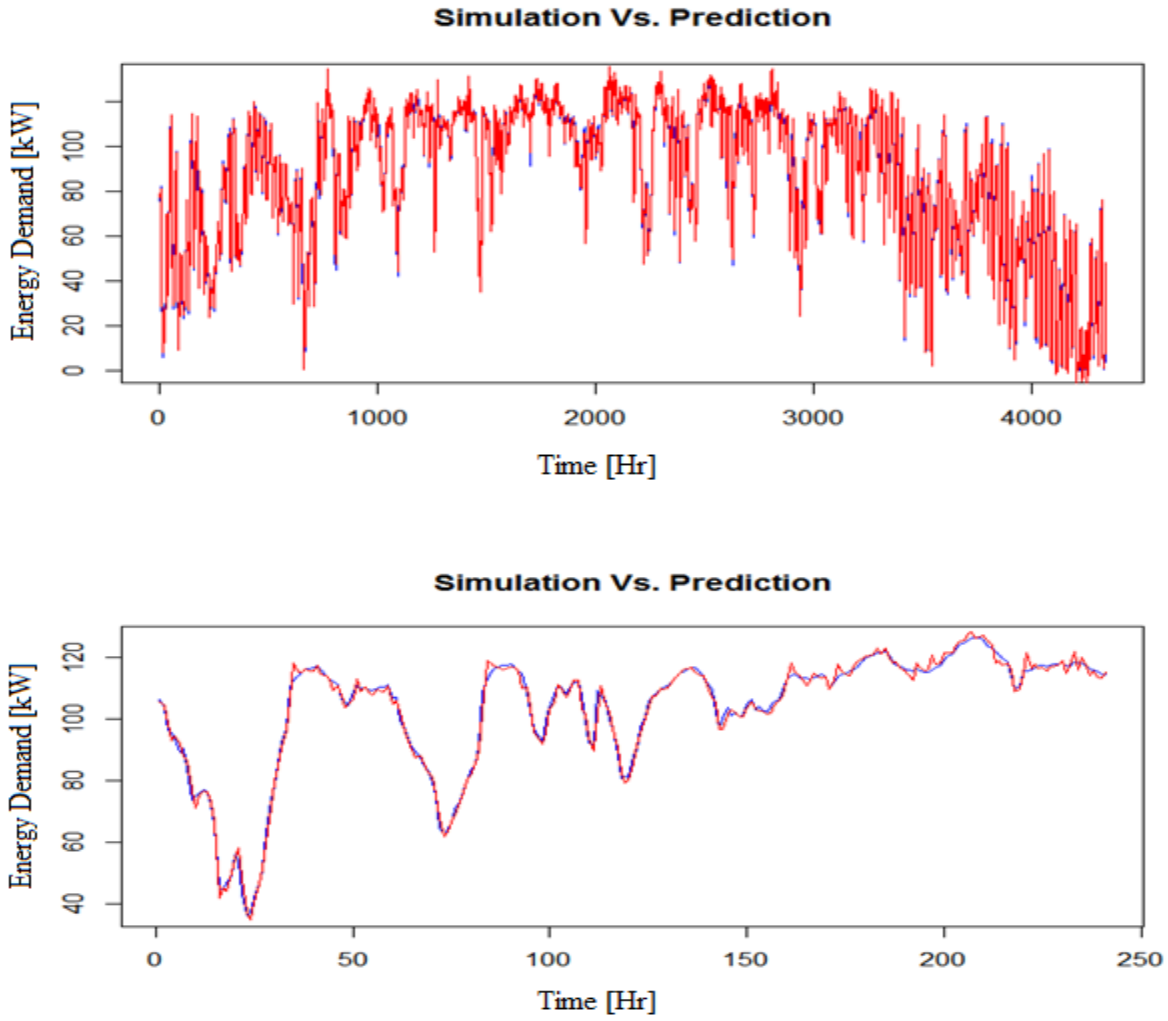


**Figure 4-3: Building "R2" heating demand profile [kW]: (Top) heating season; (Bottom) 10days' period late December till early January [hr]; Blue Line: simulation, Red Line: prediction.**

**Table 4-4: Prediction vs. simulation for building "R2"**

| Building R2 | | |
|---|---|---|
| **Building** | **MSE** | **R** |
| **R2** | 5.462 | 0.9947 |

The predicted heating demand profile for the second building "***R2***" shows a slightly lower correlation compared with the demand profile obtained from detailed simulation. However, it should be pointed out that the duration of simulation was different for two cases. It was 4341 [hr]

for "***R2***"while it was 8760 [hr] for the building "***R1"***. The MSE value for "***R1***" has been improved. **Figure *4-4*** also proves the linearity assumption made earlier in the development of the MLR methods. It also illustrates the error histogram for the "***R2***" building.

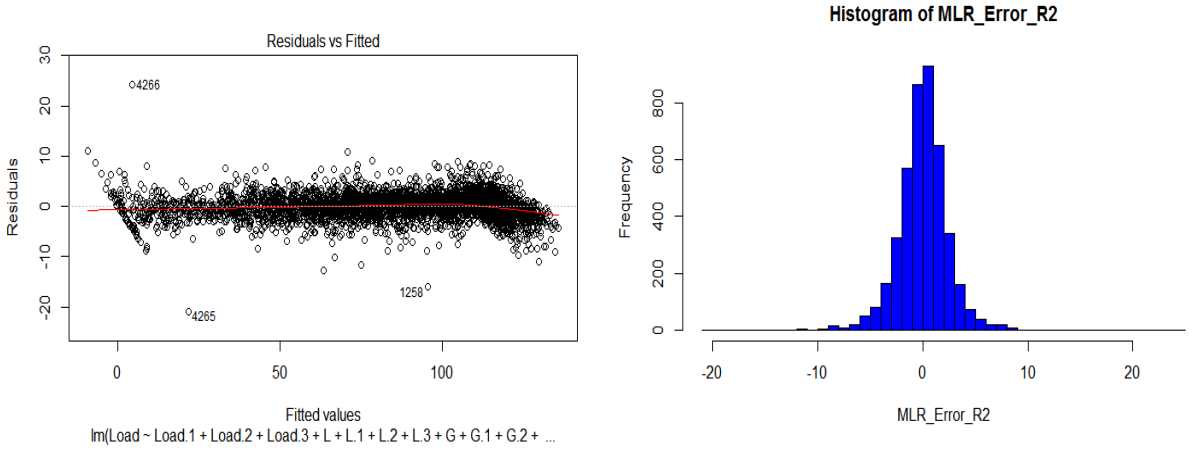


**Figure 4-4: (Left) Residual against fitted value; (Right) error histogram [kW] of the building "R1".**

### 4.1.1.2. MNLR Model

The ANN network was trained, **Appendix B (ANN, MNLR Method)** and the heating demand profile of ***R1*** and ***R2*** buildings were predicted using MNLR methods. Results obtained from the nonlinear analysis are presented in **Figure *4-5*** and **Table *4-5***. Similar to MLR methods, results obtained from MNLR method show good agreements between the predicted one and the one obtained from the detailed simulation. Unlike the MLR method, using the nonlinear model (MNLR) shows a better correlation between the predicted and the simulation profiles for the building "***R2***". This is mainly due to the fact that most of the buildings used for the training and validation stage of the ANN network were stand-alone buildings and did not have a common wall (unlike building "***R1***"). Having more diversified training data is a key point in using the MNLR method. Comparing MLR and MNLR methods shows that, in cases with a smaller training batch,

using MNLR methods is not only computationally more expensive, but it also does not result in a better prediction for all cases.

**Table 4-5: MSE and R-value of building R1 and R2 using the MNLR method**

| MNLR | | |
|---|---|---|
| **Building** | **MSE** | **R** |
| **R1** | 11.7 | 0.9961 |
| **R2** | 5.230 | 0.9978 |

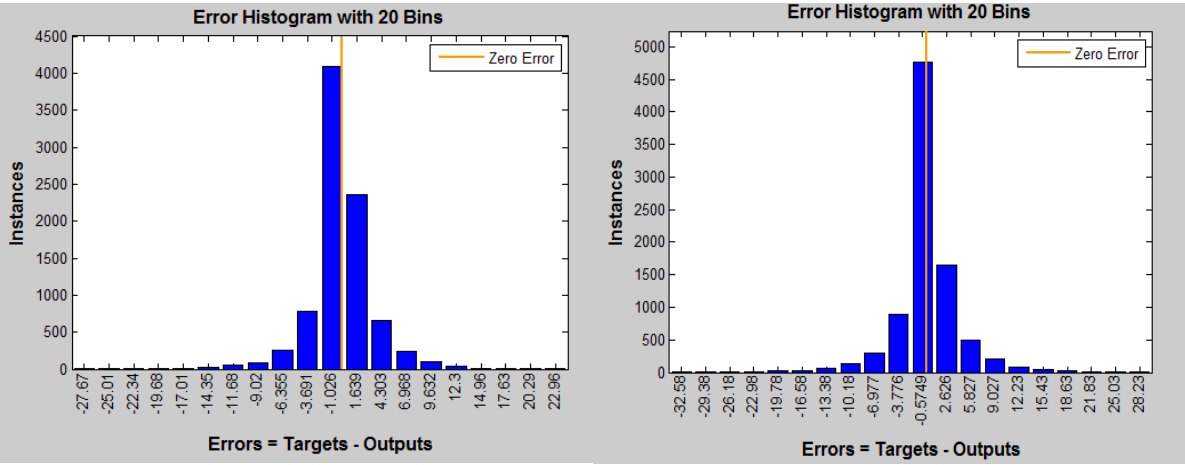


**Figure 4-5: Error histogram [kW] of building R1 and R2 using MNLR method.**

Even higher prediction accuracy expected to be obtained from using the MNLR method but, due to use of the predefined internal occupancy schedule for the entire simulation period, the prediction accuracy obtained from both MLR and MNLR method are close to each other.

### 4.1.2. Inter-model Comparison at the District Level

Since the main purpose of this study was to develop a method for predicting the heating energy demand profile of a district, in the next step, the proposed procedure was adopted in order to predict the heating energy demand profile of the DHS. To do so, three different DHSs were defined. Then, every individual user of the predefined district was modeled comprehensively using the energy simulation software, eQUEST, and the corresponding HEDP of each individual building was obtained. Utilizing the proposed procedure, the HEDP of the predefined districts were obtained and the results were compared with the one obtained from the detailed simulation. Thus, three districts were initially considered:

- **District 1:** solely comprised of 95 residential buildings
- **District 2**: solely consisting of 82 office buildings
- **District 3**: includes a mixture of 84 residential and 28 office buildings

Two validated reference buildings were selected for the study of these districts; including a residential and office buildings. The geometric parameters obtained from these buildings (i.e., number of stories, aspect ratio, orientation, net area and window-to-wall ratio) are used to define the remaining buildings of their associated community. In other words, the geometric parameters from the reference buildings were altered in accordance with these buildings in order to define other buildings within the district. These ranges were based on the likelihood of the characteristics of the buildings' archetypes within each community. Subsequently, the parameters of each building were given a random value within each of the ranges defined in **Table *4-6***.

**Table 4-6: Description of the Districts**

| Solely Residential District "District 1" | | | | | | |
|---|---|---|---|---|---|---|
| **No. of story** | **No. of Buildings** | **Area [m²]** | **Win/Wall** | **Aspect Ratio** | **Orientation with South** | **Set Point [°C]** |
| **4 Story** | 32 | 3500-4500 | 20-45% | 0.75-2.5 | ± 25º | 24 |
| **5 Story** | 36 | 3800-5000 | 20-45% | 0.75-2.5 | ± 25º | 24 |
| **6 Story** | 27 | 3500-5500 | 20-45% | 0.75-2.5 | ± 25º | 24 |
| **Solely Office District "District 2"** | | | | | | |
| **No. of story** | **No. of Buildings** | **Area [m²]** | **Win/Wall** | **Aspect Ratio** | **Orientation with South** | **Set Point [°C]** |
| **4 Story** | 21 | 10200-12000 | 25-45% | 0.75-2.5 | ± 25º | 24/20 |
| **5 Story*** | 37 | 10200-13000 | 25-45% | 0.75-2.5 | ± 25º | 24/20 |
| **6 Story** | 24 | 22500-14000 | 25-45% | 0.75-2.5 | ± 25º | 24/20 |
| **Mixed District "District 3"** | | | | | | |
| **No. of story** | **No. of Buildings** | **Area [m²]** | **Win/Wall** | **Aspect Ratio** | **Orientation with South** | **Set Point [°C]** |
| **Residential -4S** | 25 | 3500-4500 | 20-45% | 0.75-2.5 | ± 20º | 24 |
| **Residential -5S** | 32 | 3800-5000 | 20-45% | 0.75-2.5 | ± 25º | 24 |
| **Residential -6S** | 27 | 3500-5500 | 20-45% | 0.75-2.5 | ± 20º | 24 |
| **Office-4S** | 12 | 10200-12000 | 25-45% | 0.75-2.5 | ± 25º | 24/20 |
| **Office-5S*** | 10 | 10200-13000 | 25-45% | 0.75-2.5 | ± 25º | 24/20 |
| **Office-6S** | 6 | 22500-14000 | 25-45% | 0.75-2.5 | ± 25º | 24/20 |

* Detail description of the 5 story office buildings could be found in ***Appendix C (Inter-Model Comparison)***

Random values within the predefined ranges were attributed. For example, Community 1, consisting of 95 residential buildings was assigned a range of 4-6 stories per building. These buildings were further randomly defined as 32 x 4-story buildings, 36 x 5-story buildings and, 27 x 6-story buildings.

In order to further define other geometric parameters of these 4 to 6 story buildings, more randomized values were attributed. For instance, for 15% of the 4-story buildings, one other geometric parameter value was modified within its predefined range. For 25% of the 4-story buildings, two parameters were modified within their range, and finally, for 60 % of the 4-story buildings, three parameters were modified within their range. The modification of geometric parameters as described above was then assigned to the 5 and 6-story buildings.

It is important to note that 15%, 25% and 60% distribution for the modifications of the geometric parameters were also constructed based on a random process. In effect, other than the reference buildings, which are presented with realistic values, all of the other values were random and their ranges were determined based on their likelihood within their specific district. In order to define the buildings within the remaining districts 2 and 3, the same pattern of assignation of random values was applied. The schematic process of defining each district was presented in **Figure *4-6***.

After defining the buildings within each district, the heating demand profile of every individual building was obtained using both simplified MLR approach as well as eQUEST. Results obtained from detailed simulation show that the average space heating load for a low-rise multi-family residential buildings is 53.3 kWh/m$^2$/year with a maximum heating demand of 200 kW while for a low-rise office buildings, these numbers are, 55.3 kWh/m$^2$/year and 959 kW, respectively. Since the office buildings were assumed to be operating for a limited period of the time during each day, two different occupancy set point temperatures were defined. To have more consistently in the results, all buildings were assumed to use electrical heating systems.

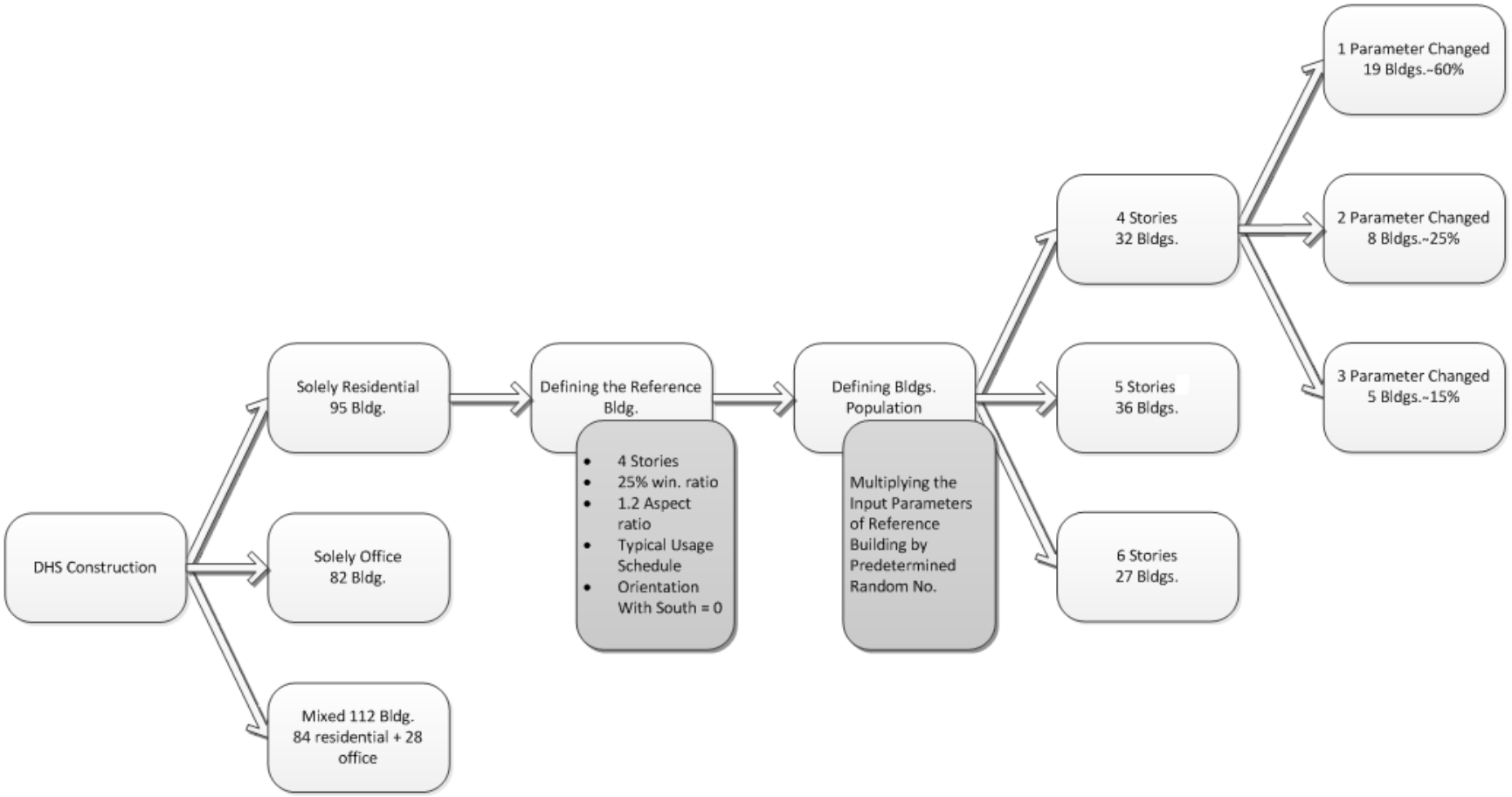


**Figure 4-6: District Generation Algorithm for Inter-modal Comparison**

Since the internal heat generation of buildings is one of the input parameters for both MLR and MNLR methods, the internal generation was determined by multiplying the density factor by usage schedule defined by ASHRAE 90.1 [149] and MNECB [142]. **Figure *4-7*** and **Figure *4-8*** show the usage schedules that were used for multi-family residential buildings as well as office buildings. More detailed description of the buildings within each district are tabulated in **Table *4-6***.

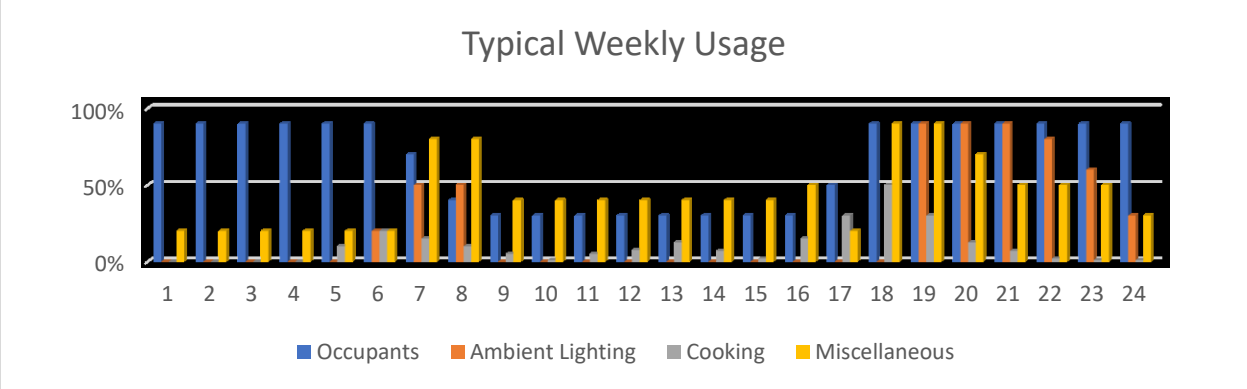


**Figure 4-7: Usage Schedule for the Residential Buildings**

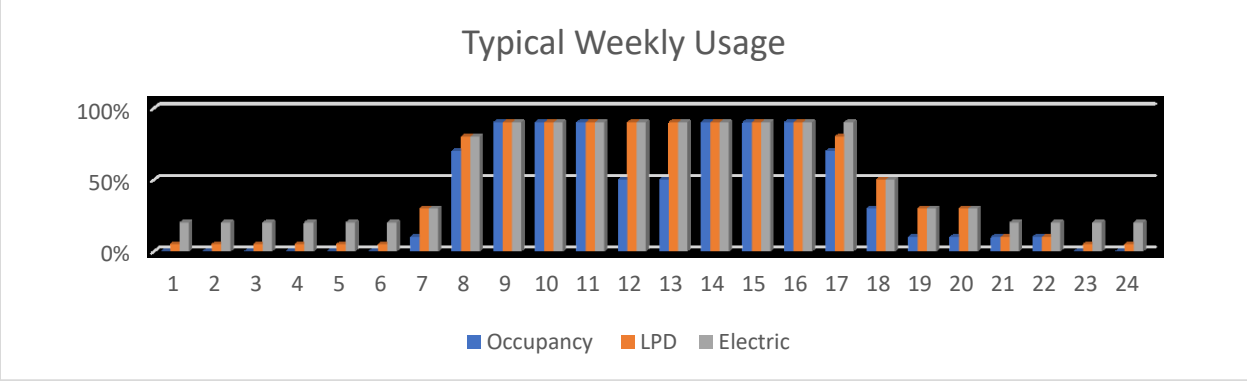


**Figure 4-8: Usage Schedule for the Office Buildings**

The MLR approach was used to predict the heating demand profile of three districts. The reference building used for modeling of the residential building is the same as the one used earlier

(*Section 4.1.1.1*). A similar approach was also used for the office buildings. Due to the characteristics of the office buildings, which have different daily usage schedule as well as temperature set point for the occupied and unoccupied periods, the results obtained from the multilinear regression analysis for the ***district 2*** shows a lower correlation between the predicted and simulated results with R = 0.9401 compared to R = 0.9966 obtained for ***district 1***. This lower correlation is due to a higher daily heating load variation in the office buildings in ***district 2*** compared with the residential buildings in ***district 1***. **Figure *4-9*** shows the daily heating load variation for the first 150 hours for ***district 1*** and ***district 2*** using the same period.

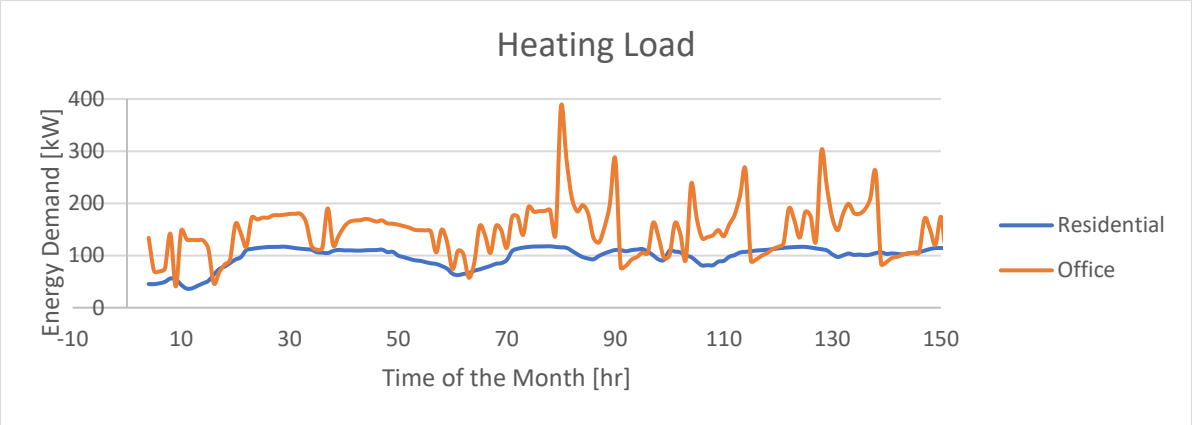


**Figure 4-9: Hourly heating load variation of the residential building against the office building**

Comparing the total heating demand load of ***district 1*** (solely residential buildings) with the schedule obtained from the summation of the profile of all individual buildings using eQUEST model shows a good agreement between them. **Figure *4-10*** and **Figure *4-11*** presents the predicted against simulated heating energy demand profile of the ***district 1*** as well as the error histogram.

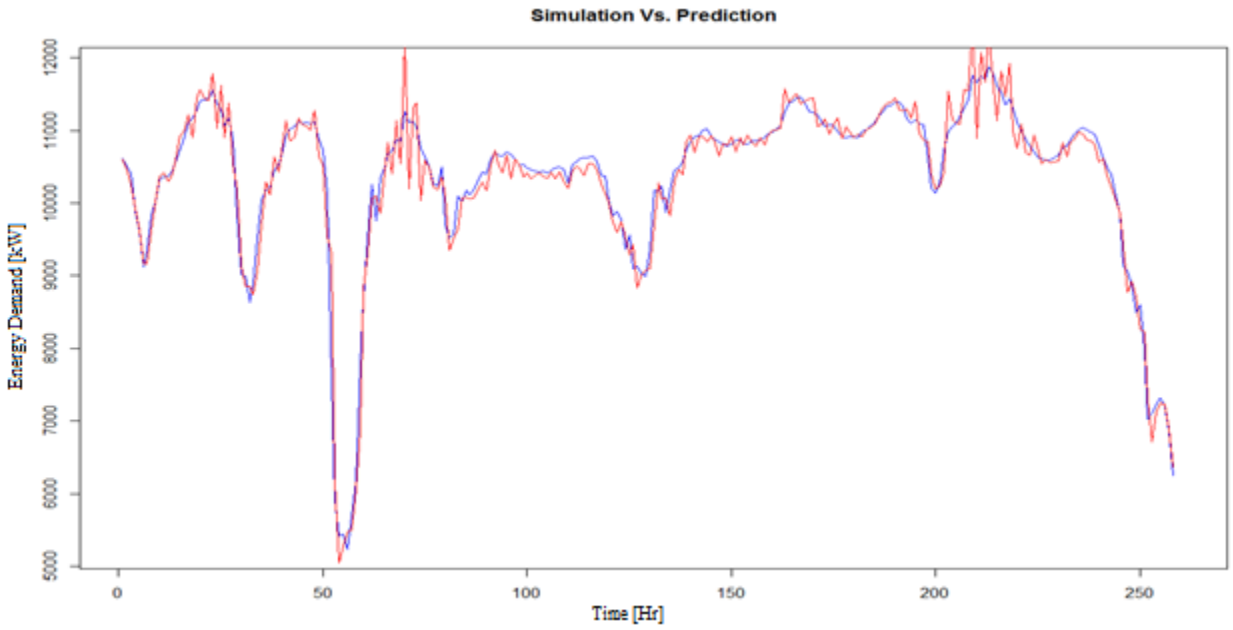


**Figure 4-10: Predicted heating demand Profile [kW] vs. simulated demand profile [kW] of district 1; Last 11 Days of December [hr]; Blue: Simulation; Red: Prediction**

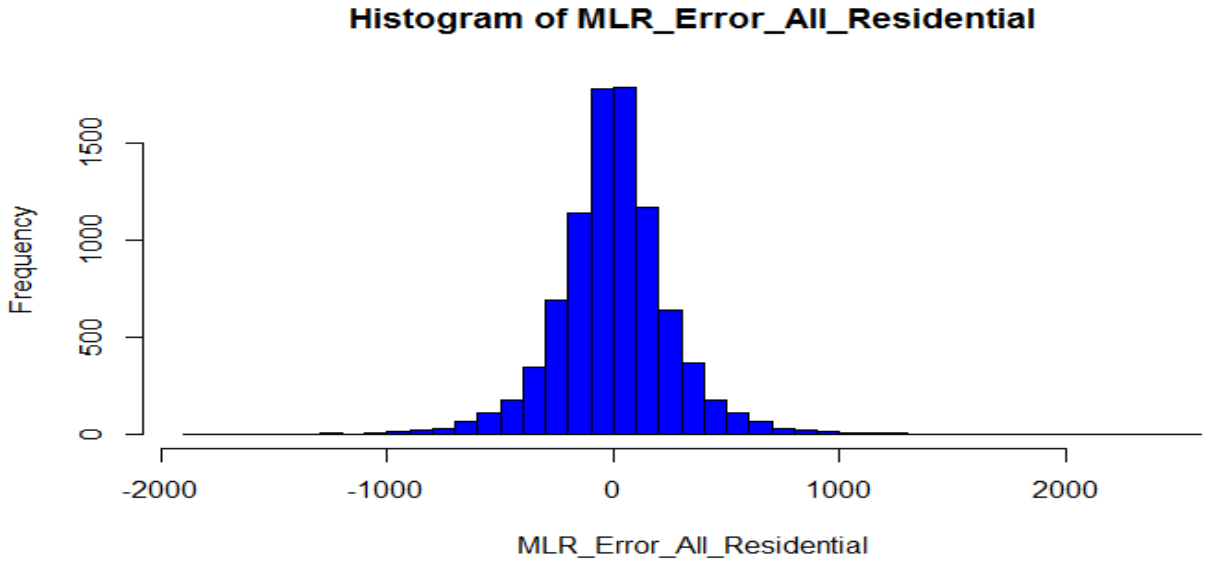


**Figure 4-11: Error Histogram [kW] for the District 1; Whole Year Period**

Based on the reference office building developed earlier, the average heating demand schedule of the office buildings within ***district 2*** was predicted and presented in **Figure *4-12*** and **Figure *4-13***. Due to the higher daily fluctuation of the heating demand schedule of the office building especially at the early morning and the late afternoon, switching between the occupied and unoccupied periods, the average standard errors for office buildings is higher and about 20.16 kW. Taking into account average office building area and average maximum peak, this value is slightly higher (1.6%) for the office buildings.

Finally, the last community was modeled using both simulation and simplified models. Results obtained for ***district 3*** shows that due to a higher number of the residential buildings within the district, the predicted profile is better fitted with the simulated schedule. The R value for ***district 3*** is about 0.9856 and the average error is about 5.2%, which is quite close to the one obtained for ***district 1*** (4.67%). **Figure *4-14*** and **Figure *4-15*** present the simulated heating demand profile against the predicted one for ***district 3.***

Aside from high prediction accuracy of the presented model, the low computational time of the model is another advantage of the proposed model over existing models. Having the heating energy demand profile of the reference building, the only time consuming step in the proposed model is the training step. After training the model, the prediction time required for predicting the heating energy demand profile of the remaining building within community is in order of less than a min per unit comparing with 5-10 min per unit for comprehensive modeling.

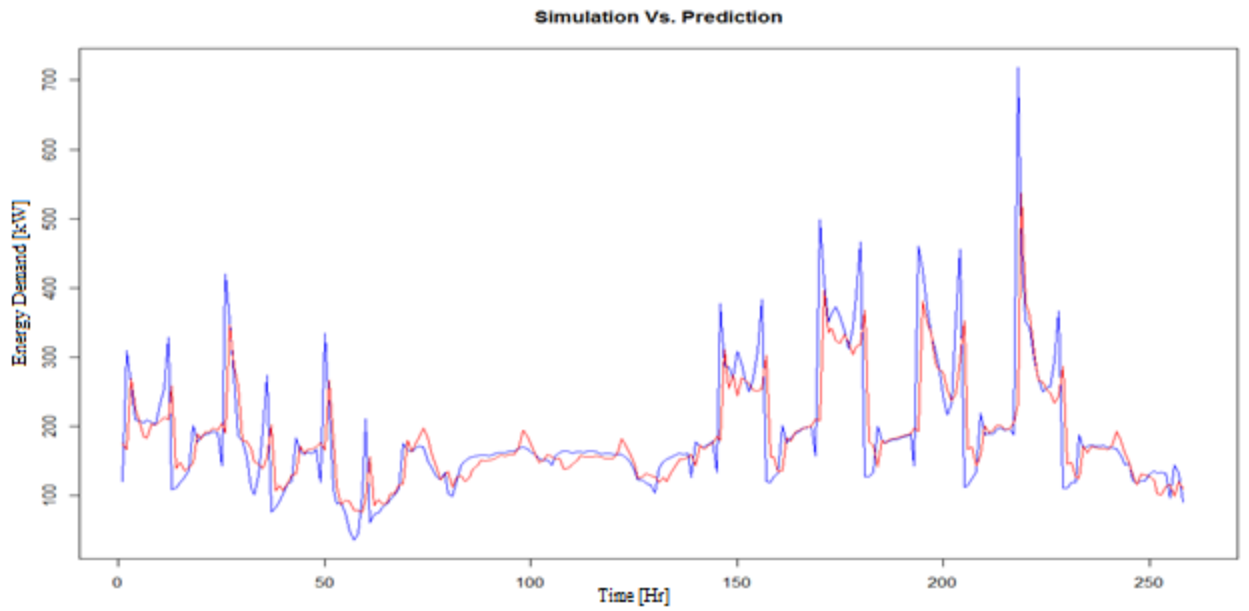


**Figure 4-12:** **Predicted heating demand Profile [kW] vs. simulated demand profile [kW] of district 2; Last 11 Days of December [hr]; Blue: Simulation; Red: Prediction**

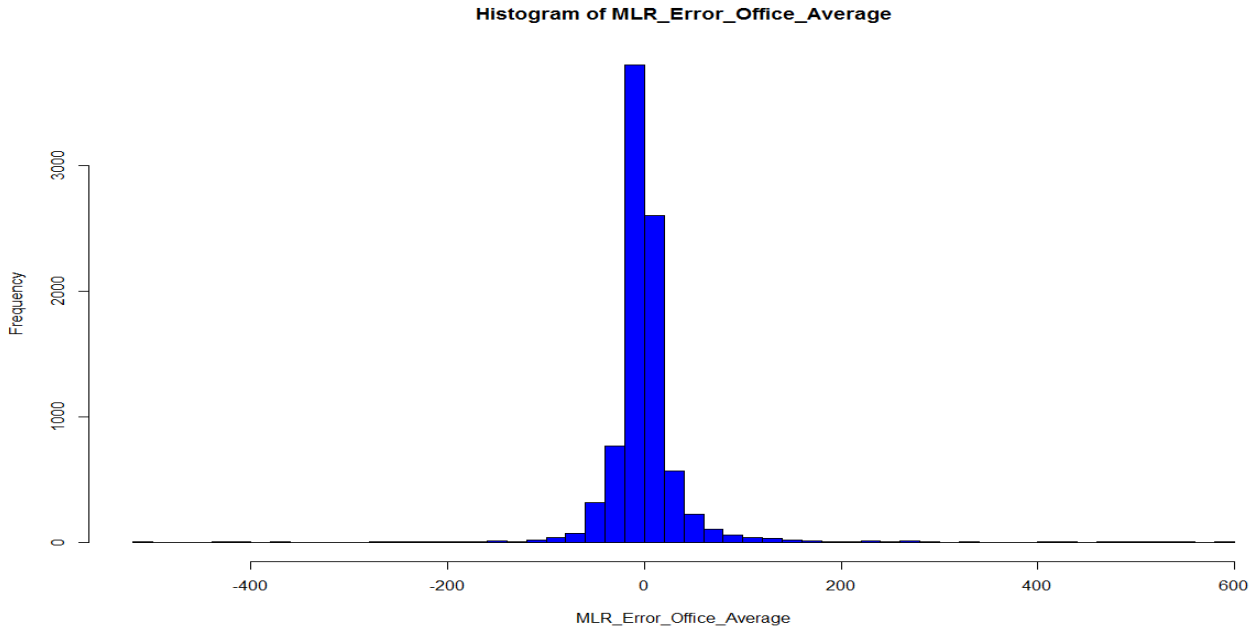


**Figure 4-13:** **Error Histogram [kW] for the District 1; Whole Year Period**

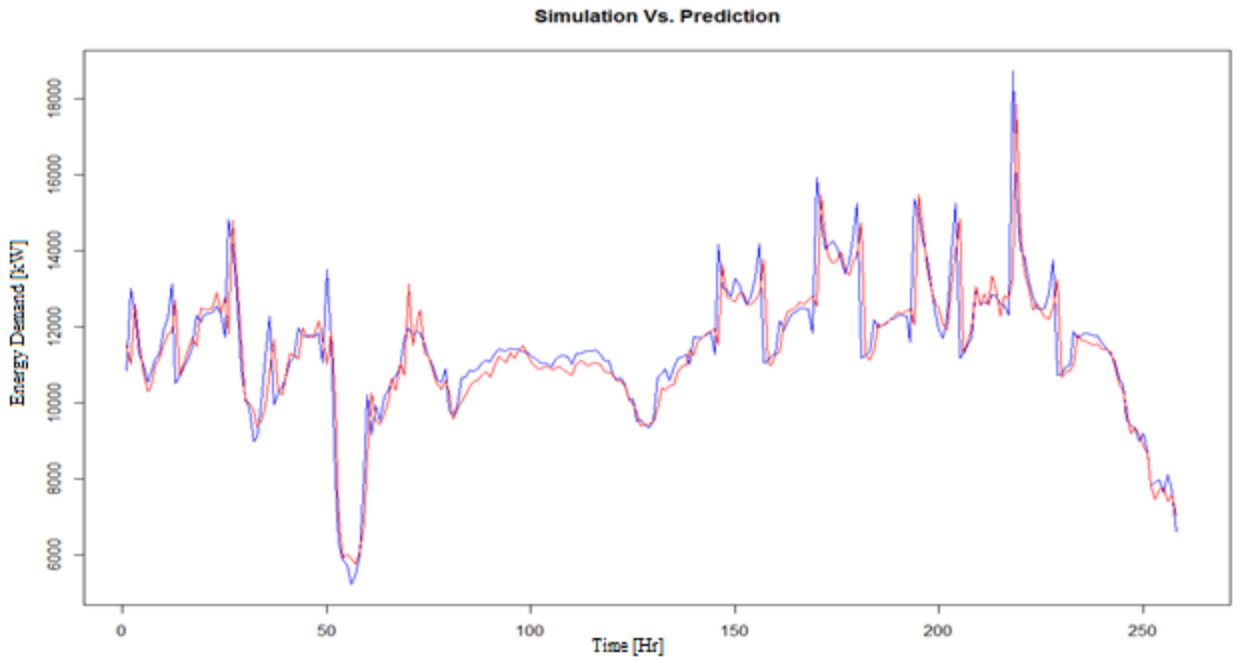


**Figure 4-14: Predicted heating demand Profile [kW] vs. simulated demand profile [kW] of district 3; Last 11 Days of December [hr]; Blue: Simulation; Red: Prediction**

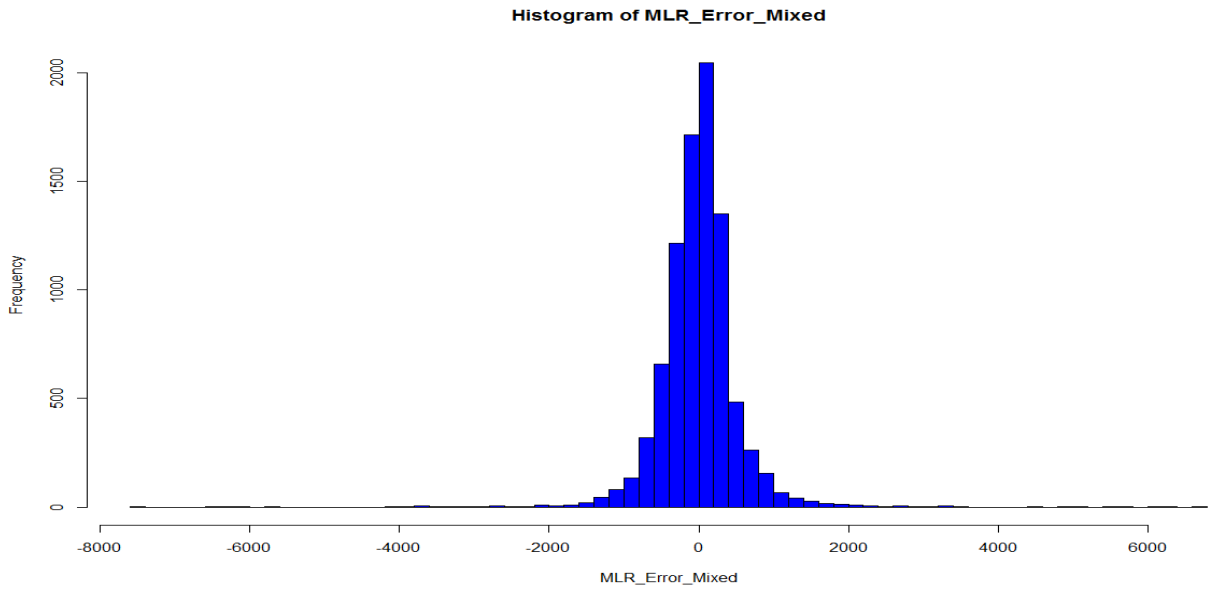


**Figure 4-15: Error Histogram [kW] for the District 1; Whole Year Period**

## 4.2. West Whitlawburn Housing Community (WWHC)

In next step, an existing H-CDHS was selected in order to validate the performance of the proposed simplified procedure. Therefore the proposed model was utilized and the HEDP of the district was predicted and results obtained from the prediction were compared with the one obtained from the measured data.

### 4.2.1. Description of the DHS

The selected Hybrid Community-District Heating System (HCDHS) is a mid-size community district heating system in Whitlawburn, Cambuslang, Scotland (WWH). The West Whitlawburn Housing Community WWH was established in 1989 to provide local community control and promote affordable quality housings for lower-income families. The community consists of 640+ dwelling units with four types of buildings. Until 2007, all buildings used the conventional individual dwelling electrical heating systems for the space heating and domestic hot water (DHW) supply. In 2007, the administration board developed their own district heating system to give the community a more affordable energy and improve the quality of the indoor environment by increasing the energy efficiency and decreasing the energy cost. Thus, after performing a feasibility study, the community management decided to develop their own DHS using a central energy center[11] a network of insulated pipework connecting the boiler house to users, and individual direct heat interface units in each dwelling. **Figure *4-16*** shows the location of buildings connected to the H-CDHS with respect to the boiler house:

1. Newly renovated towers of 12 stories (6 towers)

[11] A boiler house with a biomass boiler as its main heat generator, three backup gas boilers, and a 50m3 hot water thermal storage tank to cover potential winter peaks.

2. Newly built duplex detached houses (50 buildings)
3. 4-story terrace buildings (10 buildings)
4. Community buildings (5 buildings)

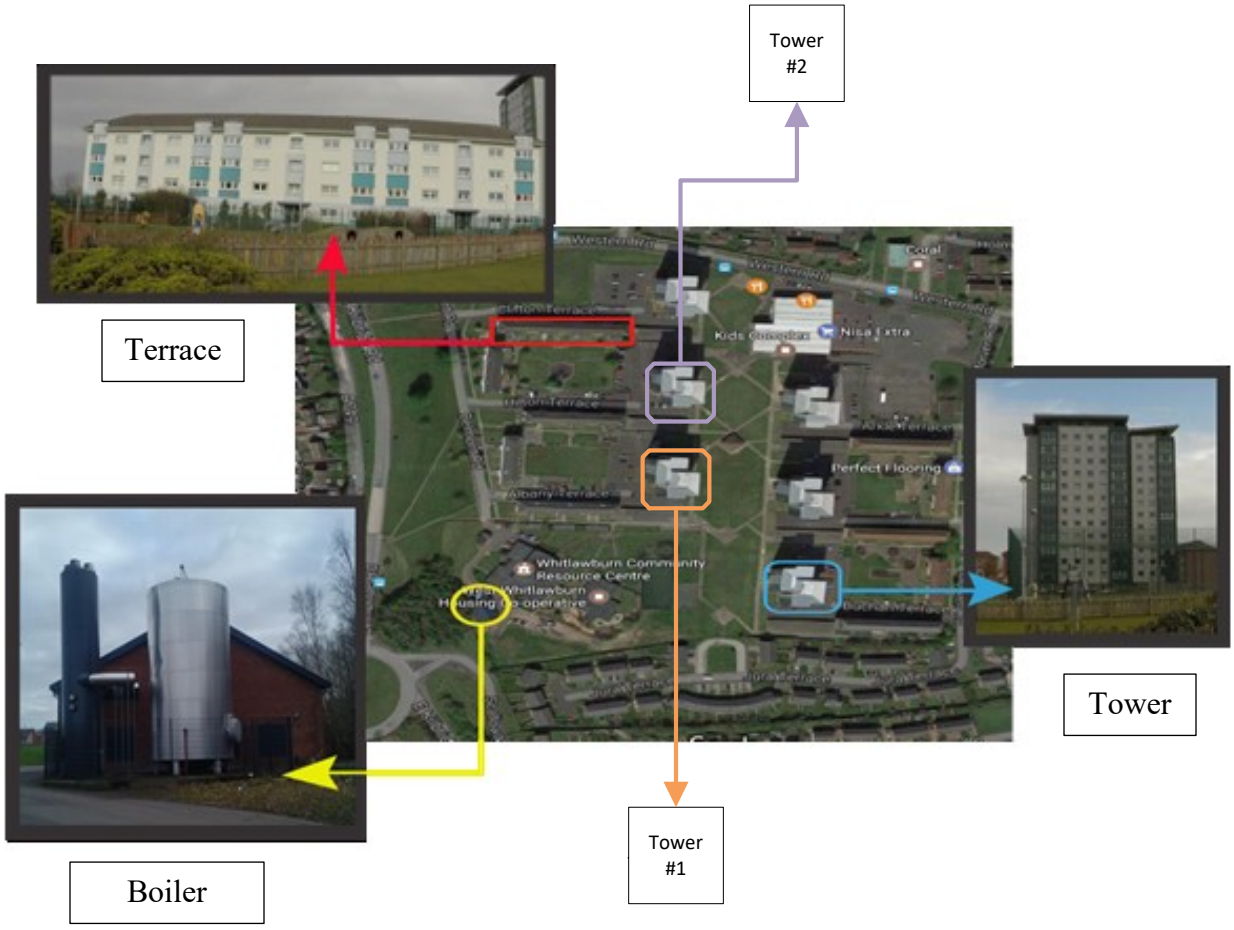


**Figure 4-16: Hybrid community-district heating system layout in Whitlawburn, Cambuslang, Scotland**

Although most recent district systems prefer using the medium to low water temperature to minimize the heat loss, an operational temperature of 80°C was chosen in this case to satisfy the minimum temperature required for DHW usage. The proposed H-CDHS can be thus categorized somewhere between the second generation (high temperature) and the third generation (energy storage) of the DHSs according to the district system's generation type (See **Figure *2-1***). In the

first development phase, six high-rise towers and five terrace buildings were connected to the H-CDHS. To size the boilers and the thermal storage tank, conservative industry standard sizing methods were used, following the Design Day method, which pre-dates the current guidance [150]. The district's energy demand was predicted based on the living space's total square meters and the Scottish building stock's annual energy consumption benchmarks [151].

### 4.2.2. Monitoring the district heating system's performance

Since 2014, the district heating system became operative and provides energy for more than 80% of the dwellings within the community. To better understand the system's heat flow, a monitoring Building Management System (BMS) interface was installed, enabling operators to monitor the system's energy generation, the distribution network loss, and energy consumed by tenants at different measuring points (MP). The main advantage of having a BMS system with multiple MPs is that the data obtained from different MPs can be used to validate and calibrate other MPs and estimate heat loss in the H-CDHS. In other words, using the data collected from the district line and smart meters helps operators to measure the energy purchased by tenants, to compare it with the energy generated by the boiler house, and to eventually determine the distribution networks' heat loss. Thus, the MPs potentially help to verify the measurements' accuracy at different stages. There are five MPs types installed in the H-CDHS at different locations and data acquisition frequencies as shown in **Figure *4-17***:

1. Smart meters located in each dwelling monitor energy consumption of both space heating (SH) and domestic hot water system every 30 minutes.
2. Energy meters installed on the dual heat exchanger units for SH and DHW inside the dwelling heat interface units (HIUs) (See **Figure *4-18***) which provides the monthly supply

and return hot water pipes' real-time mass flow rate and temperature, energy and volume pulse outputs, and accumulated energy demand.

3. Building block energy meters similar to those in the HIUs at the entrance of each building block were mainly used to measure the accumulated energy consumed.
4. District line meters measure the hot water flow rate, the HCDHS main supply line, and the boiler house's temperature every 5 minutes.
5. The boilers sensors measure the accumulated amount of the fuel consumed and the energy generated by each boiler every 15 minutes.


**Figure 4-17: (A) Smart Meter; (B) Energy Meter; (C) District and Block Meter; (D) Boiler Sensors**

**Figure 4-18: The Dual Heat Exchanger Sub-System**

A dual pipe network transfers the heated water from the boiler house to the building units, where a dual heat exchanger (sub-system) was installed to provide energy for the space heating

and domestic hot water purposes. **Figure *4-19*** and **Table *4-7*** present the schematic plan of the MPs used in the WWHC.

**Table 4-7: Location, Type and number of the MP**

| WWHC MPs | | | | | | | |
|---|---|---|---|---|---|---|---|
| ***MP*** | ***Name*** | ***Location*** | ***Number*** | ***Type*** | ***Unit*** | ***Frequency*** | ***Type*** |
| MP-1 | Building Meter | Entrance of Buildings | 6 | Energy Consumed | MWh | Monthly | ***Manual*** |
| MP-2 | Smart Meter | Each Unit | 6x72 | Energy Consumed | kWh | 30 min | ***Incremental*** |
| MP-3 | District Meter | Boiler House | 1 | Flow | $m^3$ | 15 min | ***Incremental*** |
| | | | | Supply Temp | °C | 15 min | ***Incremental*** |
| | | | | Return Temp | °C | 15 min | ***Incremental*** |
| | | | | Energy Provided | MWh | 15 min | ***Accumulative*** |
| MP-4 | Weather Sensor | WWH Site | 1 | Dry Bulb Temp | °C | 15 min | ***Incremental*** |
| Mp-5 | Thermal Storage | Thermal Storage | 1 | Mean temp | °C | 15 min | ***Incremental*** |
| | | | 6 | Different Depth | °C | 15 min | ***Incremental*** |
| Mp-6 | BioMass Boiler | Boiler House | 1 | Flow Temp | °C | 15 min | Incremental |
| | | | | Return Temp | °C | 15 min | Incremental |
| | | | | Flow | $m^3$ | 15 min | Incremental |
| | | | | Power | kW | 15 min | Incremental |
| | | | | Fuel Wood | kg | -- | Manual |
| Mp-7 | Gaz Boiler | Boiler House | 3 | Gaz Fuel | $m^3$ | -- | Manual |
| | | | | Energy Delivered | kWh | -- | Manual |
| BMS | Total Power | Boiler House | | | kW | 15 min | Incremental |

As previously mentioned, a wide range of users with different socio-economic levels and behavior demands are connected to the system. Since a large number of users are among lower income families, their energy consumption, and consequently their annual energy demand, are highly dependent on their economical state and the financial support received. Thus, the management office developed a prepaid energy credit system allowing each tenant to buy a credit in advance. The prepaid system connects to a smart meter in each unit. Smart-meters function both as an MP and a user interface that records the costs associated with the energy consumed every half hour, which tenants could use to monitor their energy usage over time.

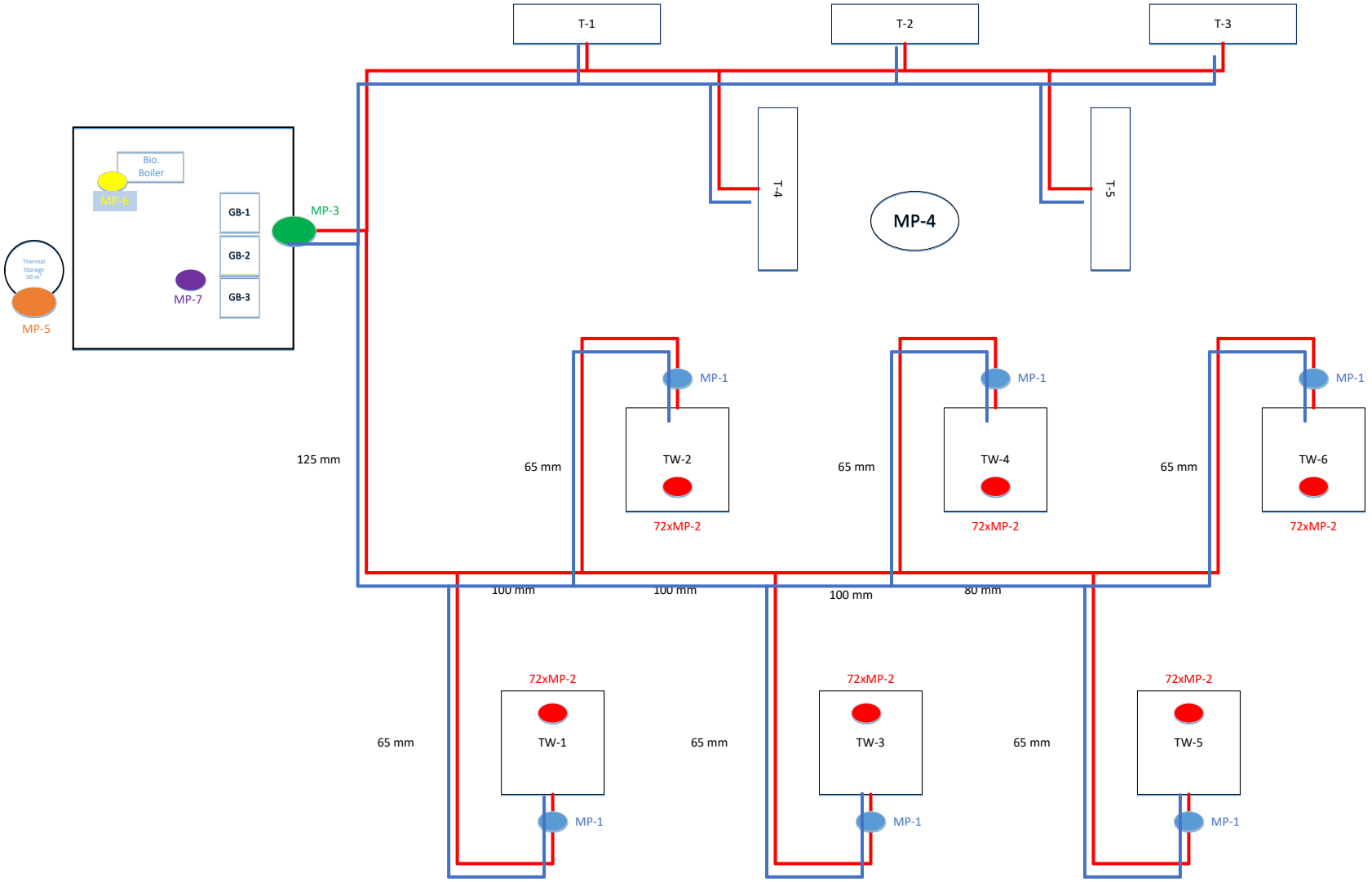


**Figure 4-19: Schematic Plan of the Type, Location and Number of each MP**

#### 4.2.2.1. Limitations in Demand Profile Prediction

After surveying the site and reviewing the plant sizing and load prediction procedures in the design stage, it was concluded that several initial simplifications were made to predict the district system's heating load:

1. All users were treated identically, irrespective of their behavior, socio-economical background, etc., leading to a potentially significant error in the load prediction. For example, while some senior tenants heat their units at a higher temperature throughout the day, younger tenants try lowering their heating bill as much as possible by turning off the system at night, and by using it for a short period of time in the evening. Those for whom social welfare is the only income could potentially tolerate lower interior temperatures and use less hot water than more affluent tenants. These factors were not considered in detail in the early design stage.
2. All units were modeled following the same benchmark assumptions, while units' characteristics (e.g. layout, orientation, insulation level, and window-to-wall ratio) were ignored. For example, on top of developing the district heating system in 2007, the exterior facade of all high-rise towers was renovated by adding a new layer over it. Also, balconies were converted to solaria, primarily on the south and west sides, which could potentially compensate a large amount of heat requirements during the day due to solar gains. This highlights the potential error in using standard benchmarks, which are commonly based on the floor area and the building age.
3. System heat loss was estimated based on the operating temperature of the distribution network supply (85°C) and return (70°C), and the constant heat loss per degree temperature throughout the building envelope. This assumption could hold for the newly renovated

buildings, but not for the partially renovated terrace buildings (the community's oldest buildings). In this case, the oversimplified assumption underestimates heat loss and thus overestimates the demand profile prediction. However, underestimating the buildings' heat loss could partly compensate for overestimating heating demands. But since the number of units in the terrace buildings is less than 20% of the total units connected to the district system, this underestimation is not enough to compensate for an exaggerated heating load prediction for the high-rise units.

Simplifications and conservative standard methods can greatly overestimate the overall energy and peak demands, causing an oversized and inefficient system with correspondingly increased capital costs provoked by short cycling, an increase in inefficient combustion maintenance requirements, and potentially shorter lifetimes and replacement periods. Therefore, an alternative method that addresses these weaknesses was evaluated.

#### 4.2.2.2. Data Validation

To ensure accuracy, all measured data were cross-validated at three different levels, including unit level, building level, and district level. The methodology was applied to Arran tower (***Tower #1***) and Arian tower (***Tower #2***). In the preliminary validation of the data collected by smart meters in the Arran Tower units over four months of heating (November 2016 to February 2017), tenant occupancy was verified and any changes in the unit occupancy was eliminated from results to avoid errors in the unit energy demand profile. After eliminating units with different tenants[12], the monthly energy demand of the remaining units was calculated using the data collected from smart meters. The monthly energy demand in units with similar tenants is expected

[12] Between November 2016 and February 2017

to correlate with the monthly outdoor temperature. Therefore, a unit's monthly usage in months with similar average outdoor temperatures should remain almost constant. To ensure building data accuracy, the cumulated monthly usage of all units in each building and the building's linearized heat loss were calculated and compared with the building meter. A similar procedure was chosen at the network level. The boiler house's total output was compared with the accumulated energy demand of all buildings with the network losses added.

### 4.2.3. Data Analysis

In the first step, the CDHS' two-year long monitored data was analyzed. Results showed that CDHS' existing condition operates less efficiently with a higher heat loss than the expected design efficiency. Moreover, the predicted heating demand load for sizing the boiler house was 2-2.5 higher than the district's actual demand power load. This overestimating caused an oversizing of the boiler house. Given this, the boiler never worked at its optimal capacity and most of the time operated at a partial capacity, which decreased the system's efficiency. Tenants' behavior is widely variable and possibly affected by individual characteristics, including economic status. The preliminary analysis of the data obtained from smart meters in each unit showed that units with almost identical physical characteristic have significantly different monthly energy demands. A field investigation and a recorded data reading revealed that only a few units used a thermostat with a given set-point value to control the space heating. The majority did not use the heating system for most of a day. In most units, the heating system was off during a day and night, or only was used briefly during the day. For tenants who turned on the heating more frequently, such unexpected behaviors were oversimplified in the CDHS' design stage, assuming that all tenants use thermostats to control space heating on a regular pattern during a day and night.

#### 4.2.3.1. Clustering

The first step in predicting the heating load, using the four-step procedure mentioned in the methodology section, is to define the number of clusters required. To do that, all the units were initially divided based on their built form and construction type into two archetypes, including the newly renovated high-rise, and partially renovated old terrace buildings. The units within each archetype were further segmented based on their occupancy behavior. A sample population dataset was selected to define the optimal number of archetypes associated with the occupants' behavior in each construction type. The total energy consumption [kWh], the number of the inner-unit heat exchanger on/off cycle per month, the peak monthly load [kW], the monthly heating degree day (HDD), and the average monthly outdoor temperature were determined as effective parameters for defining the number of archetypes. For large-scale communities with numerous users like WWHC, using all monitored data from every individual unit to determine the parameters required for defining the optimal cluster number is computationally intensive. Instead of calculating the required parameters of all units, the parameters of a smaller sample data that could represent the same distribution as the whole community were considered (***Arran tower*** with72 units). The results were extrapolated to the entire data-set (***Arian tower*** and the whole district).

**Figure 4-20** shows Arran tower's average monthly energy demand (for all dwelling units) for both DHW and SH, between November 2016 and February 2017. This figure shows the range of energy demand fluctuation when outdoor temperatures and monthly HDD do not vary considerably. Variations between 5.17°C and 5.98°C for outdoor temperature and from 312 to 331 for monthly HDD (**Figure 4-21**) are not significant for most units. Results obtained for all individual units in the Arran tower show that the monthly energy demand remains almost constant, with unit-to-unit variation generally being much greater than that of a unit's monthly variation

(except units 12, 37 and 39). Hence, most units' demand profile's monthly average is expected to remain almost constant (**Figure 4-20**).

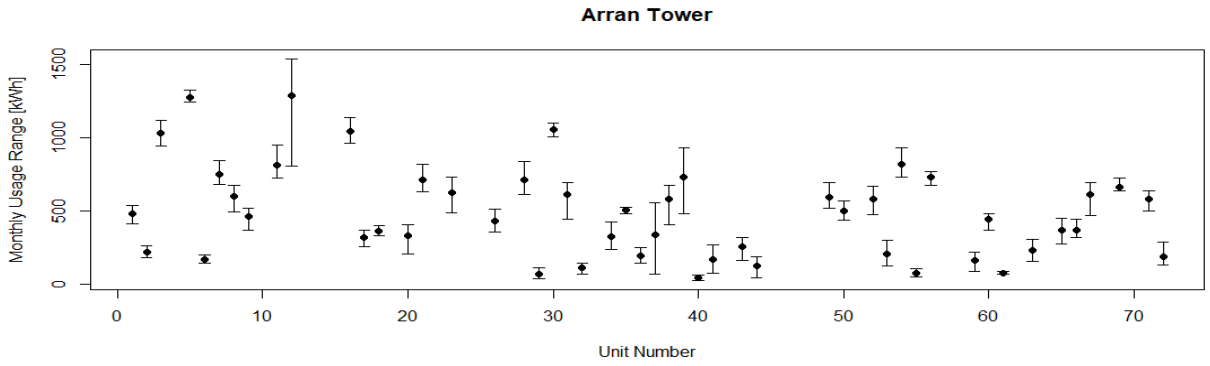


**Figure 4-20: Monthly consumption of individual units in Tower # 1, Arran Tower**

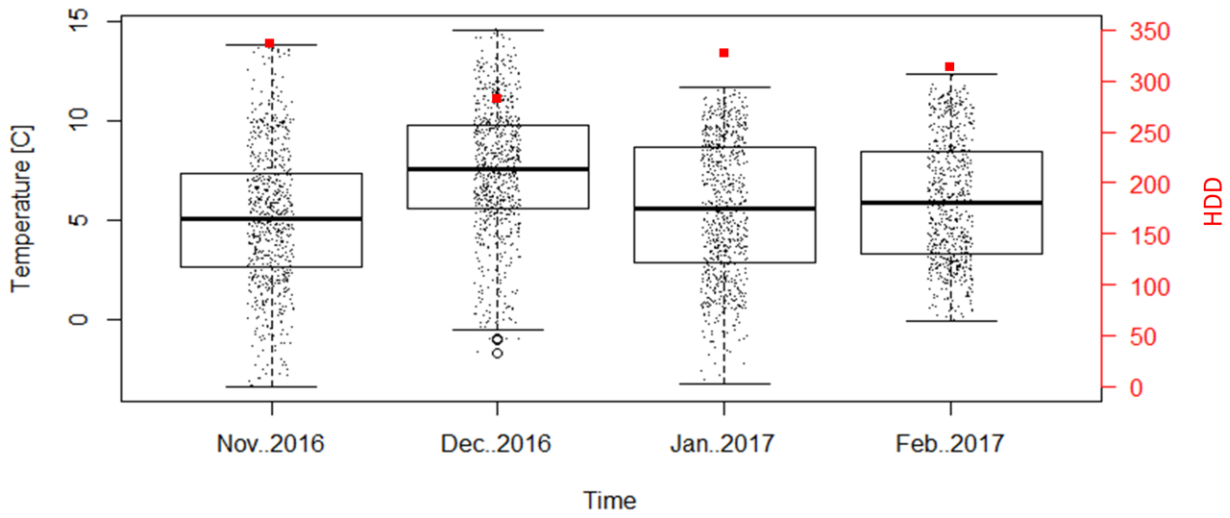


**Figure 4-21: Outdoor temperature and HDD for the 2016-17 heating season (Nov 2016eFeb 2017)**

Using the five parameters, monthly consumption, number of the inner-unit heat exchanger on/off cycle per month, monthly peak demand, monthly HDD and monthly outdoor average temperature, the K-means (number of clusters) varied between 1 and 20 to construct different

numbers of clusters. Using R software for each value of k, the square metric distance ($m^2$) of residual (R) from a reference point was determined in order to find the optimal number of archetypes (clusters) for simulation. This value was selected when the difference between the residual of two consecutive clusters became negligible. One should choose a number of clusters so that adding another cluster does not significantly increase the dataset presentation. The results are plotted in **Figure *4-22***, and it can be concluded that four to seven archetypes can be chosen as the optimal number. Here, k-means 4 was selected as the optimal number for demonstrating the method with adequate accuracy while maintaining computational costs low.

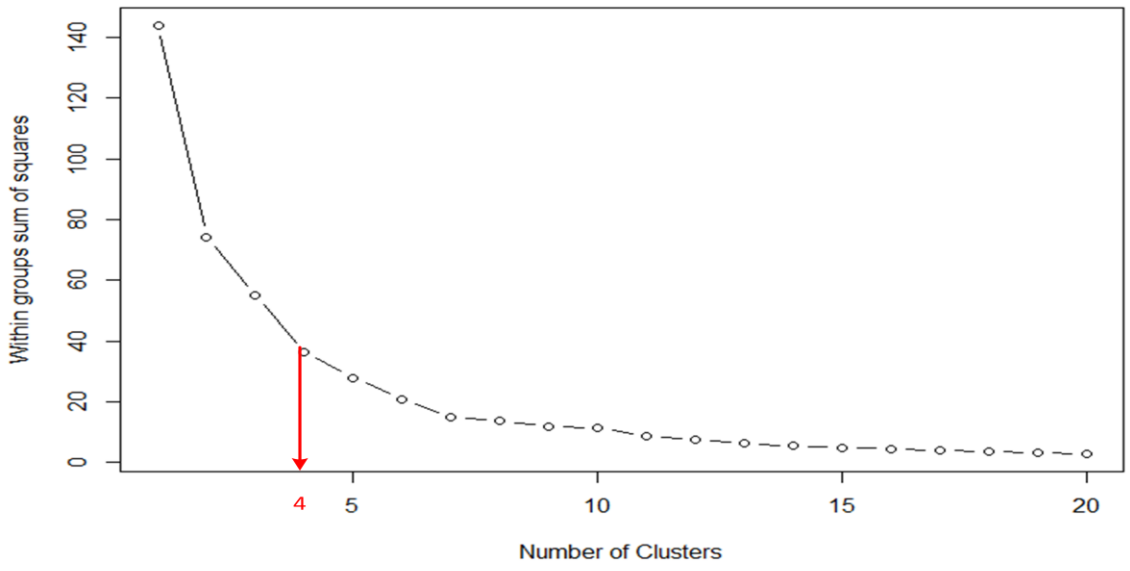


**Figure 4-22: Optimal number of archetypes**

Given the hierarchical clustering approach, all units in the sample dataset (***Tower # 1***) were divided into four different archetypes: Non-Typical High Usage (**NTHU**) as cluster 1, Non-Typical Low Usage (**NTLU**) as cluster 2, Typical Thermostat Control Usage (**TTCU**) as cluster 3, and Non-Typical Medium Usage (**NTMU**) as cluster 4 (See **Figure *4-23***). The percentage ratio of units within each archetype is shown in **Figure *4-23***. Results obtained from the clustering in ***Tower # 1*** show that only 5% of units are from the TTCU archetype. This value was assumed to be 100% in

the CDHS' design stage. The percentage of users in other archetypes are 16% (for NTLU), 24% (for NTMU), and 53% (for NTHU).

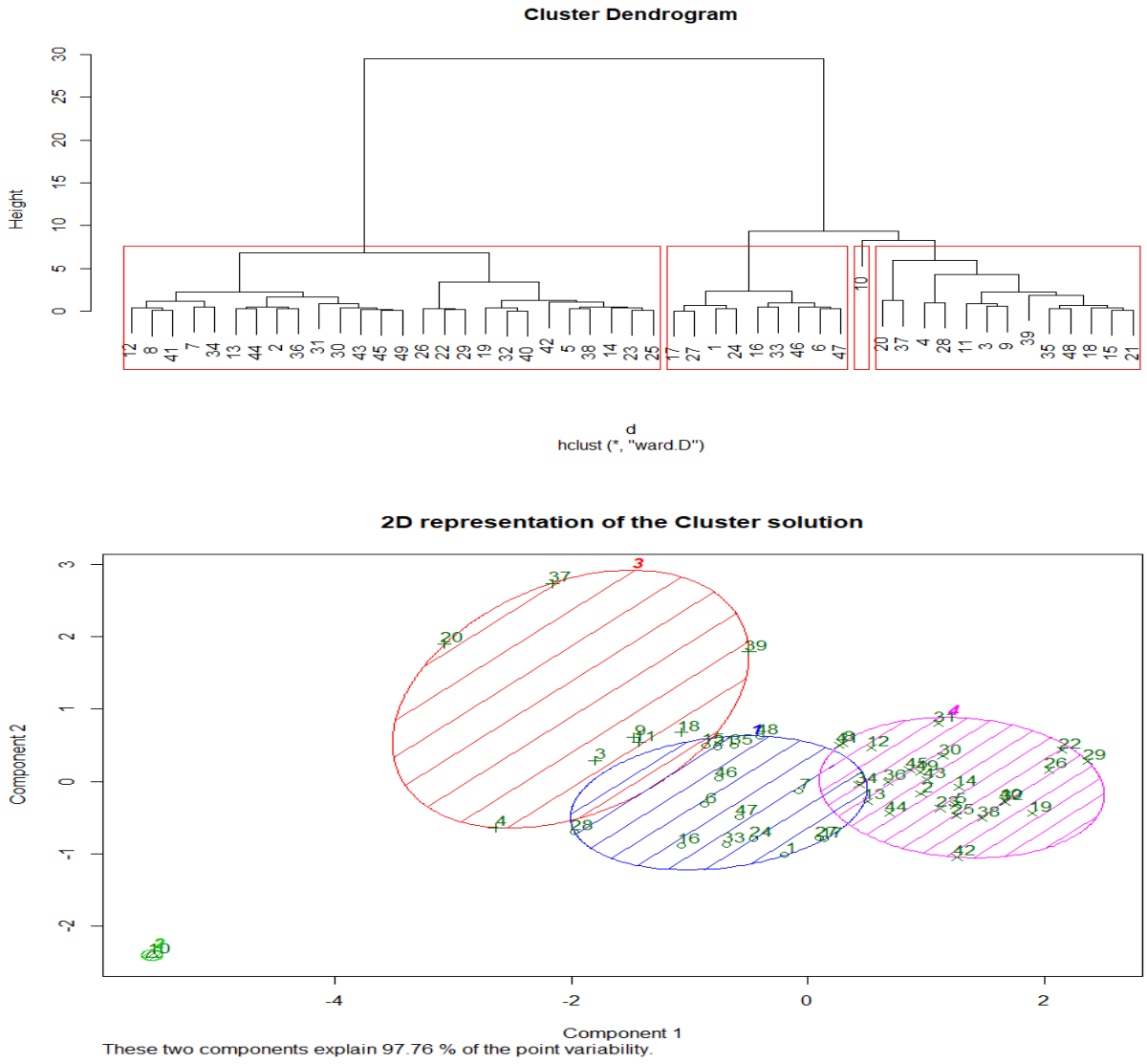


**Figure 4-23: Clustering Results for Tower#1**

**Figure *4-24*** shows the typical daily demand profile of the ***reference buildings*** associated with each defined archetype obtained from the monitored data. It is important to note that in the

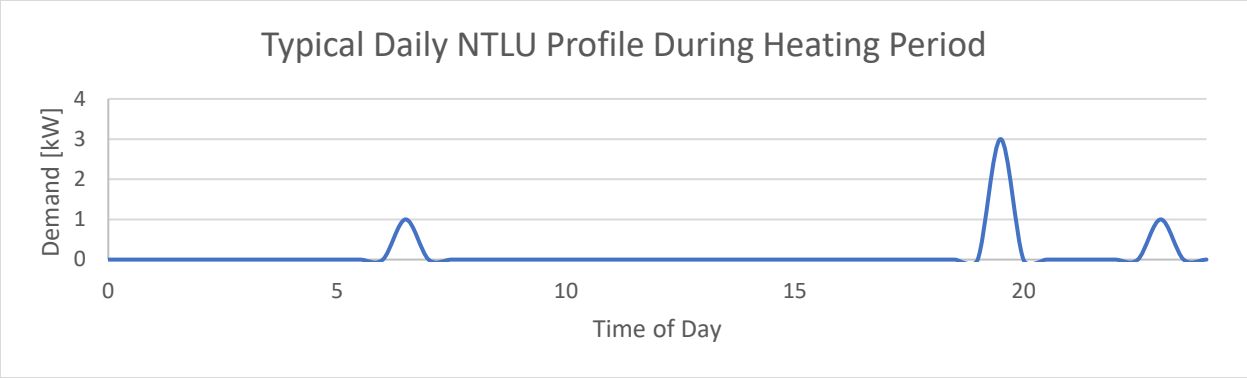


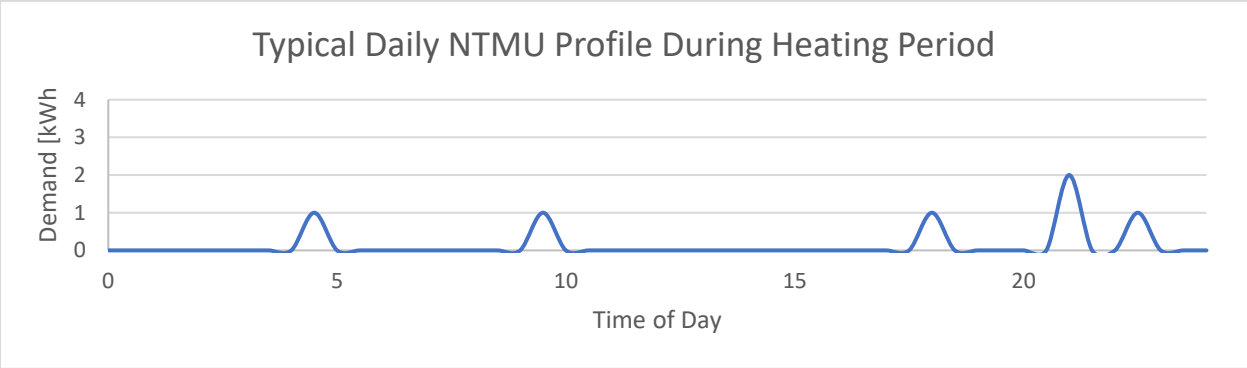


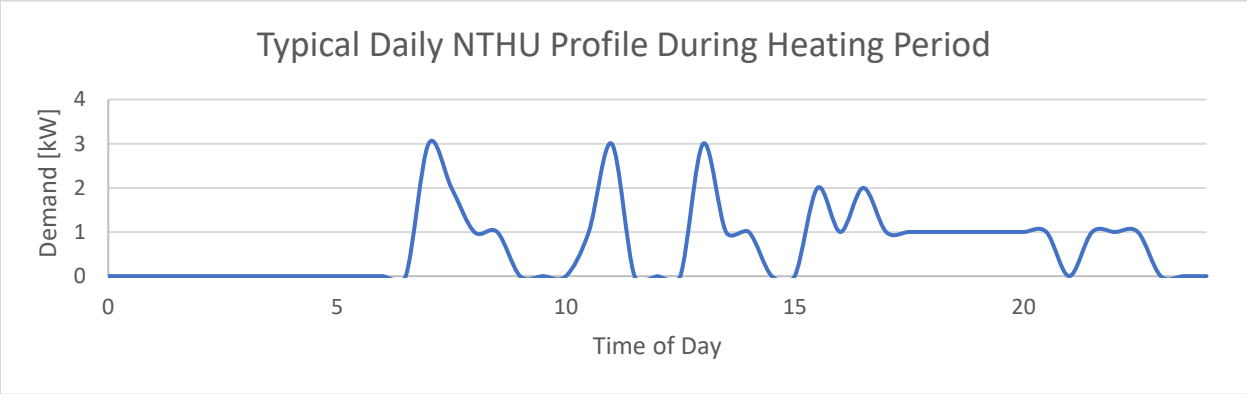


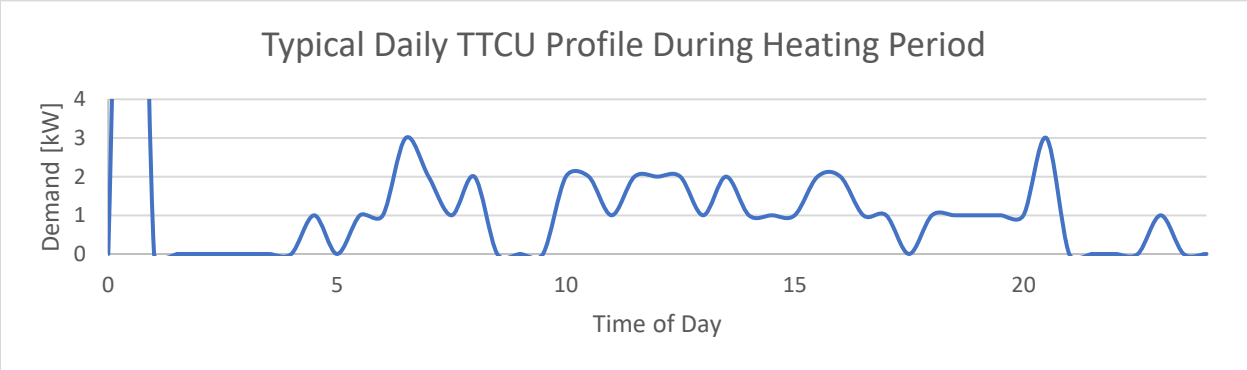


**Figure 4-24: Demand profile for reference buildings of each class NTLU (1), NTMU (2), NTHU (3), TTCU (4)**

training stage (step 3), the annual reference building's demand profile was used, while here only a typical daily demand was presented. The heating demand profile for different occupancy archetypes is similar to one reported by tenants in the field investigation. NTLU users' profile is largely dominated by a DHW usage in the morning and evening, and a slight use of space heating in the evening. NTMU users heat their space more frequently during the day, while NTHU and TTCU users generally use their thermostat to control space heating for defined periods. As a result, their heating profile is more continuous. NTHU users turn off their heating at night, while TTCU users keep it during a day, with variable night and day set points.

### 4.2.4. Predictive Model

After training the model using data from the reference buildings, and defining the input file for the remaining units, the heating demand profile of the district was predicted. The MNLR model was used here to predict WWH district's heating demand profile, trained by adopting the non-linear autoregressive model with an external Input (NARX). To account for the building's thermal mass effect on the unit's energy demand, the model used past target data, a demand profile, and other series of input parameters defined earlier in this study. To predict the demand profile in future hours, previously predicted values and input files were used at the same time. To determine the number of past hours required in the training stage, the model was trained with different past hours ranging from 2 to 8 hours. The best fit was set as the number of past hours required for representing the thermal mass of the units. For this study, 4 hours was the best fit. Also in this study, the data for real H-CDHS was used to train and validate the MLNR model using the above-mentioned four-step procedure. To verify the models' flexibility to include different users' behavior, WWH's diverse community with a wider range of users' behavior was used.

Due to limitations in acquired data, the adapted methodology (**Figure 3-1**) and developed Matlab code were slightly modified to further improve the model's accuracy, as explained below:

- In addition to the ***reference buildings'*** demand profile and three sets of input files (i.e. solar dependent, internal gain dependent, and temperature dependent data files), a time-dependent factor related to the DHW was also considered.
- In the initial model, the indoor-outdoor temperature difference was used to generate the temperature dependent data file. In this study, only the outdoor temperature was considered since the units' indoor temperature was not monitored.
- Since the internal heat generation was not monitored in each unit, the electrical energy consumed by the reference building was used to indicate the unit's internal energy generation. The existing internal generation from the British Housing Model (BHM) was thus adopted and scaled down to match the energy consumption.
- The adjusted typical thermostat control profile with a thermostat set-point of 19°C was used for the common area. For the towers, the common area accounts for about 15.8% of the total area of which only 45% is assumed to be conditioned.

Using the latter modifications, the input file for all units was generated. Moreover, the reference buildings and their demand profiles were defined earlier in the clustering step. Having the reference building's input file and demand profile, the MNLR model was trained and the related coefficients were determined. To verify the model's accuracy, its prediction was compared with measured data at three different levels. At the first level, the Arran tower's (***Tower #1***) heating demand profile[13] was predicted. At the second level, the model was applied to the Arian Tower

[13] This tower was used earlier to define the number of archetypes and the profile associated with each archetype.

(***Tower #2***) and its prediction was compared with the measured data. The entire district' total energy demand was then predicted and compared with the data acquired from the district's total energy demand.

#### 4.2.4.1. Energy demand prediction for the Arran tower (Tower #1)

In the first step, the energy demand profile of the Arran tower's *(**Tower #1**)* has been predicted. The predicted profile then was compared with the one obtained from measured data. **Figure** ***4-25*** shows the energy demand profile for the first ten days of November 2016 where appears a generally good agreement between the model's prediction and the measured data. The MSRE calculated for the hourly predicted profile was around 12.6%. A discrepancy between the two curves can be attributed largely to the inevitable lack of information about occupants' inherently stochastic behavior.

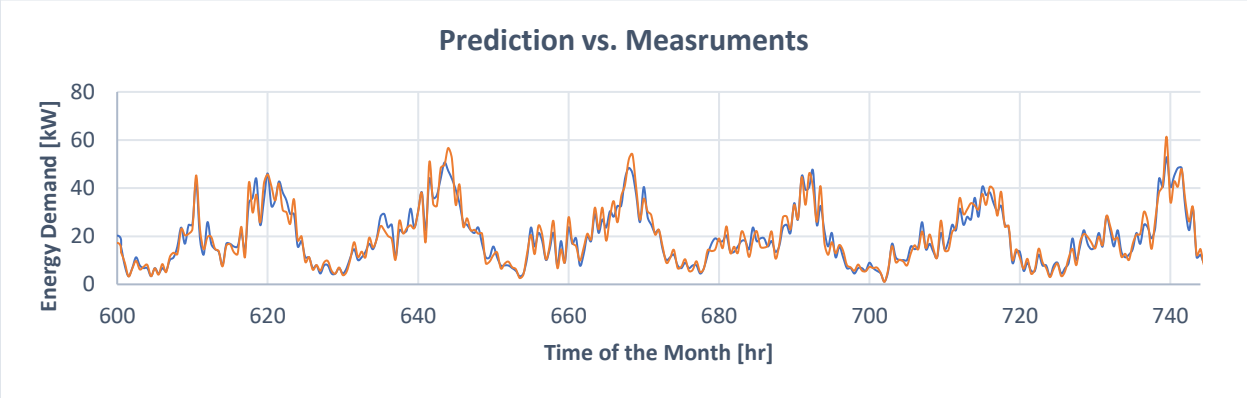


**Figure 4-25: Model prediction (Orange) vs. measured energy demand (Blue) for Tower #1.**

#### 4.2.4.2. Energy demand prediction for the Arian tower (Tower #2)

At the second level of model validation, the model's prediction is validated with the measured data for the Arian tower *(**Tower #2**)*. No data collected from this tower was previously

used to generate the model associated with the units' energy demand profile. The Arian tower holds 72 units and is approximately 300 meters away from the boiler house. **Figure *4-26*** compares the model's prediction and the measured data for the last 6 days of the December 2016, (**Appendix D (WWH Community Profiles)**). A good agreement can be observed. The MSRE calculated for the predicted data is around 21.7% for the hourly profile (entire year); 8.2% for the total consumption over the year and 6.7 total consumption over the heating season. The predicted demand's general trend matches the measured demand. Considering the data used to generate the demand profile model was based on occupants in a different tower, the result is remarkably good.

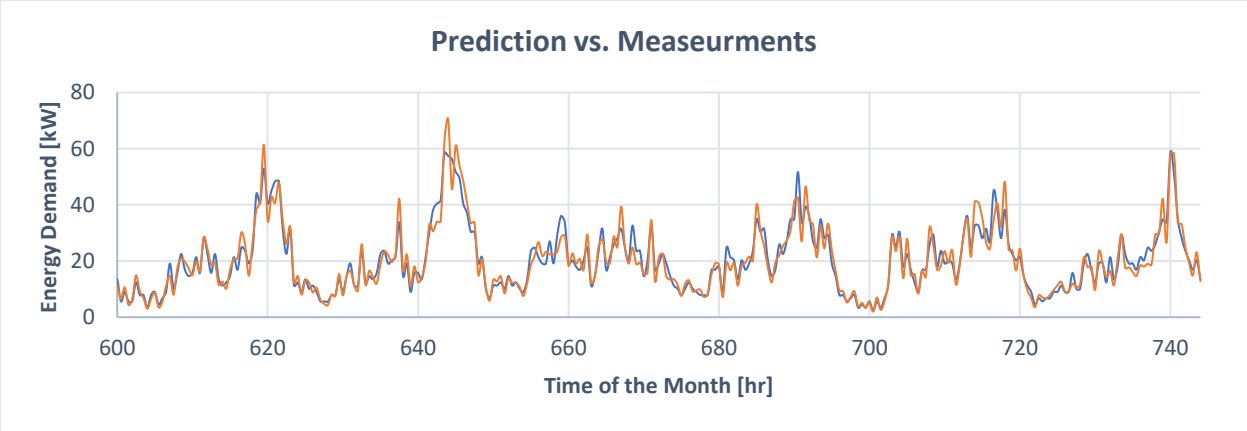


**Figure 4-26: Model prediction (Blue) vs. measured energy demand (Orange) for Tower # 2**

### 4.2.4.3. District energy demand prediction

The WWH district consists of six 12-story towers and five 4-story terrace buildings connected to the boiler house through an underground piping distribution network. To predict the entire WWH district system' total energy demand, predicting the loss and delivered energies is required and calculated in this section. To predict the entire WWH H-CDHS' demand, the demand

of each block has to be first calculated. The losses associated with the distribution system itself must be factored in.

The underground piping network has been used in this study is an insulated dual pipe network transferring hot water at a temperature of 85°C and a return temperature of 70°C with a total length of 2.4 km (1.2 km supply and 1.2 km return). **Figure *4-27*** shows the underground piping network' operational temperature.

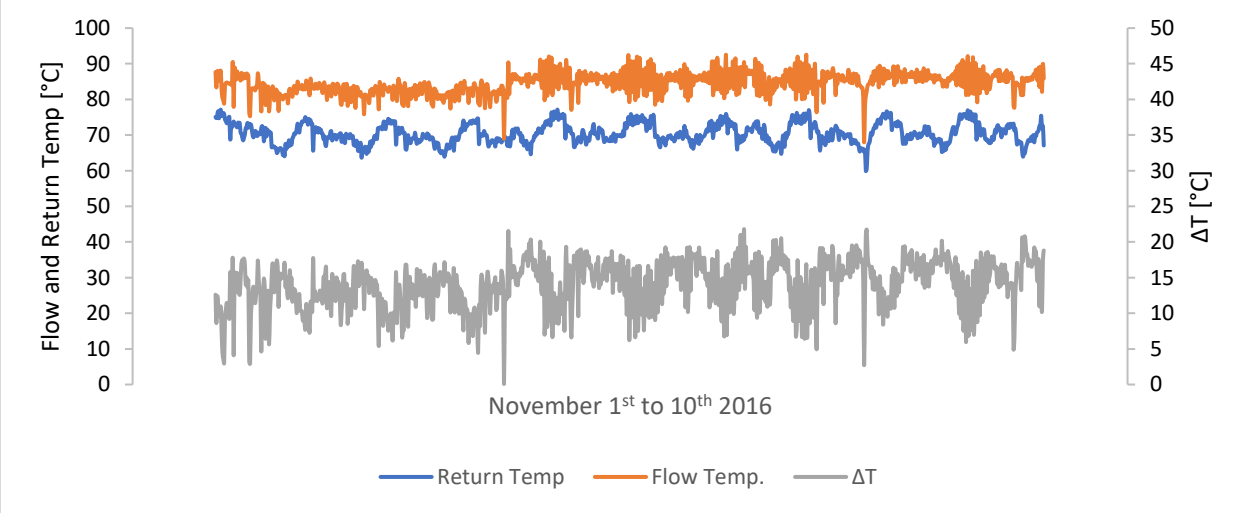


**Figure 4-27: Underground Networks Operational Temperature**

The underground network's operational temperature remains relatively constant during the year to control the amount of heat transfer from the boiler house to the consumers. This causes the system's mass flow rate to continuously vary. **Figure *4-28*** shows the fluctuating water flow rate in the first 10 days of November 2016.

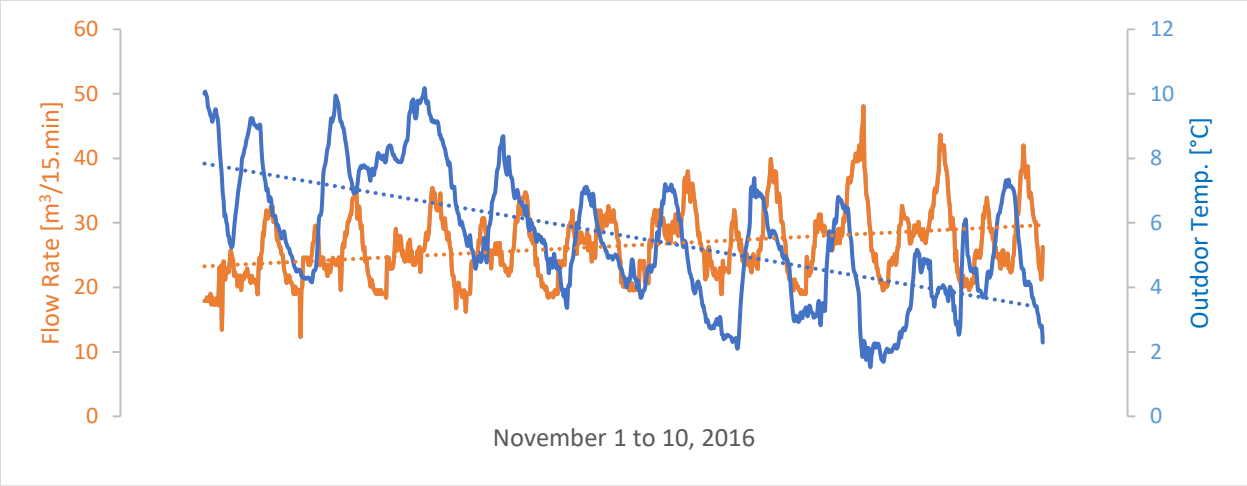


**Figure 4-28:** **Water Flow Rate vs. Outdoor Temperature in the Distribution Network**

Having the underground network's total length alongside its operational temperature, the supply and return pipes' water mass flow rate, the outdoor temperature, and the thermal properties of the soil and pipe insulations, the distribution network's total heat loss can be determined. To simplify the prediction process, a linear relation for the temperature difference between the operational temperature and surrounding environment temperatures is pre-assumed. **Figure *4-29*** shows the underground distribution network's predicted heat loss for the entire system.

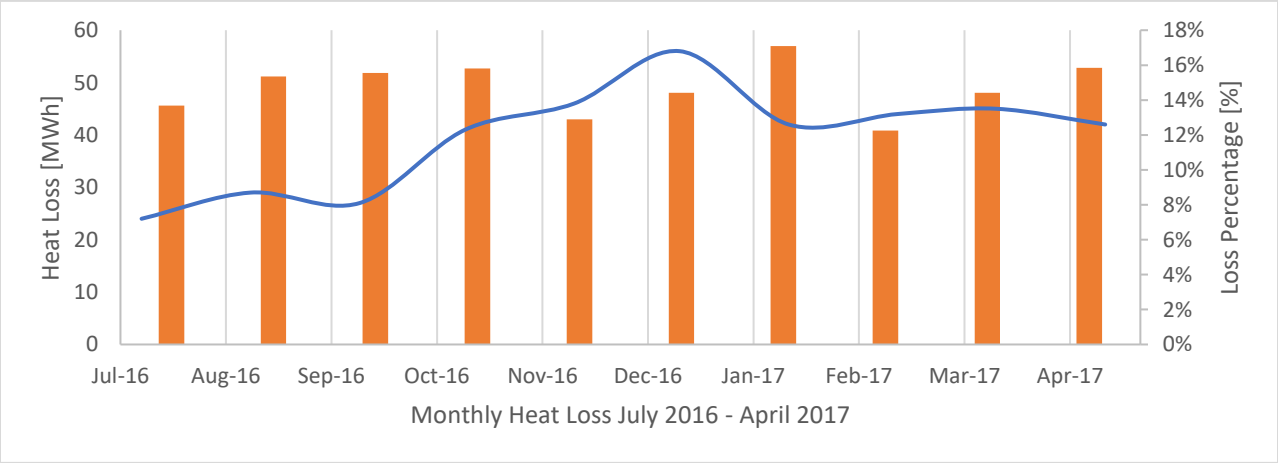


**Figure 4-29:** **Distribution network's monthly heat loss projection**

Since for many units the demand profiles are not available, the energy demand predicted for the entire system is compared with the total energy generated by the boiler house. As stated earlier, the boiler house's sensor measures only the accumulated amount of fuel consumed and the energy generated by each boiler every 15 minutes. **Figure *4-30*** and **Table *4-6*** shows the district's predicted accumulated energy demand against the energy generated by the boiler house.

**Table 4-8: Total Energy Consumption of the WWHC DHS; Prediction vs. Measurements**

| | *Predicted [kWh]* | | *Actual [kWh]* | | *Error* |
|---|---|---|---|---|---|
| | ***Monthly*** | ***Accumulated*** | ***Monthly*** | ***Accumulated*** | |
| ***Apr-16*** | 265000 | 265000 | 282000 | 282000 | 6% |
| ***May-16*** | 301003 | 566003 | 293610 | 575610 | -3% |
| ***Jun-16*** | 424837 | 990840 | 409140 | 984750 | -4% |
| ***Jul-16*** | 175360 | 1166200 | 168770 | 1153520 | -4% |
| ***Aug-16*** | 189030 | 1355230 | 185340 | 1338860 | -2% |
| ***Sep-16*** | 173552 | 1528782 | 177190 | 1516050 | 2% |
| ***Oct-16*** | 259411 | 1788193 | 266710 | 1782760 | 3% |
| ***Nov-16*** | 356885 | 2145078 | 368310 | 2151070 | 3% |
| ***Dec-16*** | 388553 | 2533631 | 429580 | 2580650 | 10% |
| ***Jan-17*** | 245779 | 2779410 | 349300 | 2929950 | 30% |
| ***Feb-17*** | 359021 | 3138431 | 358390 | 3288340 | 0% |

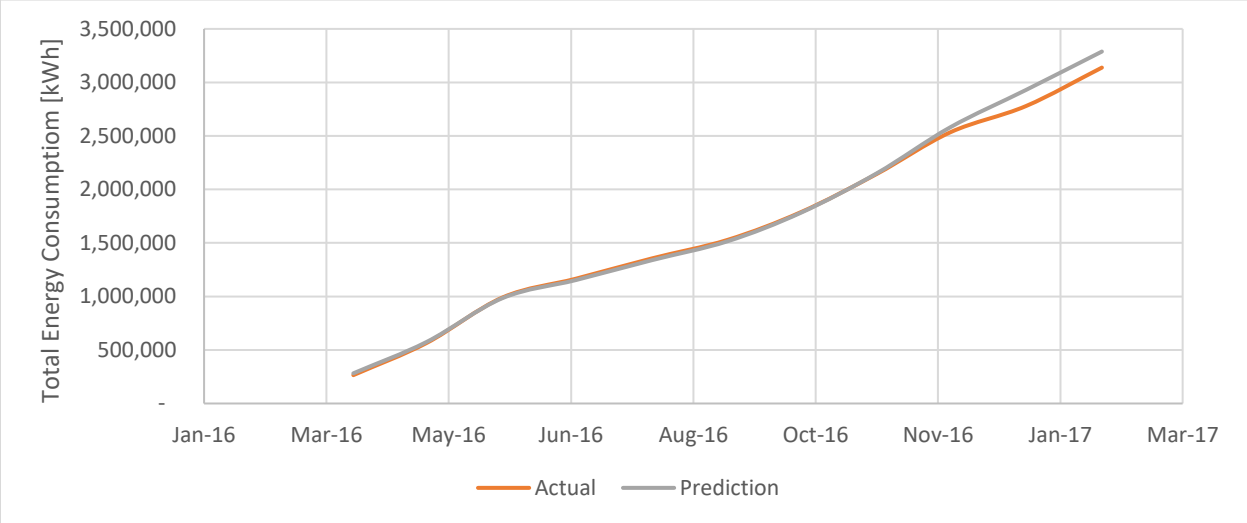


**Figure 4-30: Accumulated predicted energy delivered vs actual generated energy in the boiler house**

Results show a higher agreement between the predicted and actual energy demand with a monthly discrepancy between -4% and 6%, except in January 2017, when the error was approximately 30%. This error is due to a relatively high heat loss in the distribution network. In January 2017, given two faulty bypass valves in two different towers, the system's mass flow rate increased. Percentile and results in increasing the higher heat loss of the system are compared with the normal condition. Over a year, the accumulated energy demand predicted (3,288,340 kWh) shows a discrepancy of about 5% compared with the actual energy generated by the boiler house (3,138,431 kWh). The underestimation of the total energy demand of the district is mainly due to the buildings' heat loss, especially the older 4-stories terrace building with higher envelope deterioration. However, in the training process (Step 3), the reference profile obtained from the ***Arran tower***, which is better renovated comparing with the terrace buildings, was used with a relatively lower heat loss. It is important to note that at the training stage, the MNLR model was trained once using the reference building obtained from the ***Arran tower***. These trained models were later used to predict the heating demand profile of the remaining units, only by adopting their input file. Moreover, the ratio of the occupants' behavior considered in TTCU in the terrace buildings was slightly higher.

Regarding the heat loss of the system from the distribution network, the results obtained from **Figure *4-29*** shows that the heat loss of the system always remain within 12-16% percent of the total energy distributed by the network.

# Chapter 5: Optimisation

As mentioned earlier, the major design issue of the older district heating system (DHS) generations (1st to 3rd generation) was mainly high heat loss in the distribution network due to the high-temperature media (100°C and more) [14], [105]. In this regard, the optimization focus was on enhancing the system efficiency by controlling the heat loss from the system and subsequently, improving the system efficiency. As a result, most optimization studies have focused on minimizing the system heat loss. However, the new generation DHS (4th generation) operates at a lower temperature (50-60°C), and hence achieving higher system efficiency is possible by adopting appropriate control strategies and also through optimization of the equipment size [103], [106]. Note that, designing the 4th generation DHS based on the conventional design method, sizing the equipment based on the peak demand load, could lead to oversizing of the equipment and low system efficiency. Therefore, the adoption of an optimal approach (for cost and energy) to enhance the efficiency of the DHS while designing the 4th generation DHS became a standard practice among designers.

Considering the above-said research gap, the main objective of this study is to develop a dynamic optimization platform that could explore the optimal equipment size using the detailed demand profile in a timely manner. The developed model predicts the detailed demand profile of the DHS and uses them along with detailed energy model of the DHS and the equipment, and interaction between them to dynamically optimize the entire system. Subsequently, the optimal size of the equipment is obtained. The size of the equipment obtained from the model is later compared with the one obtained from the conventional method (design day method), as well as

using a static optimization tool, (Biomass optimization tool). In this regard, data from an existing H-CDHS with an integrated thermal energy storage system is used to optimize its boiler house to minimize its overall cost and $CO_2$ emission.

To do so, TRNSYS was used as the simulation platform to define the relationship between various system components and to couple the prediction and optimization tools. Also, a previously developed simplified load prediction model was used to dynamically predict the system demand load [66]. Results obtained from the prediction tool were fed as input to the TRNSYS file in the text format. The optimization process was then performed for an operational mode by coupling the simulation (TRNSYS software) and optimization tools (MATLAB/Simulink) as shown in **Figure *5-1***.

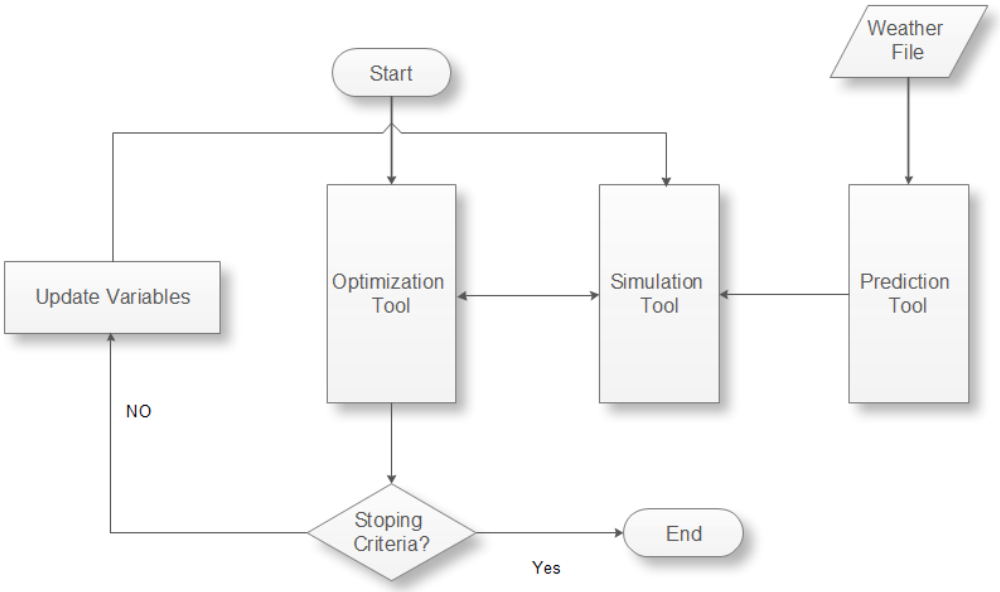


**Figure 5-1: Prediction, Simulation, and Optimization Process Flowchart**

## 5.1. Load Prediction Scenarios

To optimize an H-CDHS, the first step is to predict the hourly energy demand profile of the entire H-CDHS, which includes the energy consumption and its corresponding losses. In general, there are three different techniques to obtain a community's energy demand profile: direct measurement, a comprehensive energy simulation tool used when data is absent, and simplified prediction methods for high-level computational costs.

In this study, a simplified four-step procedure developed for load prediction, ***Section 3.1***, was used for predicting the communities' energy demand profile. The accuracy of the proposed procedure was validated using two different approaches, using both an inter-model comparison, and comparing with measured data, ***Chapter 4***. Using the validated model, the community demand profile was predicted for two different scenarios:

- ***Scenario I***: Optimizing the district's existing condition by considering users' demographic distribution regarding energy consumption habits.
- ***Scenario II***: Optimizing the community as a newly built district by using design criteria and thermostat control to simulate all users' energy behavior.

Before performing the above-said optimization scenarios, in the first step, the community demand profile was predicted. In order to predict the community demand profile, occupants were divided into four different groups based on their energy consumption habits[14]. The definition of each group and its contribution to the total population presented in more detailed in ***chapter***

[14] (*Non-Typical High Usage* (**NTHU**), *Non-Typical Medium Usage* (**NTMU**)), *Non-Typical Low Usage* (**NTLU**) and *Typical Thermostat Control Usage* (**TTCU**))

*4.2.3.1*. Once these groups' consumption habits were available, the prediction model was trained using the proportion of each group within the community, ***Chapter 3.1***.

In the ***Scenario I***, the proportion of the different occupants' type within the community remained constant and the results served as a basis of comparison for the optimization process. Leaving occupants' demographic distribution untouched, the district energy demand profile for ***Scenario I*** was predicted using the on-site weather data and it was used to validate the energy simulation tools' (TRNSYS) accuracy, as the all on-site measured data correspond with this scenario. As a result, ***Scenario I*** compare the effect of optimized equipment size and control strategy on energy consumption pattern of the existing community, its $CO_2$ emission and cost.

Conversely, in ***Scenario II***, both weather file and occupants' demographic distribution were replaced by the design condition. In this scenario, redefining the weather file (TMY3) as the prediction model input file and training it, based on the design condition, *Typical Thermostat Control Usage* (TTCU) profile can show the potential savings in the initial investment cost of major equipment (boilers and thermal storage). This assumption, using the thermostat control, works better for newly built communities (design stage) with unknown occupants' energy use behavior. Having no data regarding potential district users, the district load is determined based on the energy required to maintain the indoor air temperature at thermostat setpoint defined by a code for each building type. Comparing the TMY3 file with the onsite measured weather data file used for validating the model shows the average outdoor temperature of 9.3°C and 10.8°C, and the minimum outdoor temperature of -3.9°C and -3.3 °C for TMY3 and onsite measured data, respectively. Comparing the TMY3 average and minimum temperature, higher total load and peak demand load are expected for both scenarios.

After obtaining both scenario's typical usage behavior, a prediction model was trained based on the fraction of each community group's data. **Figure 5-2**, shows the design weather data, TMY, and onsite measured weather data, while **Figure 5-3** shows the demand heating profile for these two scenarios.

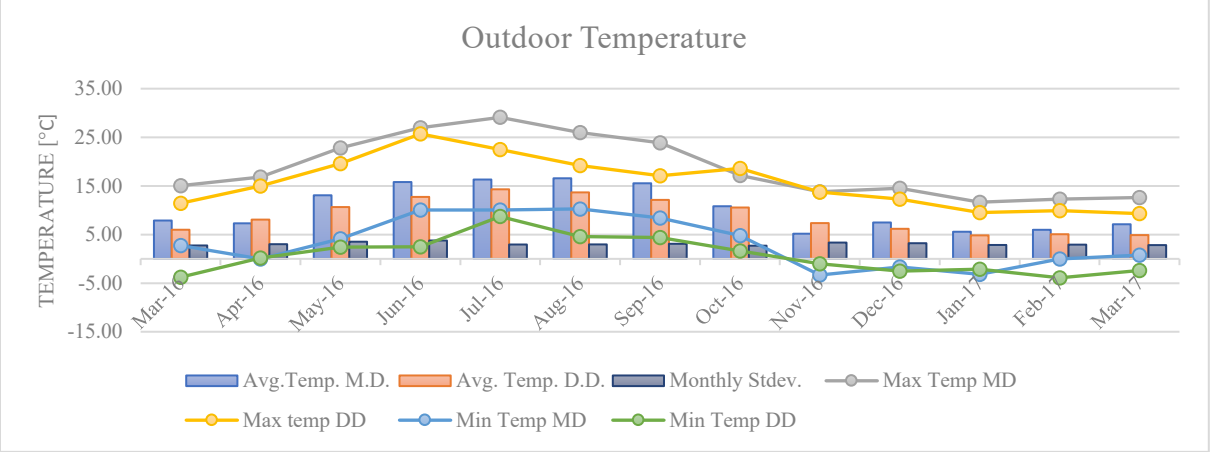


**Figure 5-2: Outdoor Weather Data (Measured Year and Design Year)**

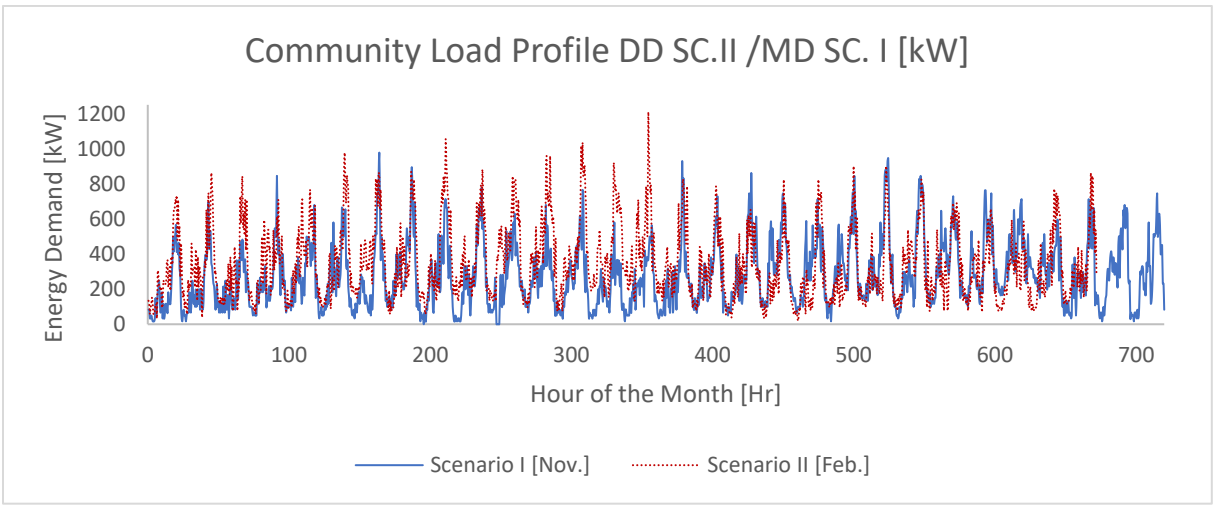


**Figure 5-3: Predicted Demand Profile for *Scenario I* (November) & *Scenario II* (February)**

Figure 5-3 shows the heating demand profile of ***Scenario I*** & ***II*** for the month when the peak demand load occurred. The inference from the figure is that the peak-heating demand load is 977.3 kW (2.8 % higher compared to the onsite measured data) in the ***Scenario I,*** and 1189 kW (25.1 % higher compared to the onsite measured data) for ***scenario II***. Note that, in ***Scenario II***, the entire community was simulated assuming all units were conditioned using the thermostat control (TTCU). It is also important to note that domestic hot water usage was constant for both scenarios. Therefore, the 25.1% increase in peak demand load was associated only with the community's higher heating demand.

## 5.2. Energy Modeling

To predict the district's energy demand profile and the interaction between its different components, TRNSYS was used while the majority of district network components and their interaction were defined. To represent other components, such as biomass boilers and building stock, the existing component types in TRNSYS were modified. In general, TRNSYS model has three major loops:

### 5.2.1. Generation Loop

The first loop (generation loop) consists of the auxiliary gas, biomass boilers, a controller, and a heat exchanger, which feeds energy into the system, as shown in Figure 5-4 and Figure 5-5. Since no specific biomass boiler type exists in TRNSYS, ***Type 700*** was modified to represent the biomass boiler by adjusting its efficiency, partial efficiency, and the control signal. After adjusting the boilers' type, two controllers were assigned to the generation loop to adjust the flow pattern between the generation/consumption loops and the storage loop. The first controller compared the network's predicted demand load with the total capacity of the boiler house and the need for the

thermal energy storage system as a backup. The second controller decides which boiler (biomass or gas) should operate to provide the required energy.

### 5.2.2. Consumption Loop

The consumption loop was constructed with ***Type 682***, which represents the demand profile of all units, (**Figure 5-3**). This ***Type*** reads the predicted demand profile through an external link. The distribution network heat loss was modeled using ***Type 952***.

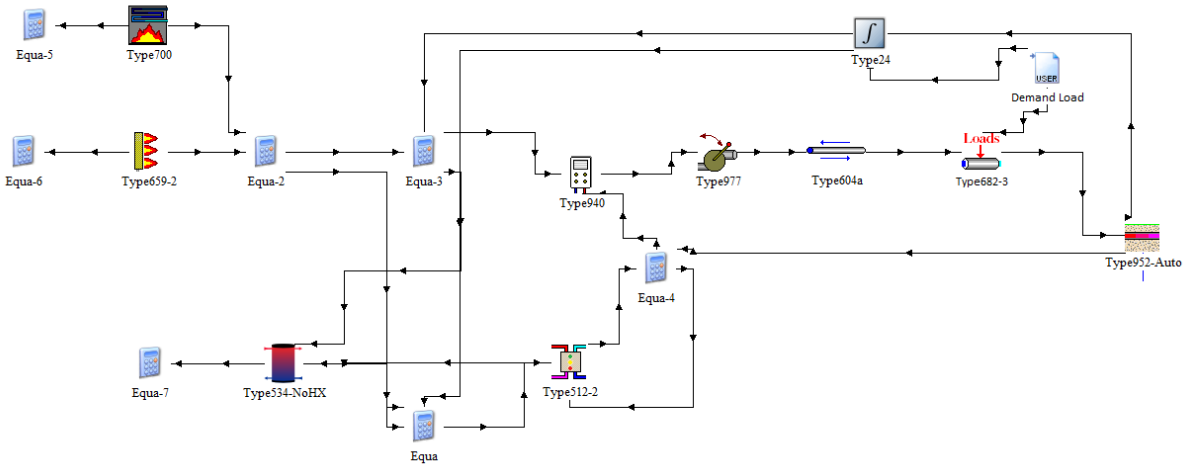


**Figure 5-4: Simultaneous charging and discharging configuration**

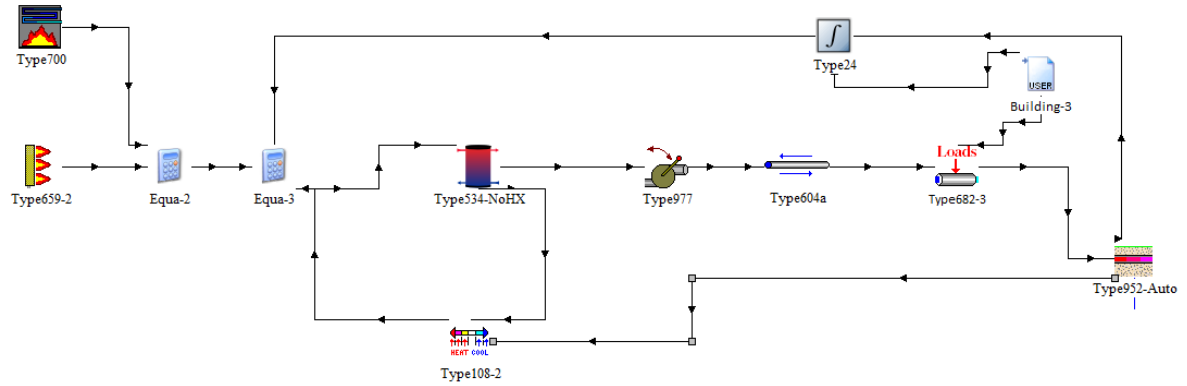


**Figure 5-5: Step-wise charging and discharging configuration**

### 5.2.3. Storage Loop

The storage loop was formed with two different configurations. The first was modeled by simultaneously charging and discharging the thermal storage as shown in **Figure *5-4***.

In other words, both the boiler house and distribution network was connected to the thermal energy storage system. While the boiler house provided energy to the thermal storage system, the latter supplied the energy to the distribution network. The second configuration was modeled using a step-wise energy storing procedure (**Figure *5-5***). In this configuration, a controller monitored the direction to the thermal storage tank (either charged or discharged). More detailed explanation on the controller will follow in ***Section 5.3***.

By comparing the preliminary results obtained from the total heat loss of the two configurations (simultaneous and stepwise), it is inferred that the step-wise charging and discharging configuration had the lower heat loss than simultaneous charging/discharging configuration due to thermal system storage size and flow direction. Also, the step-wise charging and discharging configuration has a higher overall energy efficiency compared with the simultaneous charging/discharging due to on/off frequency of the generation loop in this configuration (refer ***Figure 5-4*** & ***Figure 5-5***). More detailed explanations regarding the efficiency of the system are given in the following sections. As a result, the second configuration is used as a base for optimization.

## 5.3. Optimization Formulation

For the design stage, a dynamic multi-objective optimization method was chosen to size the main components of the district network boiler house for the two defined scenarios. The model was based on Mixed Linear Complementarity Problem (MLCP) to minimize the objective

functions, life cycle cost (LCC) and $CO_2$ emission. The optimization analysis focused on the on-site heat generation, but the option of purchasing auxiliary heating energy was also considered. This is because the primary goal of optimization is to size the main components of the boiler house to minimize the investment and operational costs over a thirty-year cycle. To account for the effects of short-term load fluctuations on components' optimal size, the optimization was conducted daily with an hourly temporal resolution. To improve model accuracy, other input data and model characteristics, including minimum and maximum output level constraints, and partial load efficiencies, were defined on an hourly basis. The system operational and fuel costs were also considered.

A controller type (Equa***.-3*** in ***Figure 5-5***) was developed to compare the energy generated at each time-step with that in the boiler house (Equa***.-2*** in ***Figure 5-5***) in accordance with the network demand load (***Type 24***)[15] and flow direction. By comparing the demand load and generation capacity, controller fed the network first and then it decides whether to use the disparity between generation and demand to charge or discharge the thermal storage system, ***Equation 5.1-5.4***. This implies that the controller regulates flow direction based on the general heat balance equation, while other constraints (such as minimum operative temperature ($T\_TS_{(t)}$)) were set for the thermal storage (***Equation 5.9***) to ensure a minimum required temperature for DHW usage:

$$\sum_{n=1}^{N} Q\_Gen_{(t,n)} + Q\_TS_{Ch.(t)} - Q\_TS_{Dis.Ch.(t)} \geq Q\_Net_{(t)} \qquad \textbf{Equ. 5-1}$$

$$Q\_Net_{(t)} = Q\_BLDG_{(t)} + Q\_Losses_{(t)} \qquad \textbf{Equ. 5-2}$$

If

[15] Type 24 is the sum of heat loss of underground pipes obtained from Type 952 and the predicted demand load of the buildings obtained from the simplified method and fed to the TRNSYS model as an external user file (Demand Load)

$$Q_{Gen_{(t,n)}} \geq Q_{Net_{(t)}} \quad \rightarrow \quad \begin{cases} Q_{Net_{(t)}} & \rightarrow \quad Loop_{DN_{(t)}} \\ Q_{Gen_{(t)}} - Q_{Net_{(t)}} & \rightarrow \quad Q_{TS_{Ch.(t)}} \end{cases} \qquad \textbf{Equ. 5-3}$$

$$Q_{Gen_{(t,n)}} < Q_{Net_{(t)}} \quad \rightarrow \quad \begin{cases} Q_{Gen_{(t)}} & \rightarrow \quad Loop_{DN_{(t)}} \\ Q\_TS_{Dis.Ch.(t)}: Q_{Net_{(t)}} - Q_{Gen_{(t)}} & \rightarrow \quad Loop_{DN_{(t)}} \end{cases} \qquad \textbf{Equ. 5-4}$$

The general equations used for modeling thermal storage, such as total energy at different time-steps and boundary conditions applied to it, are as below:

$$Q\_TS_{(t)} = Q\_TS_{(t-1)} + Q\_TS_{Ch.(t)}.\eta_{Ch.} - Q_{TS_{loss(t)}} - \left(Q_{TS_{Dis.Ch.(t)}} / \eta_{Dis.Ch.}\right) \qquad \textbf{Equ. 5-5}$$

$$Q\_TS_{(t)} \geq 0 \qquad \textbf{Equ. 5-6}$$

$$Q_{TS_{loss(t)}} = \left(T\_TS_{(t)} - T\_OA_{(t)}\right).U.A \qquad \textbf{Equ. 5-7}$$

$$T\_TS_{(t)} = T\_TS_{(t-1)} - \left(\frac{Q_{TS_{Dis.Ch.(t)}} / \eta_{Dis.Ch.}}{V.Cp_{wt.}.\rho_{wt.}}\right) + \left(\frac{Q\_TS_{Ch.(t)}.\eta_{Ch.}}{V.Cp_{wt.}.\rho_{wt.}}\right) \qquad \textbf{Equ. 5-8}$$

$$T\_TS_{(t)} \geq 70°C \qquad \textbf{Equ. 5-9}$$

After setting up the controllers, the optimization objective function ***Equation 5.10***) was set up with the aim of optimizing the size of the biomass boiler(s) and thermal storage system, and minimizing the current net cost and $CO_2$ emissions:

$$Min\{Obj(C,E)\} \qquad \textbf{Equ. 5-10}$$

where *C* and *E* are the cost and emission objectives. To make the objective function linear and to simplify it from 2D to 1D, the optimization of was employed using the equation below:

$$Obj(C,E) = \alpha.{}^{C}/_{C_0} + \beta.{}^{E}/_{E_0} \qquad \textbf{Equ. 5-1}$$

where α and β are the cost and emission importance factor in the final objective function. The cost associated function considers the entire C-DHS initial cost in addition to the present worth of the life cycle operational cost. To define the initial cost (***Equation 5.12***), the main boiler house equipment was divided into two modular modifiable parts (boilers and thermal storage system)

and fixed non-modifiable equipment (pumps and underground distribution pipelines). Note that, only the modular modifiable equipment cost was considered in the initial cost function and the initial cost of fixed non-modifiable equipment was excluded, as it remains constant regardless of the size of the modifiable equipment. For operational costs (***Equation 5.13***), the present fuel cost, the selling price of energy, and the buyout price of energy for surrounding houses for a 30-year period were considered using present worth method[16].

$$IC = (\sum_{m=1}^{N}(IC_m + LC_m.ExCap_m)) + LC_{TS}.Cap_{TS} \qquad \text{Equ. 5-2}$$

where *IC* is the linearized initial cost of the boiler house, 'n' is the number of years, FC is the fuel costs of different boilers; 'm' is the boiler number, *IN* is the annual income from selling heat to off-site users and $E_{tax}$ is the energy taxes. The initial investment cost includes the fixed and proportional variable expenses. The fixed component included the market value of the smallest size of the equipment available on the market, $LC_m$, while the proportional cost was determined by linearizing the extra cost associated with the higher capacity of the equipment, $LC_m.ExCap_m.$ , Hereafter, in the text, $IC_m$ and $LC_m.ExCap_m$ is presented as A and BX respectively.

$$OC = \left(\sum_{n=1}^{N}\sum_{m=1}^{M} FC_{n,m}.(1+i)^{-n}\right) - \left(\sum_{n=1}^{N} IN.(1+i)^{-n}\right) + \left(\sum_{n=1}^{N}\sum_{m=1}^{M} E_{tax_{n,m}}.(1+i)^{-n}\right)$$

**Equ. 5-3**

The cost function (C) is the summation of the initial and operational cost, (***Equation 5.14***)

$$C = IC + OC \qquad \text{Equ. 5-4}$$

[16] $PV_{OC} = OC_{annual}.\left({(1+i)^n - 1}/{i.(1+i)^n}\right)$ where i and n are the annual interest rate and year number, respectively, and $OC_{annual}$ is the annual operation cost.

The second objective function is defined to minimize the total $CO_2$ emission. The emission associated function was calculated using the following equation:

$$E = \sum_{n=1}^{N} \sum_{m=1}^{M} (E_{n,m}.V_{n,m}.PRFE_n + IE_{Aux}.V_{Aux}.PRFIE) \quad \text{Equ. 5-5}$$

where $E_{n.m}$ represents the fuel emissions ($kg.CO_2/kg.fuel$) used for each boiler (n) in a year (m) of the operation; $IE_{Aux}$ is the emission of the imported energy fed to the system from outside in month, (m,) of the operation ($kg\ CO_2/kg\ fuel$); $PRFE_n$ is the primary resource factor of the fuel; and $V_{n,m}$ is the fuel volume used in each month 'm' by the boiler 'n' . While calculating the costs, the wood price was discounted in order to take into account the government incentive on the price of wood pellets to encourage the small community to use biomass boilers.

To optimize the equipment size and to further minimize the overall costs, $CO_2$ emissions over the life cycle, the first step is to define the price and emissions level for the different type of fuel. **Table 5-1** represents the cost and $CO_2$ values for wood pellets and natural gas as the main fuel type for the chosen district. **Table 5-2** gives the initial cost of the major equipment.

**Table 5-1: Energy cost & emission for different fuel types**

| | Emission [kg CO2/kWh] | £/kWh |
|---|---|---|
| **Wood Pellets** | 0.039 | 0.061 |
| **Natural Gas** | 0.203 | 0.046 |
| **Buyout** | NA | 0.12 |

**Table 5-2: Investment costs**

| | Fixed £ [A] | £/kW [BX] | £/m3 |
|---|---|---|---|
| **Wood Pellets Boiler** | 125,000 | 362* | NA |
| **Gas Fired Boiler** | 132,000 | 180** | NA |
| **Wood Pellets Storage** | NA | NA | 670 |
| **Thermal Storage** | NA | NA | 1,100 |

All costs are presented in A+BX; (refer **Equation 5.12**)

Installation and other costs were added separately

* The linearized part was added after first 250 kW

** The linearized part was added after first 200 kW

### 5.3.1. Optimization Results

As mentioned in ***Section 5.1***, two different load scenarios were defined and served as a basis of comparison within existing communities (***Scenario I***) or newly built communities (***Scenario II***). Using the load demand profile for each scenario, the optimization process was applied separately, and the equipment's optimal size was determined.

#### 5.3.1.1. Scenario I (Existing Community)

The ***Scenario I*** was defined based on the current situation of the H-CDHS regarding occupants' behavior. By keeping a similar occupancy distribution to that of a real case one, the potential annual cost saving and $CO_2$ emission of the district over its life cycle was determined using the optimal equipment size and flow control (***Table 5-3***).

**Table 5-3: Optimization Results for Scenario I**

| Scenario I | | |
|---|---|---|
| **Parameters** | **Existing Situation** | **Scenario I** |
| **Peak Heating Load (kW)** | 1100 | 978 |
| **Biomass Boiler (kW)** | 870 | 477 |
| **Auxiliary Boiler (kW)** | 1300 | 609 |
| **Thermal Storage (m3)** | 50 | 16.3 |
| **Biomass Boiler Size Compared to the Peak Load (%)** | 79.1 | 49 |
| **Coverage Percentage by Biomass and Thermal Storage (%)** | NA | 95 |

The optimization results for this scenario shows a significant reduction in boiler capacities (45% for Biomass boiler and 53% for the auxiliary boiler) compared to the existing situation.

Considering that only one boiler operates at a time, this fact only achieved by utilizing a thermal storage system, which balances the demand and supply heat between the generation and consumption loops.

Comparing the optimized model results with field measurements show a dramatic drop in $CO_2$ emission (171.9 tons of $CO_2$ /year or 23%), as well as a considerable reduction in the total cost of the system (79,056 ₤/year or 17.6%). These cost and $CO_2$ reductions are partially due to the lower efficiency of the oversized equipment working at a partial load while other parts can be associated to the non-optimal control strategy of the system and missing thermal storage.

Since specific weather data and occupants' behavior was considered in the ***Scenario I*** (2016-17), the demand energy load of the community could change anytime based on the number of tenants or weather conditions. Consequently, after optimizing the system and determining the optimal equipment size, the sensitivity of the design to any change in community demand load due to change in the users' demographic distribution has been determined. To do that, two new cases (**High and Low usage**) were defined. These newly defined cases included a change in the fraction of occupants' types[17] in the community compared with the existing condition obtained from clustering results. In the ***High usage case***, the fraction of NTLU and NTMU users dropped, were added to the NTHU and TTCU users to represent a higher demand load, see Table 4. In the ***Low usage case***, the number of NTHU users dropped was added to the lower energy consumers such as NTLU and NTMU, see ***Table 5-4***

[17] NTLU, NTMU, NTHU, TTCU

Table 5-4: **Fraction of the Occupants' Types in Different Scenarios**

| Sensitivity analysis scenarios | | | |
|---|---|---|---|
| | ***Low Usage*** | ***Scenario I*** | ***High Usage*** |
| ***NTLU*** | 23% | 16% | 10% |
| ***NTMU*** | 39% | 24% | 15% |
| ***NTHU*** | 33% | 53% | 65% |
| ***TTCU*** | 5% | 15% | 10% |
| ***Peak Load*** | 884 kW | 978 kW | 1086 kW |

By changing the fraction of occupants, the energy demand profile of the newly defined cases was predicted and fed to the energy model (see ***Figure 5-5***). The boiler house equipment size remained similar to the ***Scenario I***. After modeling these newly defined cases, the system performance under new conditions was determined. Comparing the percentage of the biomass boiler and thermal storage, which can cover the demand load of the community between the ***Scenario I*** and ***High Usage Case*** (see ***Table 5-5***), shows that in the ***High Usage Case*** with 12% higher pick, the percentage coverage time by biomass boiler dropped by 1.1%.

Table 5-5: **Performance of the Optimized System under New Demand Profile Load**

| Sensitivity Results | | | |
|---|---|---|---|
| **Technology** | **Low Usage** | **Scenario I** | **High Usage** |
| **Peak Heating Load (kW)** | 884 | 978 | 1086 |
| **Biomass Boiler (kW)** | 477 | 477 | 477 |
| **Auxiliary Boiler (kW)** | 609 | 609 | 609 |
| **Thermal Storage ($m^3$)** | 16.3 | 16.3 | 16.3 |
| **Biomass Boiler Size Compared to the Peak Load (%)** | 54 | 49 | 44 |
| **Coverage Percentage by Biomass and Thermal Storage (%)** | 97.8 | 95.0 | 93.9 |

#### 5.3.1.2. Scenario II (Design Stage)

In the ***Scenario II***, the weather file was changed and the occupants' distribution was altered to the TTCU to represent the design criteria for the newly build buildings. **Table 5-6** presents the optimal equipment sizes, resulting from the optimization of the boiler house for the ***Scenario II***.

Table 5-6: **Optimization Results for the Second Scenario**

| Scenario II | | |
|---|---|---|
| **Technology** | **Existing Situation** | **Scenario I** |
| **Biomass Boiler (kW)** | 870 | 661 |
| **Auxiliary Boiler (MW)** | 1.3 | 0.738 |
| **Thermal Storage** | 50 $m^3$ | 32.8 $m^3$ |
| **Peak Heating Load** | 1100 kW | 1189 kW |
| **Bio. Percentage during Peak** | 66.9% | 56% |
| **Percentage from Bio.** | NA | 98.8% |

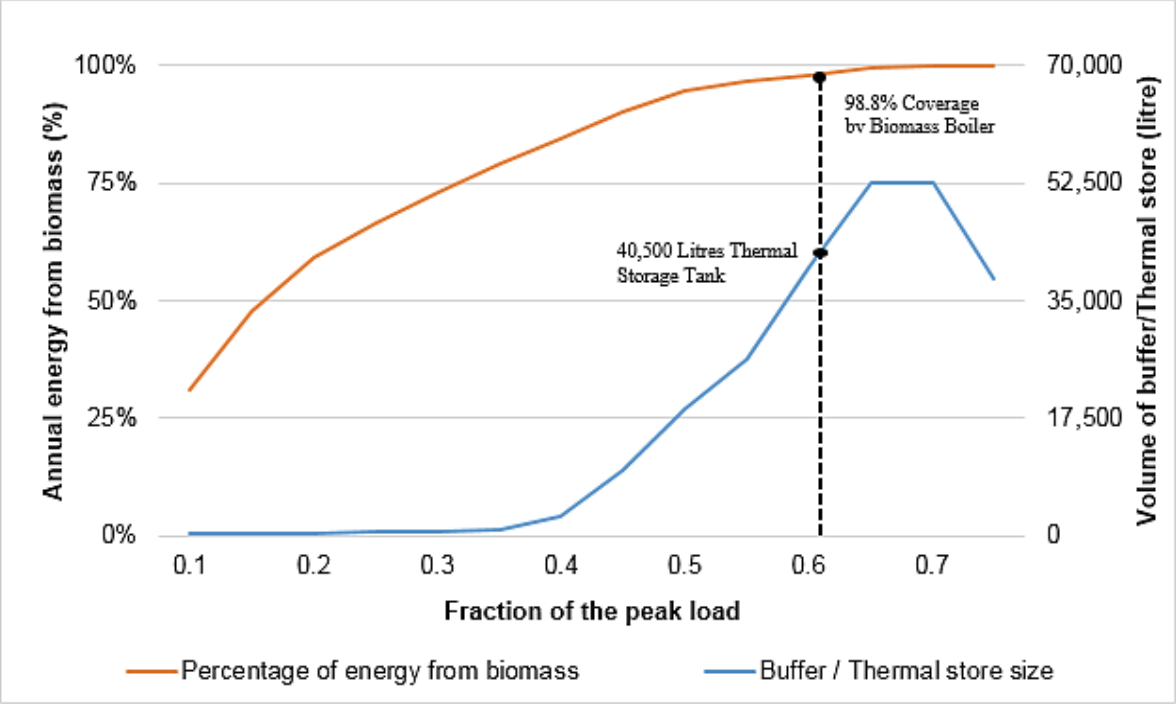


Figure 5-6: **Optimal Equipment Size, Size of the biomass boiler as a percentage of a peak load for different annual % of energy from a biomass boiler**

Similar to the ***Scenario I***, the capacity of the boiler optimal size, biomass and auxiliary boiler, used less than 60% of their capacity to respond to the peak demand load. In order to find the optimal size of the equipment using the static optimized sizing tools such as Biomass Boiler Sizing Tool (version 6.8.2), primarily the same annual biomass energy coverage (98.8%) was determined. Using the same coverage percentage, the sizing tool suggests the biomass boiler with

the capacity size of 62% of the peak load and 40.5 $m^3$ thermal storage tank (refer to **Figure 5-6**). **Table 5-7** and presents the equipment size and cost associated with each design method.

**Table 5-7: Comparison of the Equipment Size, Cost for Different Design Strategies**

| Results Obtained from Different Design Strategies | | | | | |
|---|---|---|---|---|---|
| | **Conventional** | **Static Optimization Tool** | | **Proposed Dynamic Optimization Process** | |
| | | **Size** | **Size Reduction [%]** | **Size** | **Size Reduction [%]*** |
| **Biomass Boiler [kW]** | 870 | 737 | 15.3 | 661 | 24.0 |
| **Auxiliary Boiler [kW]** | 1300 | 0.891 | 31.5 | 0.738 | 43.2 |
| **Thermal Storage [$m^3$]** | 50 | 40.5 | 19.0 | 32.5 | 35.0 |
| **Cost** | 734,440 | 602,224 | 18.0 | 538,372 | 26.7 |

* Reductions calculated comparing with conventional method

Considering that only one boiler operates at a time, 98.8% coverage by biomass boiler was achieved using only thermal storage to balance between the generation and consumption loop. As shown in ***Table 5-7***, this solution can reduce the size of both auxiliary and main biomass boilers into a fraction of their original size and, as a result, decrease the system heat loss while improving the district energy efficiency. The reduction in major equipment size of the district using the proposed dynamic optimization method caused a 196,068 £ or 26.7% drop only in the system initial investment cost. Also, knowing the fact that the efficiency of the biomass boiler is lower when operated partially, two scenarios could be assumed for a non-optimal size equipment: 1) the biomass boiler works at its full capacity all the time while keeping the generation efficiency at maximum value; this can result in generation of an excessive amount of heat, which eventually is accounted as loss, and 2) the boiler works at partial load only to meet the network demand. This decreases generation efficiency due to the boilers lower partial capacity efficiency [152]. In both scenarios, the overall efficiency of the system drops.

### 5.3.1.3. Impact of Dynamic Optimization in Determining the Operational Period of the System

As mentioned earlier in ***Section 5.1***, the main difference between the static and dynamic optimization is in dependency of the decision-making process with respect to time. In other words, dynamic optimization, by breaking the demand profile into smaller periods and determining a solution for each period, considers the effects of demand at the previous hour on the optimal solution. **Table *5-5 (a)***, presents the charging/discharging profile of the thermal storage over the 10 days period in November, obtained from the ***Scenario I*** and **Table *5-5 (b)*** represents the thermal energy storage mean temperature and the district demand load.

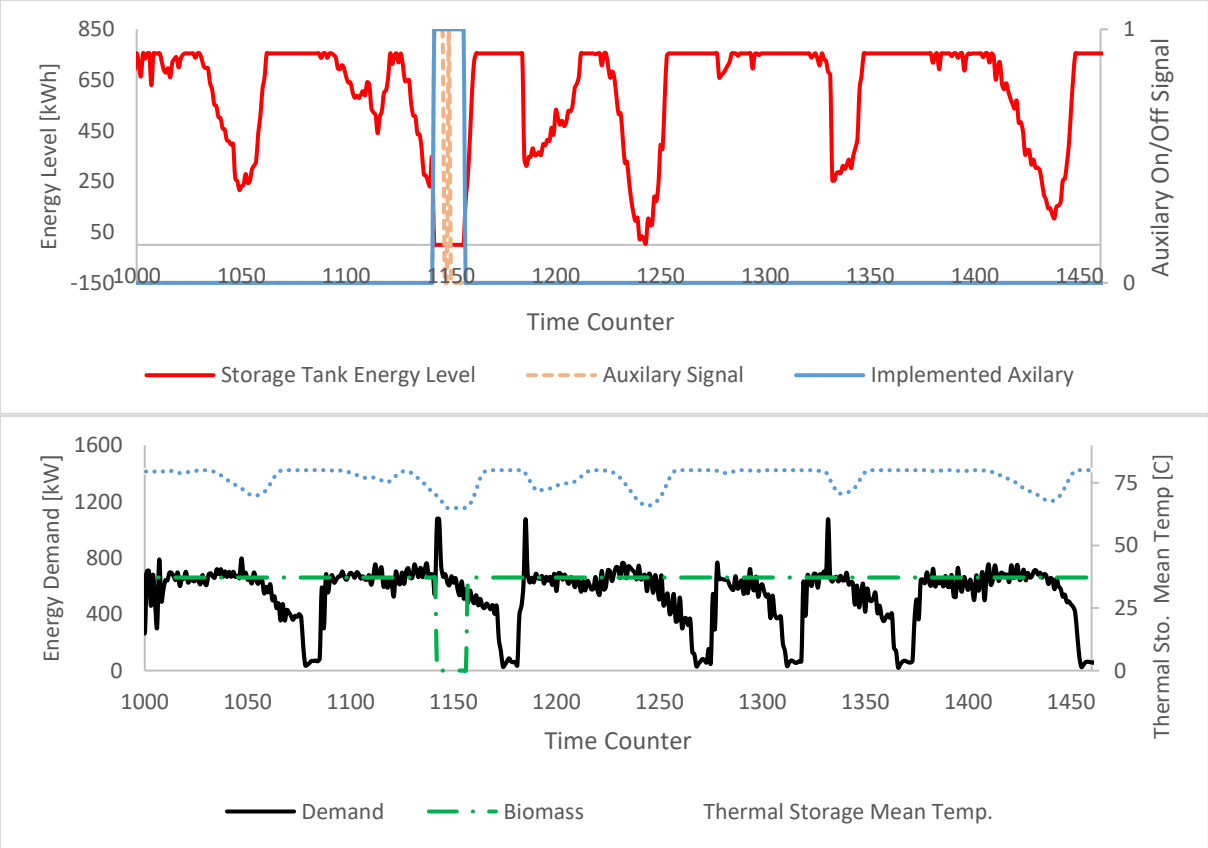


**Figure 5-7: (a) Thermal storage energy level for a 10-day period in November; (b) Thermal storage temperature and district demand load for the same 10-days (Bottom)**

In static optimization by only considering the peak demand in finding the optimal solution, the effects of the energy demand at previous hours on determining the optimal solution will be neglected. On the other hand, in dynamic optimization, by considering the effects of the demand profile at a previous hour in determining the optimal solution can result in better utilizing of the thermal storage and lower size of the equipment. For instance, as presented in **Table *5-5***, the response of the system to an identical demand varied based on the energy demand of the previous hours. In case of the first peak (shown in **Table *5-5 (b)***), due to the high demand of the system prior to the peak, the thermal storage has been partially discharged, and as a result, the axillary energy is required to respond to the energy demand of the system. On the other hand, due to lower demand of the network prior to the second and third peak, the thermal storage is fully charged, and no auxiliary energy is required.

Apart from determining the optimal size of the equipment, the optimal performance of the system could be determined from the proposed dynamic optimization method. As shown in ***Table 5-5 (b)***, since the biomass boiler works constantly, the district demand load can be met by a nominal size of the biomass boiler. However, when the demand load of the DHS is higher than the capacity of the biomass boiler, the deficit energy is met from the thermal energy storage. On the other hand, when the demand load drops, the surplus energy is stored in the thermal energy storage and the energy storage level swiftly increases. In peak demand period, the instantaneous auxiliary system (gas boiler in this case), along with thermal storage, provide required energy demanded by the district network since the biomass boiler cannot provide enough energy for the system. Using this strategy while running the biomass boiler constantly at full capacity for the optimized sized system, step-wise charging/discharging the thermal storage can eliminate the need for the auxiliary energy 98.8% of the time while maintaining the system's maximum overall efficiency.

# Chapter 6: Conclusion and Recommendations:

## 6.1. Summary and Conclusions:

The rapid increase in energy demand in multiple domains such as the building sector results in fossil fuel overuse which is currently the most dominant energy source world-wide. In effect, the overconsumption of fossil fuels in last decades has provoked the rise of CO2-equivalent emission levels in the atmosphere which has led to the inevitability and irreversibility of global warming.

Providing a secure and clean source of energy to respond to households demand is and will continue to be an upmost fundamental challenge faced by energy planners. Different energy conservation strategies have been applied at various levels, including in the arenas of energy production, conversion, and, user-demand but the most promising solutions have reached a higher level known as energy management. Hybrid Community-District Heating System (H-CDHS) is a unique type of energy management integrating thermal storage within its renewable fed system. Since energy generated by renewable sources is intermittent in nature, thermal storage allows the system to regulate the demand. Indeed, the integration of thermal storage decreases the dependence on non-renewable energies since it controls the system's energy flow. Obtaining an accurate prediction of the heating energy demand profile of the system at small intervals (e.g., on an hourly basis) is the first step in designing an efficient H-CDHS.

Establishing the hourly demand profile of the system allows the controllers to regulate the supply and demand by storing and utilizing energy when there is excess or shortage respectively. Due to lack of an easy to use and reliable tool, which could be used to predict the heating demand profile of large-scale district networks (e.g., within the urban sector) in a timely manner and with

a high accuracy, designers have developed several simplified models. Most of these prediction methods have been introduced mainly based on the assumption of the stand-alone building, barely representing the complexity of an urban/district setting (e.g., unmeasured effects of the neighborhood on buildings such as shared walls and also the solar blockage by the adjacent shadow casted from other buildings).

Another drawback of these models is that they are not applicable to different types of buildings and are mainly used for sole prediction of residential buildings' heating demand. Also, most of these existing methods focus on the building's total energy consumption instead of its energy profile. Finally, aside from the type of prediction, the accuracy of the existing models is pre-dominantly low due to oversimplifying the process and use of scaling methods in their prediction process, while more accurate models are not feasible for a larger scale community due to level of information required for their modeling and their computational time.

Accordingly, this dissertation focused on the development of a simplified energy prediction procedure, which could be used to accurately predict the detail HEDPs, ranging from mid to large scale communities in a timely manner, with a least amount of the required information, and with a high resolution accuracy. To do so, a procedure has been developed using two different mathematical method MLR and MNLR. Then the proposed procedure has been validated at different levels, including building level and community level, using both intermodal comparison and measured data following the below steps:

- By adopting a clustering method and utilizing a prediction algorithm, the building stock has been segmented into different archetypes. Segmentation of the building stock model especially in the case of the communities with more diverse building types, increased the accuracy of the prediction.

- In order to find the optimal number of the cluster required for segmenting the building stock model, Elbow method has been adopted. It will define the optimal number of the cluster by comparing the difference between the within-cluster sums of the square (WSS) of two consecutive cluster numbers.
- Unlike most present works, the proposed model do not use the scaling methods in predicting the HEDP of the district, but it predicts the HEDP of every individual units within the district.
- In order to predict the HEDP, the proposed method used basic physical and geometrical properties of the units along with climatological information to generate the input file for the model.
- Using the reference building of each cluster, the MLR/MNLR model has been trained separately for each cluster. Each trained model has been used for predicting the HEDP of all individual units within that cluster.
- The heat loss from of the distribution network has been predicted separately presuming a linear relation between an average operational temperature of the distribution network and the surrounding environment temperature.

The proposed procedure later has been validated at different level, e.g. building & district level, using both intermodal comparison and the measured data obtained from a mid-size hybrid district heating community. At first, intermodal comparison has been used:

- In order to validate the procedure at a building level, then HEDP of two mid-rise residential buildings, **R1** and **R2**, has been predicted using both MLR and MNLR methods.

- One of the mid-rise residential buildings used for the inter-model comparison is modeled based on the specification of the urban setting (**R2**), having a common wall with other buildings, while the other building (**R1**) assumed to be a stand-alone building.
- MSRE of the prediction at a building level obtained about 11.7kW (8.48%) for the **R2** and 5.23kW (4.25%) for the **R1**.
- In order to validate the procedure at a community level three different districts with 85-112 buildings were modeled using the random number and their HEDP determined using both simplified procedure as well as a comprehensive simulation using eQUEST.
- For the proposed districts, the computational time required using the proposed method is less than on tenth of the time required by comprehensive modeling, eQUEST.
- Since the only time consuming step in the proposed model is the training step, by increasing the number of the units, the computational time saving percentage will increase.
- The accuracy of the prediction for three communities obtained to be:
    1. Solely residential: R=0.9966 with an average error of 4.7%
    2. Solely office building: R=0.9401 with an average error of 6.8%
    3. Mixed community: R=0.9856 with an average error of 5.2%
- Even though, in all three communities, predicted results show a high agreement with the one obtained from comprehensive modeling, due to non-uniform daily usage of the office buildings compared with residential buildings, the average error

for district 2 in all office building, was slightly higher than the community with all residential buildings (1.6%).

After performing the intermodal comparison, the proposed model validated using the measured data:

- At an early design stage, the community's heating demand profile was predicted following a simplified model with an average national energy benchmark for Scotland. The only adjustment made to the benchmark was a 20% reduction in the overall energy consumption and peak demand to compensate for the occupants' economic status. The results of this oversimplification was overestimating the peak energy demand by a factor of 2.
- The prediction shows high correlations between the predicted and actual profiles even though the heating demand profile consist of both SH and DHW usage. The suggested procedure captured the profile with an acceptable accuracy level 11.2% in the annual RMSE, and 8.2% in the seasonal RMSE
- Results shows that the prediction accuracy remains close both at the building and community levels due to the models' flexibility in capturing the demand profile of every individual unit. Unlike most existing models, which extrapolates the data based on the number of the users or total floor area, this model predicts the community load by envisaging that for every single user.

Considering the mentioned research gap, a dynamic optimization model that explores optimal equipment size using the detailed demand profile has been developed. The developed model predicts the detailed demand profile of the DHS and it uses it along with the detailed energy model of the DHS, detailed model of the equipment and interaction between them to dynamically

optimize the entire system and subsequently provide the optimal size of the equipment. The size of the equipment obtained from the model is later compared with the one obtained from the conventional methods, including the design day method, the static optimization tool, and Biomass optimization tool. In this regard, data from an existing H-CDHS with an integrated thermal energy storage system is used to optimize its boiler house to minimize its overall cost and $CO_2$ emission. Optimization performed to calculate the overall size of the major energy generation and storing equipment, and operational control strategy for the community under different scenarios.

- In case of the existing community, ***Scenario I*** as the existing district, comparing the optimal equipment sizes with the existing non-optimal equipment sizes, a considerable difference was found for equipment sizes, including 45% smaller biomass boiler, 53% smaller auxiliary boiler and finally 67% smaller thermal storage size. This is mainly due to the fact that the existing boiler house has been designed based on the conventional methods. Aside from the huge drop in the initial cost of the system, (£267,716 or 38.1%), the annual life cycle cost and $CO_2$ footprint of the district also dropped by £79,056/year (17.6%) and 171.9 tons of $CO_2$ /year (23%), respectively. these drops are mainly results in a higher efficiency of the system due to a full load operation of the equipment.
- In case of newly build district, ***Scenario II*** as the newly built district, three different design methods have been used to size the equipment, including conventional, static commercial optimization tool and the developed dynamic optimization process. The results indicate that initial cost of the system using the proposed dynamic optimization method could drop by 26.7% comparing with conventional method while using the static optimization tool could only result in 18% drop in the initial

cost of the system. These facts emphasized on the importance of dynamic optimization of the system in order to achieve a better optimal solution.

## 6.2. Future Works Recommendations:

The recommended future research work on the energy prediction and optimization of the hybrid community district heating system are:

1. As mentioned earlier, based on the Lund classification [8], one of the main distinguishing points between the 4$^{th}$ generation of the DHS compared to the earlier generations, is in design of the system to provide both heating and cooling load by utilizing the cold storage and centralized cooling plants, **Figure *2-1***. To this end, predicting the Cooling Energy Demand Profile (CEDP) of the users is an essential task worth studying. Do to the absence of the measured data for cooling load, and the limitation of the current work, this study only focused on predicting the heating demand load of the users, including both domestic hot water usage as well as space heating.
2. While optimizing the system, the energy distribution network layout of the system was not taken into account in the energy model and only the total heat loss of the distribution network consider while predicting the HEDP. In order to have more efficient district system, optimizing the energy distribution network layout and studying the effect of the optimal layout on the overall performance of the system could be done for a future works.

# References:


[1] IEA, “Energy Technology Perspectives 2017 - Executive Summary,” *Iea*, p. 371, 2017.

[2] UN DESA, “World Population Prospects The 2017 Revision Key Findings and Advance Tables,” *World Popul. Prospect. 2017*, pp. 1–46, 2017.

[3] NASA, “NASA GLOBAL CLIMATE CHANGE,” *February 2018*. [Online]. Available: https://climate.nasa.gov/vital-signs/carbon-dioxide/.

[4] European Commission, “Directive 2006/32 EC of the European parliment and the councile of 5 April on energy end-use efficiency and energy services and repealing Council Directive 93/76/EEC,” *Off. J. Eur. Union*, pp. 12–25, 2006.

[5] EC, “The Directive 2010/31/EU of the European Parliament and of the Council of 19 May 2010 on the energy performance of buildings,” *Off. J. Eur. Union*, vol. 53, pp. 1–6, 2010.

[6] National Energy Board (NEB), *Canada’s Energy Future: Energy Supply and Demand Projections to 2035*, no. November. 2011.

[7] P. Christoff, “The promissory note: COP 21 and the Paris Climate Agreement,” *Env. Polit.*, vol. 25, no. 5, pp. 765–787, 2016.

[8] H. Lund, S. Werner, R. Wiltshire, S. Svendsen, J. E. Thorsen, F. Hvelplund, and B. V. Mathiesen, “4th Generation District Heating (4GDH),” *Energy*, vol. 68, pp. 1–11, Apr. 2014.

[9] I. Ben Hassine and U. Eicker, “Impact of load structure variation and solar thermal energy integration on an existing district heating network,” *Appl. Therm. Eng.*, vol. 50, no. 2, pp. 1437–1446, Feb. 2013.

[10] M. Kuosa, M. Aalto, M. El Haj Assad, T. Mäkilä, M. Lampinen, and R. Lahdelma, "Study of a district heating system with the ring network technology and plate heat exchangers in a consumer substation," *Energy Build.*, vol. 80, pp. 276–289, Sep. 2014.

[11] M. a. Ancona, M. Bianchi, L. Branchini, and F. Melino, "District Heating Network Design and Analysis," *Energy Procedia*, vol. 45, pp. 1225–1234, 2014.

[12] H. Madsen and K. E. N. Sejling, "on Flow a N D Supply Temperature Control in District Heating Systems," vol. 14, no. 6, pp. 613–620, 1994.

[13] H. Lund, S. Werner, R. Wiltshire, S. Svendsen, J. E. Thorsen, F. Hvelplund, and B. V. Mathiesen, "4th Generation District Heating (4GDH). Integrating smart thermal grids into future sustainable energy systems.," *Energy*, vol. 68, pp. 1–11, 2014.

[14] W. Wang, X. Cheng, and X. Liang, "Optimization modeling of district heating networks and calculation by the Newton method," *Appl. Therm. Eng.*, vol. 61, no. 2, pp. 163–170, Nov. 2013.

[15] J. Dahm, "District Heating Pipelines in the Ground - Simulation Model -," no. May, pp. 1–22, 2001.

[16] M. Kuosa, K. Kontu, T. Mäkilä, M. Lampinen, and R. Lahdelma, "Static study of traditional and ring networks and the use of mass flow control in district heating applications," *Appl. Therm. Eng.*, vol. 54, no. 2, pp. 450–459, May 2013.

[17] I. Ben Hassine and U. Eicker, "Simulation and optimization of the district heating network in Scharnhauser Park," no. 0, pp. 1–18, 2011.

[18] H. Palsson, *Methods for planning and operating decentralised combined heat and power*

*plants*. 2000.

[19] A. Keçebaş, M. A. Alkan, İ. Yabanova, and M. Yumurtacı, "Energetic and economic evaluations of geothermal district heating systems by using ANN," *Energy Policy*, vol. 56, pp. 558–567, May 2013.

[20] C. T. C. Arsene and A. Bargiela, "MODELLING AND SIMULATION OF WATER SYSTEMS BASED ON LOOP EQUATIONS," vol. 5, no. 1, pp. 61–72, 1989.

[21] H. Chenoweth, C. Crawford, H. Chenoweth, and C. Crawford, "Pipe Network Analysis Published by : American Water Works Association Pipe Network Analysis," vol. 66, no. 1, pp. 55–58, 2018.

[22] R. P. Donachie, "Digital Program for Water Network Analysis," *J. Hydraul. Div.*, vol. 100, no. 3, pp. 393–403, 1974.

[23] A. G. Collins, R. L. Johnson, and R. L. Johnson, "Finite-Element Method for Water-Distribution Networks Published by : American Water Works Association Finite-Element Method for Networks," vol. 67, no. 7, pp. 385–389, 2018.

[24] M. Calì and R. Borchiellini, "SA NE M SC PL O E – C EO AP LS TE S PL O E –," vol. II.

[25] H. Gopalakrishnan and D. Kosanovic, "Economic optimization of combined cycle district heating systems," *Sustain. Energy Technol. Assessments*, vol. 7, pp. 91–100, Sep. 2014.

[26] C. Weber, F. Maréchal, and D. Favrat, "Design and optimization of district energy systems Design and optimization of district energy systems," no. September, 2006.

[27] I. Hassine and U. Eicker, "Simulation and optimization of the district heating network in Scharnhauser Park," *2nd Eur. Conf. Polygeneration*, vol. 49, no. 0, pp. 1–18, 2011.

[28] a. Dalla Rosa, R. Boulter, K. Church, and S. Svendsen, "District heating (DH) network design and operation toward a system-wide methodology for optimizing renewable energy solutions (SMORES) in Canada: A case study," *Energy*, vol. 45, no. 1, pp. 960–974, Sep. 2012.

[29] a. Dalla Rosa and J. E. Christensen, "Low-energy district heating in energy-efficient building areas," *Energy*, vol. 36, no. 12, pp. 6890–6899, Dec. 2011.

[30] D. Buoro, P. Pinamonti, and M. Reini, "Optimization of a Distributed Cogeneration System with solar district heating," *Appl. Energy*, vol. 124, pp. 298–308, Jul. 2014.

[31] I. Ben Hassine and U. Eicker, "Control Aspects of Decentralized Solar Thermal Integration into District Heating Networks," *Energy Procedia*, vol. 48, pp. 1055–1064, 2014.

[32] T. Nuytten, B. Claessens, K. Paredis, J. Van Bael, and D. Six, "Flexibility of a combined heat and power system with thermal energy storage for district heating," *Appl. Energy*, vol. 104, pp. 583–591, Apr. 2013.

[33] M. Noussan, G. Cerino Abdin, A. Poggio, and R. Roberto, "Biomass-fired CHP and heat storage system simulations in existing district heating systems," *Appl. Therm. Eng.*, pp. 1–7, Nov. 2013.

[34] M. Guadalfajara, M. a. Lozano, and L. M. Serra, "Comparison of Simple Methods for the Design of Central Solar Heating Plants with Seasonal Storage," *Energy Procedia*, vol. 48, pp. 1110–1117, 2014.

[35] a Hlebnikov, N. Dementjeva, and a Siirde, "Optimization of Narva District Heating Network and Analysis of Competitiveness of Oil Shale Chp Building in Narva," *Oil Shale*,

vol. 26, no. 3, p. 269, 2009.

[36] M. Pirouti, A. Bagdanavicius, J. Ekanayake, J. Wu, and N. Jenkins, “Energy consumption and economic analyses of a district heating network,” *Energy*, vol. 57, pp. 149–159, Aug. 2013.

[37] S. M. Sanaei and T. Nakata, “Optimum design of district heating: Application of a novel methodology for improved design of community scale integrated energy systems,” *Energy*, vol. 38, no. 1, pp. 190–204, Feb. 2012.

[38] V. Verda, G. Baccino, A. Sciacovelli, and S. Lo Russo, “Impact of district heating and groundwater heat pump systems on the primary energy needs in urban areas,” *Appl. Therm. Eng.*, vol. 40, pp. 18–26, Jul. 2012.

[39] E. Dotzauer, “Simple model for prediction of loads in district-heating systems,” *Appl. Energy*, vol. 73, no. 3–4, pp. 277–284, 2002.

[40] T. Sharp, “Energy Benchmarking In Commercial Office Buildings,” *ACEEE Summer Study Energy Effic. Build.*, vol. 4, pp. 321–329, 1995.

[41] C. S. Barnaby, J. D. Spitler, and D. Xiao, “The Residential Heat Balance Method for Heating and Cooling Load Calculations,” *ASHRAE Trans.*, vol. 111, no. Ashrae, pp. 291–307, 2005.

[42] TRNSYS, “User Manual: TRNSYS 17 a TRaN sient SYstem Simulation program,” *TRNSYS Libr. Vol. 4 Math. Ref. Sol. Energy Lab. Univ. Wisconsin-Madison, USA*, vol. 3, pp. 1–486, 2009.

[43] D. B. Crawley, L. K. Lawrie, F. C. Winkelmann, W. F. Buhl, Y. J. Huang, C. O. Pedersen,

R. K. Strand, R. J. Liesen, D. E. Fisher, M. J. Witte, and J. Glazer, “EnergyPlus : Creating a New-Generation Building Energy Simulation Program EnergyPlus : creating a new-generation building energy simulation program,” vol. 33, pp. 319–331, 2001.

[44] J. Ortiga, J. C. Bruno, A. Coronas, and I. E. Grossman, “Review of optimization models for the design of polygeneration systems in district heating and cooling networks,” *Comput. Aided Chem. Eng.*, vol. 24, pp. 1121–1126, Jan. 2007.

[45] M. de Guadalfajara, M. a. Lozano, and L. M. Serra, “Evaluation of the Potential of Large Solar Heating Plants in Spain,” *Energy Procedia*, vol. 30, pp. 839–848, Jan. 2012.

[46] E. J. Kim, G. Plessis, J. L. Hubert, and J. J. Roux, “Urban energy simulation: Simplification and reduction of building envelope models,” *Energy Build.*, vol. 84, pp. 193–202, 2014.

[47] S. Wang and X. Xu, “Simplified building model for transient thermal performance estimation using GA-based parameter identification,” *Int. J. Therm. Sci.*, vol. 45, no. 4, pp. 419–432, 2006.

[48] M. S. Al-Homoud, “Computer-aided building energy analysis techniques,” *Build. Environ.*, vol. 36, no. 4, pp. 421–433, 2001.

[49] R. Yao and K. Steemers, “A method of formulating energy load profile for domestic buildings in the UK,” *Energy Build.*, vol. 37, no. 6, pp. 663–671, 2005.

[50] L. Fei and H. Pingfang, “A baseline model for office building energy consumption in hot summer and cold winter region,” *Proc. - Int. Conf. Manag. Serv. Sci. MASS 2009*, 2009.

[51] G. Y. Yun and K. Steemers, “Behavioural, physical and socio-economic factors in household cooling energy consumption,” *Appl. Energy*, vol. 88, no. 6, pp. 2191–2200, 2011.

[52] H. S. Hippert, C. E. Pedreira, and R. C. Souza, “Neural networks for short-term load forecasting: a review and evaluation,” *IEEE Trans. Power Syst.*, vol. 16, no. 1, pp. 44–55, 2001.

[53] G. Gross and F. D. Galiana, “Short-term load forecasting,” *Proc. IEEE*, vol. 75, no. 12, pp. 1558–1573, 1987.

[54] Z. Tang, C. De Almeida, C. de Almeida, P. A. Fishwick, Z. Tang, and C. De Almeida, “Time series forecasting using neural networks vs. Box- Jenkins methodology,” *Simulation*, vol. 57, no. 5, pp. 303–310, 1991.

[55] N. Amjady, “Short-term hourly load forecasting using time-series modeling with peak load estimation capability,” *IEEE Trans. Power Syst.*, vol. 16, no. 4, pp. 798–805, 2001.

[56] C. M. Lee and C. N. Ko, “Short-term load forecasting using lifting scheme and ARIMA models,” *Expert Syst. Appl.*, vol. 38, no. 5, pp. 5902–5911, 2011.

[57] O. P. Palsson, “Stochastic Modeling, Control and Optimization of District Heating Systems.” 1993.

[58] E. S. Gardner, “Exponential smoothing: The state of the art,” *J. Forecast.*, vol. 4, no. 1, pp. 1–28, 1985.

[59] G. Zhang, B. Eddy Patuwo, and M. Y. Hu, “Forecasting with artificial neural networks:,” *Int. J. Forecast.*, vol. 14, no. 1, pp. 35–62, 1998.

[60] B.-J. Chen, M.-W. M.-W. Chang, and C.-J. C.-J. Lin, “Load Forecasting Using Support Vector Machines: A Study on EUNITE Competition 2001,” *IEEE Trans. Power Syst.*, vol. 19, no. 4, pp. 1821–1830, 2004.

[61] F. Haghighat, H. Brohus, and J. Rao, “Modelling air infiltration due to wind fluctuations—a review,” *Build. Environ.*, vol. 35, no. 5, pp. 377–385, 2000.

[62] F. Haghighat, T. E. Unny, and M. Chandrashekar, “Stochastic Modeling of Transient Heat Flow Through Walls.,” *J. Sol. Energy Eng. Trans. ASME*, vol. 107, no. 3, 1985.

[63] H. A. Nielsen and H. Madsen, “Modelling the heat consumption in district heating systems using a grey-box approach,” *Energy Build.*, vol. 38, no. 1, pp. 63–71, 2006.

[64] Y. Zhang, K. Soga, R. Choudhary, and S. Bains, “GSHP Application for Heating and Cooling at ‘ City Scale ’ for the City of Westminster,” *Proc. World Geotherm. Congr.*, no. April, pp. 19–25, 2015.

[65] B. Talebi, P. A. Mirzaei, A. Bastani, and F. Haghighat, “A Review of District Heating Systems: Modeling and Optimization,” *Front. Built Environ.*, vol. 2, pp. 2665–2676, 2016.

[66] B. Talebi, F. Haghighat, and P. A. Mirzaei, “Simplified model to predict the thermal demand profile of districts,” *Energy Build.*, vol. 145, pp. 213–225, 2017.

[67] Y. Shimoda, T. Fujii, T. Morikawa, and M. Mizuno, “Residential end-use energy simulation at city scale,” *Build. Environ.*, vol. 39, no. 8 SPEC. ISS., pp. 959–967, 2004.

[68] S. Heiple and D. J. Sailor, “Using building energy simulation and geospatial modeling techniques to determine high resolution building sector energy consumption profiles,” *Energy Build.*, vol. 40, no. 8, pp. 1426–1436, 2008.

[69] A. Mavrogianni, M. Davies, M. Kolokotroni, and I. Hamilton, “A GIS-based bottom-up space heating demand model of the London domestic stock,” *Int. Build. Perform. Simul. Assoc. Build. Simul.*, pp. 1061–1067, 2009.

[70] G. Dall'o', A. Galante, and M. Torri, "A methodology for the energy performance classification of residential building stock on an urban scale," *Energy Build.*, vol. 48, pp. 211–219, 2012.

[71] P. Caputo, G. Costa, and S. Ferrari, "A supporting method for defining energy strategies in the building sector at urban scale," *Energy Policy*, vol. 55, pp. 261–270, 2013.

[72] A. Mastrucci, O. Baume, F. Stazi, and U. Leopold, "Estimating energy savings for the residential building stock of an entire city: A GIS-based statistical downscaling approach applied to Rotterdam," *Energy Build.*, vol. 75, pp. 358–367, 2014.

[73] M. Aksoezen, M. Daniel, U. Hassler, and N. Kohler, "Building age as an indicator for energy consumption," *Energy Build.*, vol. 87, pp. 74–86, 2015.

[74] S. K. Firth and K. J. Lomas, "Investigating Co2 Emission Reductions in Existing Urban Housing Using a Community Domestic Energy Model," *Build. Simul.*, pp. 2098–2105, 2009.

[75] I. Ballarini, S. P. Corgnati, and V. Corrado, "Use of reference buildings to assess the energy saving potentials of the residential building stock: The experience of TABULA project," *Energy Policy*, vol. 68, pp. 273–284, 2014.

[76] I. Theodoridou, A. M. Papadopoulos, and M. Hegger, "A typological classification of the Greek residential building stock," *Energy Build.*, vol. 43, no. 10, pp. 2779–2787, 2011.

[77] A. A. Famuyibo, A. Duffy, and P. Strachan, "Developing archetypes for domestic dwellings - An Irish case study," *Energy Build.*, vol. 50, pp. 150–157, 2012.

[78] É. Mata, A. Sasic Kalagasidis, and F. Johnsson, "Building-stock aggregation through

archetype buildings: France, Germany, Spain and the UK," *Build. Environ.*, vol. 81, pp. 270–282, 2014.

[79] P. Tuominen, R. Holopainen, L. Eskola, J. Jokisalo, and M. Airaksinen, "Calculation method and tool for assessing energy consumption in the building stock," *Build. Environ.*, vol. 75, pp. 153–160, 2014.

[80] L. Filogamo, G. Peri, G. Rizzo, and A. Giaccone, "On the classification of large residential buildings stocks by sample typologies for energy planning purposes," *Appl. Energy*, vol. 135, pp. 825–835, 2014.

[81] J. A. Fonseca and A. Schlueter, "Integrated model for characterization of spatiotemporal building energy consumption patterns in neighborhoods and city districts," *Appl. Energy*, vol. 142, pp. 247–265, 2015.

[82] R. Nouvel, C. Schulte, U. Eicker, D. Pietruschka, and V. Coors, "CityGML-Based 3D City Model for Energy Diagnostics and Urban Energy Policy Support," *Proc. BS2013 13th Conf. Int. Build. Perform. Simul. Assoc.*, pp. 218–225, 2013.

[83] K. M. Powell, A. Sriprasad, W. J. Cole, and T. F. Edgar, "Heating, cooling, and electrical load forecasting for a large-scale district energy system," *Energy*, vol. 74, no. C, pp. 877–885, 2014.

[84] F. G. H. Koene, L. G. Bakker, D. Lanceta, and S. Narmsara, "SIMPLIFIED BUILDING MODEL OF DISTRICTS," in *Fifth German-Austrian IBPSA Conference*, 2015, pp. 152–159.

[85] H. Gadd and S. Werner, "Daily heat load variations in Swedish district heating systems,"

*Appl. Energy*, vol. 106, pp. 47–55, 2013.

[86] M. T. Ali, M. Mokhtar, M. Chiesa, and P. Armstrong, "A cooling change-point model of community-aggregate electrical load," *Energy Build.*, vol. 43, no. 1, pp. 28–37, 2011.

[87] Y. S. Lee and L. I. Tong, "Forecasting energy consumption using a grey model improved by incorporating genetic programming," *Energy Convers. Manag.*, vol. 52, no. 1, pp. 147–152, 2011.

[88] A. Goia, C. May, and G. Fusai, "Functional clustering and linear regression for peak load forecasting," *Int. J. Forecast.*, vol. 26, no. 4, pp. 700–711, 2010.

[89] A. Mavrogianni, M. Davies, Z. Chalabi, P. Wilkinson, M. Kolokotroni, and J. Milner, "Space heating demand and heatwave vulnerability: London domestic stock," *Build. Res. Inf.*, vol. 37, no. 5–6, pp. 583–597, 2009.

[90] L. Pedersen, J. Stang, and R. Ulseth, "Load prediction method for heat and electricity demand in buildings for the purpose of planning for mixed energy distribution systems," *Energy Build.*, vol. 40, no. 7, pp. 1124–1134, 2008.

[91] J. Tanimoto, A. Hagishima, and H. Sagara, "A methodology for peak energy requirement considering actual variation of occupants' behavior schedules," *Build. Environ.*, vol. 43, no. 4, pp. 610–619, 2008.

[92] P. Sehrawat and K. Kensek, "URBAN ENERGY MODELING: GIS AS AN ALTERNATIVE TO BIM," in *ASHRAE/IBPSA-USA Bldg Simulation Conf.*

[93] K. Orehounig, G. Mavromatidis, and R. Evins, "Predicting energy consumption of a neighbourhood using building performance simulations," in *Proceedings of BSO14*.

[94] S. Chu and A. Majumdar, “Opportunities and challenges for a sustainable energy future,” *Nature*, vol. 488, no. 7411, pp. 294–303, 2012.

[95] J. Zeng, J. Han, and G. Zhang, “Diameter optimization of district heating and cooling piping network based on hourly load,” *Appl. Therm. Eng.*, vol. 107, pp. 750–757, 2016.

[96] M. Åberg and D. Henning, “Optimisation of a Swedish district heating system with reduced heat demand due to energy efficiency measures in residential buildings,” *Energy Policy*, vol. 39, no. 12, pp. 7839–7852, 2011.

[97] D. Henning, S. Amiri, and K. Holmgren, “Modelling and optimisation of electricity, steam and district heating production for a local Swedish utility,” *Eur. J. Oper. Res.*, vol. 175, no. 2, pp. 1224–1247, 2006.

[98] J. A. Wright, H. A. Loosemore, and R. Farmani, “Optimization of building thermal design and control by multi-criterion genetic algorithm,” *Energy Build.*, vol. 34, no. 9, pp. 959–972, 2002.

[99] A. Keçebaş and İ. Yabanova, “Thermal monitoring and optimization of geothermal district heating systems using artificial neural network: A case study,” *Energy Build.*, vol. 50, pp. 339–346, Jul. 2012.

[100] J. Söderman and F. Pettersson, “Structural and operational optimisation of distributed energy systems,” *Appl. Therm. Eng.*, vol. 26, no. 13, pp. 1400–1408.

[101] H. Lu, Z. Yu, K. Alanne, L. Zhang, L. Fan, X. Xu, and I. Martinac, “Transition path towards hybrid systems in China: Obtaining net-zero exergy district using a multi-objective optimization method,” *Energy Build.*, vol. 85, pp. 524–535, 2014.

[102] E. D. Mehleri, H. Sarimveis, N. C. Markatos, and L. G. Papageorgiou, “Optimal design and operation of distributed energy systems: Application to Greek residential sector,” *Renew. Energy*, vol. 51, pp. 331–342, Mar. 2013.

[103] E. D. Mehleri, H. Sarimveis, N. C. Markatos, and L. G. Papageorgiou, “A mathematical programming approach for optimal design of distributed energy systems at the neighbourhood level,” *Energy*, vol. 44, no. 1, pp. 96–104, 2012.

[104] J. Söderman, “Optimisation of structure and operation of district cooling networks in urban regions,” *Appl. Therm. Eng.*, vol. 27, no. 16 SPEC. ISS., pp. 2665–2676, 2007.

[105] J. Wang, Z. Zhou, and J. Zhao, “A method for the steady-state thermal simulation of district heating systems and model parameters calibration,” *Energy Convers. Manag.*, vol. 120, pp. 294–305, 2016.

[106] A. Chauhan and R. P. Saini, “Discrete harmony search based size optimization of Integrated Renewable Energy System for remote rural areas of Uttarakhand state in India,” *Renew. Energy*, vol. 94, pp. 587–604, 2016.

[107] D. Olsthoorn, F. Haghighat, and P. A. Mirzaei, “Integration of storage and renewable energy into district heating systems: A review of modelling and optimization,” *Sol. Energy*, vol. 136, pp. 49–64, 2016.

[108] Z. Zhou, P. Liu, Z. Li, E. N. Pistikopoulos, and M. C. Georgiadis, “Impacts of equipment off-design characteristics on the optimal design and operation of combined cooling; heating and power systems,” *Comput. & Chem. Eng.*, vol. 48, no. 0, p. -, 2012.

[109] C. Bordin, A. Gordini, and D. Vigo, “An optimization approach for district heating strategic

network design," *Eur. J. Oper. Res.*, vol. 252, no. 1, pp. 296–307, 2016.

[110] M. Ameri and Z. Besharati, "Optimal design and operation of district heating and cooling networks with CCHP systems in a residential complex," *Energy Build.*, vol. 110, pp. 135–148, 2016.

[111] T. Fang and R. Lahdelma, "Genetic optimization of multi-plant heat production in district heating networks," *Appl. Energy*, vol. 159, pp. 610–619, 2015.

[112] A. R. Razani and I. Weidlich, "A genetic algorithm technique to optimize the configuration of heat storage in DH networks," *Int. J. Sustain. Energy Plan. Manag.*, vol. 10, no. 0, pp. 21–32, 2016.

[113] S. Barberis, M. Rivarolo, A. Traverso, and A. F. Massardo, "Thermo-economic analysis of the energy storage role in a real polygenerative district," *J. Energy Storage*, vol. 5, pp. 187–202, 2016.

[114] L. T. Biegler and I. E. Grossmann, "Retrospective on optimization," *Comput. Chem. Eng.*, vol. 28, no. 8, pp. 1169–1192, 2004.

[115] S. Attia, M. Hamdy, W. O'Brien, and S. Carlucci, "Assessing gaps and needs for integrating building performance optimization tools in net zero energy buildings design," *Energy Build.*, vol. 60, pp. 110–124, 2013.

[116] S. Akhtari, T. Sowlati, and K. Day, "Economic feasibility of utilizing forest biomass in district energy systems – A review," *Renew. Sustain. Energy Rev.*, vol. 33, pp. 117–127, May 2014.

[117] D. Connolly, H. Lund, B. V. Mathiesen, S. Werner, B. Möller, U. Persson, T. Boermans, D.

Trier, P. a. Østergaard, and S. Nielsen, “Heat Roadmap Europe: Combining district heating with heat savings to decarbonise the EU energy system,” *Energy Policy*, vol. 65, pp. 475–489, Feb. 2014.

[118] D. Henning, “Optimisation of Local and National Energy Systems Development and Use of the MODEST Model.”

[119] L. Magnier and F. Haghighat, “Multiobjective optimization of building design using TRNSYS simulations, genetic algorithm, and Artificial Neural Network,” *Build. Environ.*, vol. 45, no. 3, pp. 739–746, 2010.

[120] E. Asadi, M. Gameiro, C. H. Antunes, and L. Dias, “A multi-objective optimization model for building retrofit strategies using TRNSYS simulations, GenOpt and MATLAB,” *Build. Environ.*, vol. 56, pp. 370–378, 2012.

[121] M. Vesterlund, A. Toffolo, and J. Dahl, “Optimization of multi-source complex district heating network, a case study,” *Energy*, vol. 126, pp. 53–63, 2017.

[122] H. Wang, H. Wang, Z. Haijian, and T. Zhu, “Optimization modeling for smart operation of multi-source district heating with distributed variable-speed pumps,” *Energy*, vol. 138, pp. 1247–1262, 2017.

[123] M. Rivarolo, A. Cuneo, A. Traverso, and A. F. Massardo, “Design optimisation of smart poly-generation energy districts through a model based approach,” *Appl. Therm. Eng.*, vol. 99, pp. 291–301, 2016.

[124] P. E. Campana, S. J. Quan, F. I. Robbio, A. Lundblad, Y. Zhang, T. Ma, B. Karlsson, and J. Yan, “Optimization of a residential district with special consideration on energy and water

reliability," *Appl. Energy*, vol. 194, pp. 751–764, 2017.

[125] G. Schweiger, P. O. Larsson, F. Magnusson, P. Lauenburg, and S. Velut, "District heating and cooling systems – Framework for Modelica-based simulation and dynamic optimization," *Energy*, vol. 137, pp. 566–578, 2017.

[126] T. Falke, S. Krengel, A. K. Meinerzhagen, and A. Schnettler, "Multi-objective optimization and simulation model for the design of distributed energy systems," *Appl. Energy*, vol. 184, pp. 1508–1516, 2016.

[127] L. Li, H. Mu, N. Li, and M. Li, "Economic and environmental optimization for distributed energy resource systems coupled with district energy networks," *Energy*, vol. 109, pp. 947–960, 2016.

[128] L. Jie, X. Xin, B. Fani, F. C. A., Z. Baoguo, D. Guangming, S. Xin, and L. Hongwei, "Data driven mathematical modeling and global optimization framework for entire petrochemical planning operations," *AIChE J.*, vol. 62, no. 9, pp. 3020–3040.

[129] T. Mertz, S. Serra, A. Henon, and J. M. Reneaume, "A MINLP optimization of the configuration and the design of a district heating network: Academic study cases," *Energy*, vol. 117, pp. 450–464, 2016.

[130] H. Lu, K. Alanne, and I. Martinac, "Energy quality management for building clusters and districts (BCDs) through multi-objective optimization," *Energy Convers. Manag.*, vol. 79, pp. 525–533, Mar. 2014.

[131] D. Buoro, M. Casisi, A. De Nardi, P. Pinamonti, and M. Reini, "Multicriteria optimization of a distributed energy supply system for an industrial area," *Energy*, vol. 58, pp. 128–137,

2013.

[132] D. Dobersek and D. Goricanec, “Optimisation of tree path pipe network with nonlinear optimisation method,” *Appl. Therm. Eng.*, vol. 29, no. 8–9, pp. 1584–1591, 2009.

[133] T. M. Kodinariya and P. R. Makwana, “Review on determining number of Cluster in K-Means Clustering,” *Int. J. Adv. Res. Comput. Sci. Manag. Stud.*, vol. 1, no. 6, pp. 2321–7782, 2013.

[134] A. Saltelli, “Sensitivity Analysis,” *PhD-course Numbers policy Pract. Probl. Quantif.*, p. Esbergen, 2017.

[135] C. H. Frey and S. R. Patil, “Indentification and Review of Sensitivity Analysis Methods,” *Risk Anal.*, vol. 22, no. 3, pp. 553–578, 2002.

[136] S. K. Firth, K. J. Lomas, and A. J. Wright, “Targeting household energy-efficiency measures using sensitivity analysis,” *Build. Res. Inf.*, vol. 38, no. 1, pp. 24–41, 2010.

[137] A. Saltelli and P. Annoni, “How to avoid a perfunctory sensitivity analysis,” *Environ. Model. Softw.*, vol. 25, no. 12, pp. 1508–1517, 2010.

[138] V. Cheng and K. Steemers, “Modelling domestic energy consumption at district scale: A tool to support national and local energy policies,” *Environ. Model. Softw.*, vol. 26, no. 10, pp. 1186–1198, 2011.

[139] T. Turányi, “Lecture 1-2 Local sensitivity analysis,” pp. 1–50.

[140] S. Wilcox and W. Marion, “Users manual for TMY3 data sets,” *Renew. Energy*, no. May, p. 51, 2008.

[141] A. Engineers, “ANSI/ASHRAE Standard 55-2010,” pp. 3–6, 2010.

[142] U. Whole and H. Performance, “Performance Compliance for Houses,” no. March, 1999.

[143] J. Pfafferott, S. Herkel, and J. Wapler, “Thermal building behaviour in summer: Long-term data evaluation using simplified models,” *Energy Build.*, vol. 37, no. 8, pp. 844–852, 2005.

[144] “2017 ASHRAE Handbook—Fundamentals.”

[145] M. Ezekiel and K. A. Fox, *Methods of correlation and regression analysis: Linear and curvilinear, 3rd ed.* Oxford, England: John Wiley, 1959.

[146] G. E. S., “Exponential smoothing: The state of the art,” *J. Forecast.*, vol. 4, no. 1, pp. 1–28, Sep. 2006.

[147] J. Adamowski, H. Fung Chan, S. O. Prasher, B. Ozga-Zielinski, and A. Sliusarieva, “Comparison of multiple linear and nonlinear regression, autoregressive integrated moving average, artificial neural network, and wavelet artificial neural network methods for urban water demand forecasting in Montreal, Canada,” *Water Resour. Res.*, vol. 48, no. 1, pp. 1–14, 2012.

[148] T. Lu and M. Viljanen, “Prediction of indoor temperature and relative humidity using neural network models: Model comparison,” *Neural Comput. Appl.*, vol. 18, no. 4, pp. 345–357, 2009.

[149] S. G. Halverson, M, M.Rosenberg, W.Wang, J. Zhang, V.Mendon, R.Athalye, Y Xie, R.Hart, “ANSI / ASHRAE / IES Standard 90.1-2013. Determination of Energy Savings : Quantitative Analysis,” no. August, 2014.

[150] CIBSE, “Energy benchmarks,” *Building*, vol. CIBSE TM46, p. 26, 2008.

[151] H. Bruhns, P. Jones, R. Cohen, B. Bordass, and H. Davies, “CIBSE Review of Energy

Benchmarks for Display Energy Certificates - Analysis of DEC results to date (ANNEX - Energy distibution charts),” no. May, 2011.

[152] S. M. Camporeale, B. Fortunato, M. Torresi, F. Turi, A. M. Pantaleo, and A. Pellerano, “Part Load Performance and Operating Strategies of a Natural Gas—Biomass Dual Fueled Microturbine for Combined Heat and Power Generation,” *J. Eng. Gas Turbines Power*, vol. 137, no. 12, p. 121401, 2015.

# Appendix A (MLR Method)

Regression coefficients obtained from training of the reference building:

**Table A-1: Summary Output**

| *Regression Statistics* | |
|---|---|
| Multiple R | 0.998307557 |
| R Square | 0.996617977 |
| Adjusted R Square | 0.996612174 |
| Standard Error | 2.645153621 |
| Observations | 8757 |

**Table A-2: Regression Coefficient**

| | *Coefficients* | *Standard Error* | *t Stat* | *P-value* | *Lower 95%* | *Upper 95%* | *Lower 95.0%* | *Upper 95.0%* |
|---|---|---|---|---|---|---|---|---|
| Intercept | -4.0896477 | 0.54333 | -7.52707 | 0.00000 | -5.15469 | -3.02460 | -5.15469 | -3.02460 |
| Load-1 | 1.4092226 | 0.01055 | 133.56586 | 0.00000 | 1.38854 | 1.42990 | 1.38854 | 1.42990 |
| Load-2 | -0.3713752 | 0.01782 | -20.84614 | 0.00000 | -0.40630 | -0.33645 | -0.40630 | -0.33645 |
| Load-3 | -0.1085372 | 0.01048 | -10.35315 | 0.00000 | -0.12909 | -0.08799 | -0.12909 | -0.08799 |
| TD | 0.0044513 | 0.00006 | 80.30940 | 0.00000 | 0.00434 | 0.00456 | 0.00434 | 0.00456 |
| TD-1 | -0.0057457 | 0.00009 | -60.60852 | 0.00000 | -0.00593 | -0.00556 | -0.00593 | -0.00556 |
| TD-2 | 0.0009605 | 0.00011 | 8.56908 | 0.00000 | 0.00074 | 0.00118 | 0.00074 | 0.00118 |
| TD-3 | 0.0007492 | 0.00007 | 10.30722 | 0.00000 | 0.00061 | 0.00089 | 0.00061 | 0.00089 |
| SD | -0.0000077 | 0.00000 | -22.40160 | 0.00000 | -0.00001 | -0.00001 | -0.00001 | -0.00001 |
| SD-1 | 0.0000079 | 0.00000 | 15.09332 | 0.00000 | 0.00001 | 0.00001 | 0.00001 | 0.00001 |
| SD-2 | 0.0000005 | 0.00000 | 1.00940 | 0.31281 | 0.00000 | 0.00000 | 0.00000 | 0.00000 |
| SD-3 | -0.0000022 | 0.00000 | -6.38566 | 0.00000 | 0.00000 | 0.00000 | 0.00000 | 0.00000 |
| IG | 0.0401457 | 0.01972 | 2.03548 | 0.04183 | 0.00148 | 0.07881 | 0.00148 | 0.07881 |
| IG-1 | -0.0057327 | 0.03465 | -0.16544 | 0.86860 | -0.07366 | 0.06219 | -0.07366 | 0.06219 |
| IG-2 | -0.1887608 | 0.03465 | -5.44829 | 0.00000 | -0.25667 | -0.12085 | -0.25667 | -0.12085 |
| IG-3 | 0.2289462 | 0.01946 | 11.76536 | 0.00000 | 0.19080 | 0.26709 | 0.19080 | 0.26709 |

TD: Thermal Dependence; SD: Solar Dependence; IG: Internal Gain

## Appendix B (ANN, MNLR Method)

The Artificial Neural Network (ANN) is as a data-driven approach, which predicts the results using existing data history. The ANN, has the ability to approximate any linear or non-linear complex relation which could not be obtained by other analytical approaches. Due to its usefulness, this method has been used widely in order to predict the noisy values of multivariate time series, using the time series history.

The ANN has been used for this study is the NARX, Nonlinear autoregressive model with external Input, which predicts the series Y(t) given d past values of Y(t) and another series X(t), method generated by Matlab Neural Network Fitting Tool, NNFT. The network has been used, has a feedforward structure with 23 hidden units. The number of the hidden unites decided to be 23 based on Lu [33] suggestion who suggests, the best number of hidden units for the system is equal with two times the number of input layer plus one.

For the purpose of the training, validation and testing, the heating energy demand profile of the reference building has been obtained using comprehensive modeling. Having the input and target data, the model has been trained and the used for prediction the heating energy demand profile of the ***R1*** and ***R2*** buildings. **Error! Reference source not found.** and **Error! Reference source not found.** present the nonlinear regression results obtained from ANN model.

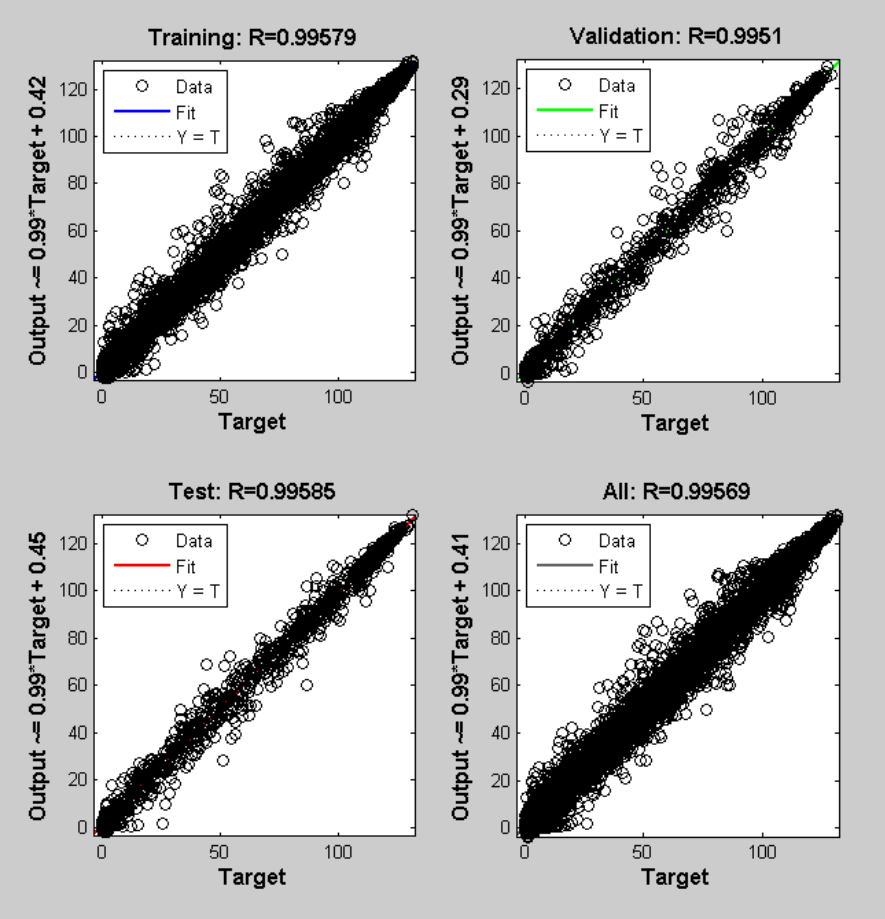


**Figure B-1:** **Regression Results Obtained from ANN Model**

**Table B-1:** **Regression Results Obtained from ANN Model**

| | R |
|---|---|
| *Training* | 9.956E-01 |
| *Validation* | 9.951E-01 |
| *Testing* | 9.958E-01 |
| *All* | 9.957E-01 |

## Appendix C (Inter-Model Comparison)

For a purpose of the inter-model comparison, 289 simulations have been performed, using a validated eQUEST model. The simulations were conducted over a range of buildings type, residential and office buildings, by multiplying the selected input parameter(s) by a random number within the predefined range. As mentioned in ***Section 4.1.2***, the simulations were done by changing a single parameter in 15% of the cases. While in remaining 85%, 2 parameters in 25% of the cases, and 3 parameters in 60% of the cases were changed. Then the heating demand profiles obtained from detailed simulation (eQUEST) were used to obtain the total heating energy demand profile of the district. Out of 289 buildings, 47 of them are 5 story office buildings including 37 buildings in ***District 2*** and 10 buildings in ***District 3***. Fifty seven 5-Story office buildings have been simulated and 47 of them have been picked randomly to be used in ***District 2 & 3***.

**Table C-1: Range of the Buildings Parameters**

| 5-Story Office Buildings | | |
|---|---|---|
| **Parameters** | **District 2** | **District 3** |
| **Number** | 37 | 10 |
| **Area [ft$^2$]** | 110-140K | 110-150k |
| **Aspect Ratio** | 0.7-2.5 | 0.7-2.5 |
| **Win/Wall** | 25-45% | 25-45% |
| **Occupancy Density [ft$^2$/ person]** | 85 -110 | 85 -110 |
| **Orientation with South** | 0 - 90º | 0 - 90º |

**Table C-2: Distribution of the 5-Story Office Buildings with 3, 2, 1 parameters changed in each District**

| Distribution of the Varied Parameters | | | |
|---|---|---|---|
| **District 2** | | | |
| **3-Parameters** | 60% | 22.2 | 22 |
| **2-Parametes** | 25% | 9.25 | 9 |
| **1-Parameter** | 15% | 5.55 | 6 |
| **Total** | | 37 | 37 |
| **District 3** | | | |
| **3-Parameters** | 60% | 6 | 6 |
| **2-Parametes** | 25% | 2.5 | 3 |
| **1-Parameter** | 15% | 1.5 | 1 |
| **Total** | | 10 | 10 |

## Table C-3: Detail Description of a Simulated Buildings

| District 2: Solely Commercial [5S-Office] | | | | | | | | | | | | | | |
|---|---|---|---|---|---|---|---|---|---|---|---|---|---|---|
| Name | Area | | Stories | Aspect Ratio | Dimensions | | | | | | Win/Wall | Orientation | Int. | Note |
| | [sq.ft] | [sq.m] | | | X1[ft] | X1[m] | Y1[ft] | Y1[m] | Flr-Flr[ft] | Flr-Flr[m] | | | | |
| **Base 5S** | 125000.00 | 11612.88 | 5 | 1.00 | 158.10 | 48.19 | 158.10 | 48.19 | 13.00 | 3.96 | 30% | North | 1 | 0 |
| **Base 5S-1** | 110000.00 | 10219.33 | 5 | 1.00 | 148.30 | 45.20 | 148.30 | 45.20 | 13.00 | 3.96 | 30% | North | 1 | 1E |
| **Base 5S-2** | 140000.00 | 13006.43 | 5 | 1.00 | 167.35 | 51.01 | 167.35 | 51.01 | 13.00 | 3.96 | 30% | North | 1 | 2 |
| **Base 5S-3** | 125000.00 | 11612.88 | 5 | 0.60 | 122.45 | 37.32 | 204.10 | 62.21 | 13.00 | 3.96 | 30% | North | 1 | 0 |
| **Base 5S-4** | 125000.00 | 11612.88 | 5 | 0.80 | 141.40 | 43.10 | 176.80 | 53.89 | 13.00 | 3.96 | 30% | North | 1 | 1E |
| **Base 5S-5** | 125000.00 | 11612.88 | 5 | 1.20 | 173.20 | 52.79 | 144.35 | 44.00 | 13.00 | 3.96 | 30% | North | 1 | 1W |
| **Base 5S-6** | 125000.00 | 11612.88 | 5 | 1.50 | 193.65 | 59.02 | 129.10 | 39.35 | 13.00 | 3.96 | 30% | North | 1 | 2 |
| **Base 5S-7** | 125000.00 | 11612.88 | 5 | 1.00 | 158.10 | 48.19 | 158.10 | 48.19 | 13.00 | 3.96 | 20% | North | 1 | 0 |
| **Base 5S-8** | 125000.00 | 11612.88 | 5 | 1.00 | 158.10 | 48.19 | 158.10 | 48.19 | 13.00 | 3.96 | 25% | North | 1 | 2 |
| **Base 5S-9** | 125000.00 | 11612.88 | 5 | 1.00 | 158.10 | 48.19 | 158.10 | 48.19 | 13.00 | 3.96 | 35% | North | 1 | 1W |
| **Base 5S-10** | 125000.00 | 11612.88 | 5 | 1.50 | 433.01 | 131.98 | 288.68 | 87.99 | 13.00 | 3.96 | 30% | South | 1 | 0 |
| **Base 5S-11** | 136000.00 | 12634.81 | 5 | 1.00 | 368.78 | 112.40 | 368.78 | 112.40 | 13.00 | 3.96 | 30% | East | 1 | 1N |
| **Base 5S-12** | 125000.00 | 11612.88 | 5 | 2.50 | 559.02 | 170.39 | 223.61 | 68.16 | 13.00 | 3.96 | 30% | West | 1 | 2 |
| **Base 5S-13** | 150000.00 | 13935.46 | 5 | 1.00 | 387.30 | 118.05 | 387.30 | 118.05 | 14.00 | 4.27 | 30% | North | 2 | 1E, AIS |
| **Base 5S-14** | 142000.00 | 13192.23 | 5 | 1.00 | 376.83 | 114.86 | 376.83 | 114.86 | 15.00 | 4.57 | 30% | North | 2 | 2, AIS |
| **Base 5S-15** | 117000.00 | 10869.66 | 5 | 1.80 | 458.91 | 139.88 | 254.95 | 77.71 | 13.00 | 3.96 | 30% | North | 1 | 1W |
| **Base 5S-16** | 132000.00 | 12263.20 | 5 | 0.90 | 344.67 | 105.06 | 382.97 | 116.73 | 13.00 | 3.96 | 30% | North | 1 | 2 |
| **Base 5S-17** | 125000.00 | 11612.88 | 5 | 1.00 | 353.55 | 107.76 | 353.55 | 107.76 | 13.00 | 3.96 | 23% | North | 1 | 1W |
| **Base 5S-18** | 125000.00 | 11612.88 | 5 | 1.00 | 353.55 | 107.76 | 353.55 | 107.76 | 13.00 | 3.96 | 28% | North | 1 | 2 |
| **Base 5S-19** | 125000.00 | 11612.88 | 5 | 1.00 | 353.55 | 107.76 | 353.55 | 107.76 | 13.00 | 3.96 | 30% | South East | 1 | 1SW |
| **Base 5S-20** | 125000.00 | 11612.88 | 5 | 1.00 | 353.55 | 107.76 | 353.55 | 107.76 | 13.00 | 3.96 | 30% | North West | 1 | 2 |
| **Base 5S-21** | 125000.00 | 11612.88 | 5 | 1.00 | 353.55 | 107.76 | 353.55 | 107.76 | 13.50 | 4.11 | 36% | North | 2 | 1E |
| **Base 5S-22** | 125000.00 | 11612.88 | 5 | 1.00 | 353.55 | 107.76 | 353.55 | 107.76 | 14.50 | 4.42 | 28% | North | 2 | 2 |
| **Base 5S-23** | 125000.00 | 11612.88 | 5 | 1.30 | 403.11 | 122.87 | 310.09 | 94.51 | 13.00 | 3.96 | 45% | North | 2 | 1W |
| **Base 5S-24** | 113000.00 | 10498.04 | 5 | 0.85 | 309.92 | 94.46 | 364.61 | 111.13 | 13.00 | 3.96 | 25% | North | 2 | 2 |
| **Base 5S-25** | 135000.00 | 12541.91 | 5 | 2.00 | 519.62 | 158.38 | 259.81 | 79.19 | 13.00 | 3.96 | 30% | North | 3 | 1E |
| **Base 5S-26** | 125000.00 | 11612.88 | 5 | 0.70 | 295.80 | 90.16 | 422.58 | 128.80 | 13.00 | 3.96 | 35% | North | 2 | 1E |
| **Base 5S-27** | 116000.00 | 10776.75 | 5 | 0.90 | 323.11 | 98.48 | 359.01 | 109.43 | 13.00 | 3.96 | 28% | North | 1 | 2 |
| **Base 5S-28** | 138000.00 | 12820.62 | 5 | 0.85 | 342.49 | 104.39 | 402.93 | 122.81 | 13.00 | 3.96 | 32% | North | 1 | 2 |
| **Base 5S-29** | 112000.00 | 10405.14 | 5 | 0.95 | 326.19 | 99.42 | 343.36 | 104.66 | 13.00 | 3.96 | 40% | South West | 1 | 1SE |
| **Base 5S-30** | 132000.00 | 12263.20 | 5 | 1.20 | 397.99 | 121.31 | 331.66 | 101.09 | 13.00 | 3.96 | 40% | North West | 1 | 2 |
| **Base 5S-31** | 146000.00 | 13563.84 | 5 | 1.00 | 382.10 | 116.46 | 382.10 | 116.46 | 13.30 | 4.05 | 45% | North | 2 | 0 |
| **Base 5S-32** | 118000.00 | 10962.56 | 5 | 0.70 | 287.40 | 87.60 | 410.57 | 125.14 | 13.70 | 4.18 | 30% | North | 2 | 2 |
| **Base 5S-33** | 122000.00 | 11334.17 | 5 | 1.00 | 349.28 | 106.46 | 349.28 | 106.46 | 13.00 | 3.96 | 36% | North | 1 | 1W |
| **Base 5S-34** | 127000.00 | 11798.69 | 5 | 1.00 | 356.37 | 108.62 | 356.37 | 108.62 | 13.00 | 3.96 | 42% | East | 1 | 1W |
| **Base 5S-35** | 110000.00 | 10219.33 | 5 | 1.50 | 406.20 | 123.81 | 270.80 | 82.54 | 13.00 | 3.96 | 30% | North | 1 | 1W |
| **Base 5S-36** | 116000.00 | 10776.75 | 5 | 1.00 | 340.59 | 103.81 | 340.59 | 103.81 | 13.00 | 3.96 | 25% | South | 1 | 2 |
| **Base 5S-37** | 130000.00 | 12077.40 | 5 | 1.00 | 360.56 | 109.90 | 360.56 | 109.90 | 13.50 | 4.11 | 30% | North | 1 | 0 |
| **Base 5S-38** | 146000.00 | 13563.84 | 5 | 0.80 | 341.76 | 104.17 | 427.20 | 130.21 | 13.00 | 3.96 | 35% | North | 1 | 0 |
| **Base 5S-39** | 131000.00 | 12170.30 | 5 | 1.30 | 412.67 | 125.78 | 317.44 | 96.76 | 13.00 | 3.96 | 30% | West | 1 | 1N |
| **Base 5S-40** | 116000.00 | 10776.75 | 5 | 1.80 | 456.95 | 139.28 | 253.86 | 77.38 | 14.00 | 4.27 | 25% | North | 1 | 0 |
| **Base 5S-41** | 135000.00 | 12541.91 | 5 | 0.60 | 284.60 | 86.75 | 474.34 | 144.58 | 13.00 | 3.96 | 30% | North | 2 | 1W |
| **Base 5S-42** | 118000.00 | 10962.56 | 5 | 1.50 | 420.71 | 128.23 | 280.48 | 85.49 | 14.50 | 4.42 | 30% | West | 1 | 2 |
| **Base 5S-43** | 115000.00 | 10683.85 | 5 | 1.00 | 339.12 | 103.36 | 339.12 | 103.36 | 13.00 | 3.96 | 30% | South East | 3 | 2 |
| **Base 5S-44** | 116000.00 | 10776.75 | 5 | 1.20 | 373.10 | 113.72 | 310.91 | 94.77 | 15.00 | 4.57 | 30% | North | 2 | 1W |
| **Base 5S-45** | 140000.00 | 13006.43 | 5 | 1.00 | 374.17 | 114.05 | 374.17 | 114.05 | 13.00 | 3.96 | 25% | North | 3 | 0 |
| **Base 5S-46** | 125000.00 | 11612.88 | 5 | 2.50 | 559.02 | 170.39 | 223.61 | 68.16 | 13.00 | 3.96 | 32% | North West | 1 | 2 |
| **Base 5S-47** | 121000.00 | 11241.27 | 5 | 0.70 | 291.03 | 88.71 | 415.76 | 126.72 | 13.00 | 3.96 | 40% | North | 1 | 0 |
| **Base 5S-48** | 125000.00 | 11612.88 | 5 | 1.00 | 353.55 | 107.76 | 353.55 | 107.76 | 15.00 | 4.57 | 34% | North | 3 | 0 |
| **Base 5S-49** | 125000.00 | 11612.88 | 5 | 1.40 | 418.33 | 127.51 | 298.81 | 91.08 | 13.00 | 3.96 | 28% | South West | 1 | 1SW |

| | | | | | | | | | | | | | | |
|---|---|---|---|---|---|---|---|---|---|---|---|---|---|---|
| **Base 5S-50** | 110000.00 | 10219.33 | 5 | 0.80 | 296.65 | 90.42 | 370.81 | 113.02 | 13.00 | 3.96 | 35% | North | 1 | 0 |
| **Base 5S-51** | 135000.00 | 12541.91 | 5 | 1.00 | 367.42 | 111.99 | 367.42 | 111.99 | 14.00 | 4.27 | 30% | South | 3 | 2 |
| **Base 5S-52** | 125000.00 | 11612.88 | 5 | 1.20 | 387.30 | 118.05 | 322.75 | 98.37 | 13.00 | 3.96 | 25% | West | 1 | 2 |
| **Base 5S-53** | 120000.00 | 11148.36 | 5 | 2.50 | 547.72 | 166.95 | 219.09 | 66.78 | 15.00 | 4.57 | 20% | North | 1 | 0 |
| **Base 5S-54** | 125000.00 | 11612.88 | 5 | 0.60 | 273.86 | 83.47 | 456.44 | 139.12 | 13.50 | 4.11 | 45% | East | 1 | 0 |
| **Base 5S-55** | 115000.00 | 10683.85 | 5 | 1.10 | 355.67 | 108.41 | 323.33 | 98.55 | 13.00 | 3.96 | 30% | North East | 1 | 2 |
| **Base 5S-56** | 150000.00 | 13935.46 | 5 | 1.00 | 387.30 | 118.05 | 387.30 | 118.05 | 14.50 | 4.42 | 22% | South West | 1 | 2 |
| **Base 5S-57** | 125000.00 | 11612.88 | 5 | 1.50 | 433.01 | 131.98 | 288.68 | 87.99 | 13.20 | 4.02 | 32% | North | 2 | 0 |

**Int.: Internal Generation Schedule; Note: number of common walls and their location**

# Appendix D (WWH Community Profiles)

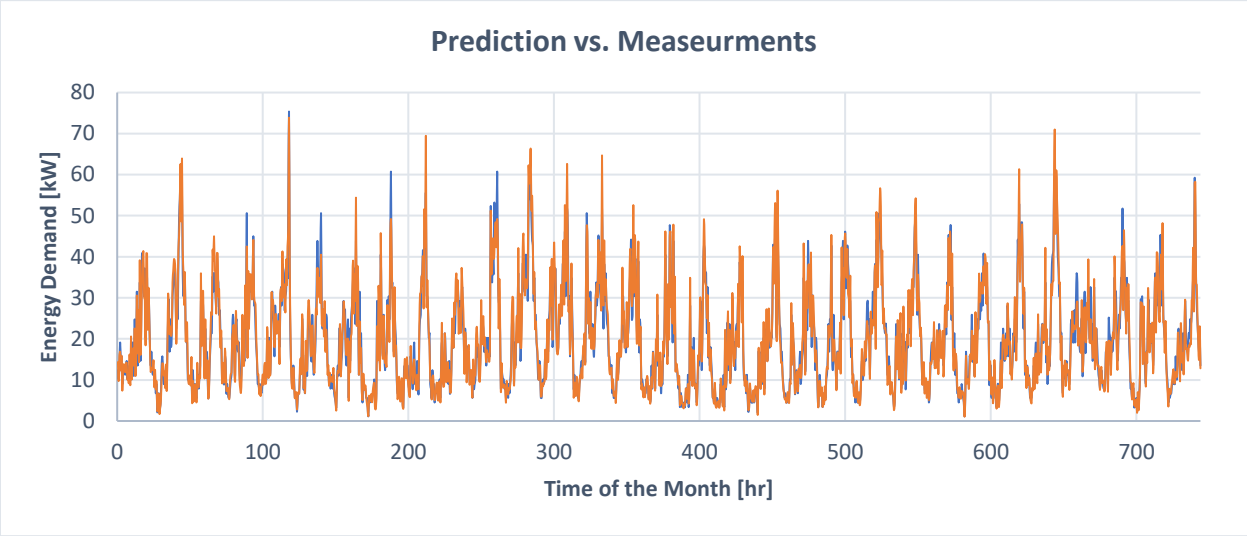


**Figure D-1: Model prediction (Blue) vs. measured energy demand (Orange) for Tower # 2; December 2016**

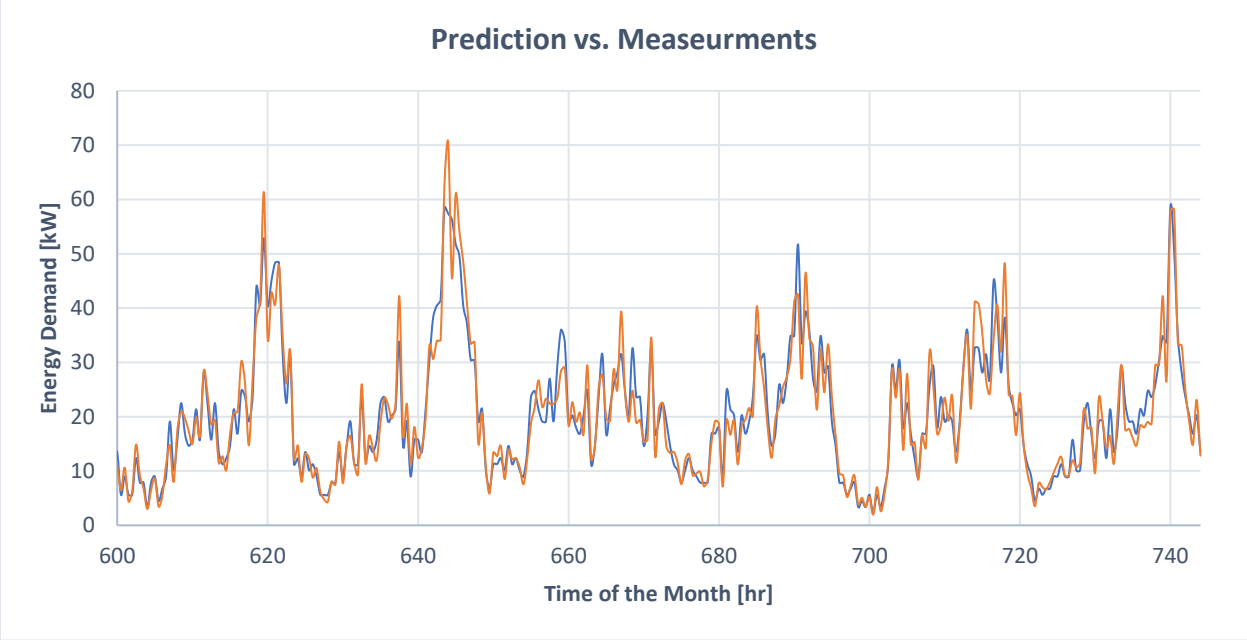


**Figure D-2: Model prediction (Blue) vs. measured energy demand (Orange) for Tower # 2; last 6 days of December 2016**

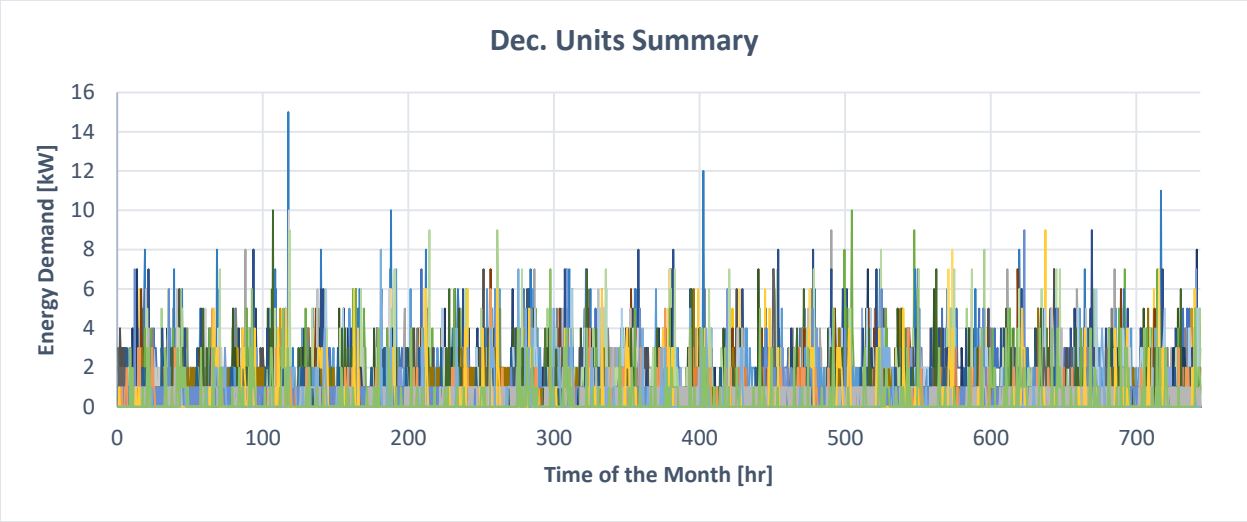


**Figure D-3: Predicted Energy Demand of different Units Tower # 2; December 2016**

# Appendix E (Optimization)

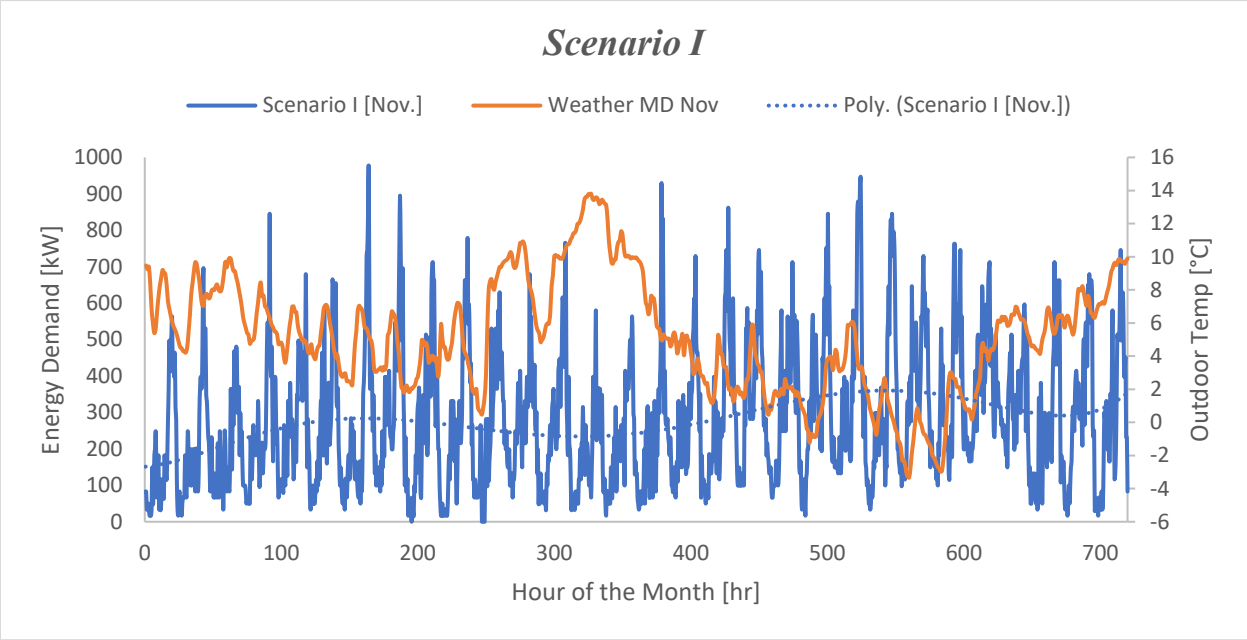


**Figure E-1: Predicted Demand Profile for the Scenario I; November 2016**

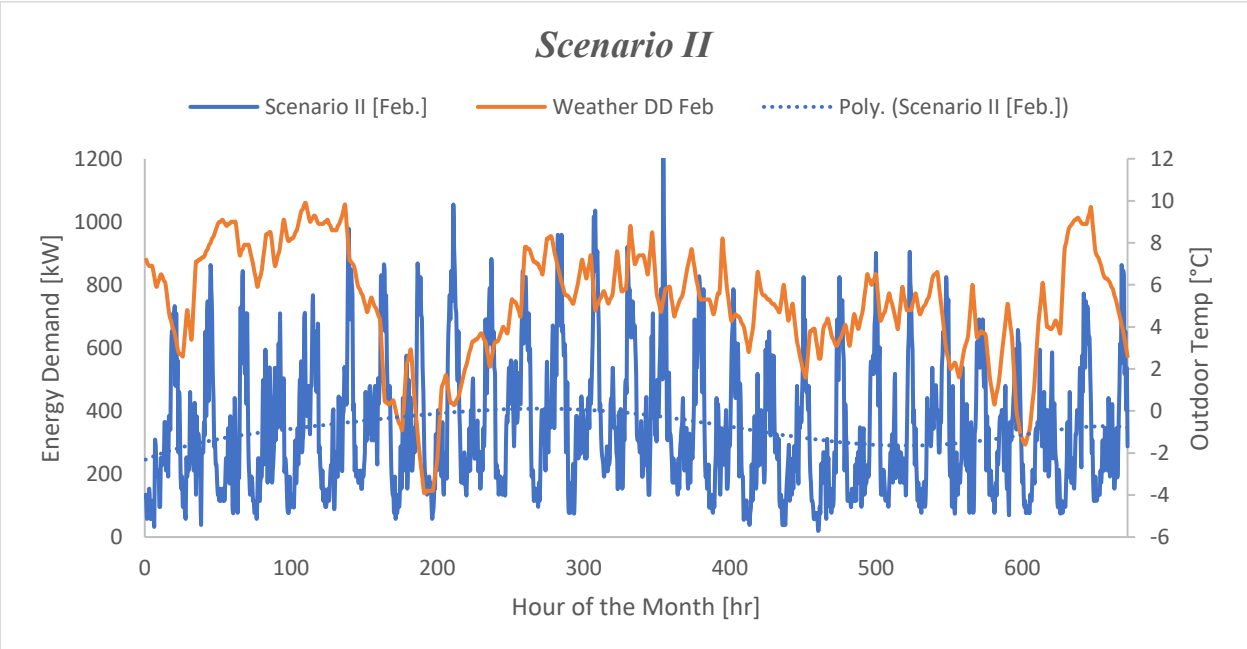


**Figure E-2: Predicted Demand Profile for the Scenario II; February**